Prediction of Gas and Liquid Leak Rates in Compression Packing at Room Temperature

by

Ali Salah Omar AWEIMER

MANUSCRIPT-BASED THESIS PRESENTED TO ÉCOLE DE
TECHNOLOGIE SUPÉRIEURE IN PARTIAL FULFILLMENT FOR THE
DEGREE OF DOCTOR OF PHILOSOPHY
PH.D.

MONTREAL, SEPTEMBER, 10, 2019

ÉCOLE DE TECHNOLOGIE SUPÉRIEURE
UNIVERSITÉ DU QUÉBEC

ACKNOWLEDGMENT

Prédiction des taux de fuite de gaz et de liquides dans les garnitures d'étanchéité à température ambiante

Ali Salah Omar AWEIMER

RESUMÉ

Le joint d'étanchéité est l'élément clé de tout assemblage mécanique pressurisé. Un mauvais choix ou tout simplement l'utilisation non appropriée d'un joint d'étanchéité peut engendrer des fuites intolérables ou des infiltrations de contaminateurs potentiellement dangereux pour l'humain ou l'environnement. À la suite des nouvelles réglementations sur les émissions, de même que de nombreux incidents dus aux fuites, il devient impératif de développer de nouvelles méthodes de conception de joints d'étanchéité pour les équipements pressurisés, en se basant notamment sur la fuite maximale à tolérer. L'écoulement d'un fluide à travers les joints d'étanchéité a été étudié intensivement par plusieurs chercheurs lesquels ont élaboré des modèles théoriques et numériques pour prédire les fuites. Néanmoins, très peu d'études ont portés sur les fuites à travers les garnitures de valves et de presse-étoupes. En effet, même si la majorité des problèmes de fuites signalés par les industriels sont engendrés par les valves et les pompes qui utilisent des garnitures de presse-étoupes très peu de travaux existent dans la littérature. Par ailleurs, il n'existe malheureusement pas de norme de conception de presse-étoupes et les procédures d'essais se focalisent sur la control de la qualité sans donner d'importance à la performance. Les bancs d'essai existant pour tester les garnitures ne sont pas assez sophistiqués pour permettre de caractériser les matériaux et obtenir les propriétés mécaniques. Donc il convient de développer des montages instrumentés afin de pouvoir implémenter des modèles appropriés pour la prédiction des fuites à travers les garnitures de presse-étoupes.

L'objectif principal de ce projet de doctorat est donc la prédiction des fuites laquelle sera valider par des essais expérimentaux sur plusieurs types de garnitures de presse-étoupes à différentes pressions de fluide et plusieurs niveaux de compression des garnitures. On s'intéressera spécifiquement aux mesures expérimentales de fuites de gaz et de liquides et au développement de nouvelles approches théoriques pour les prédire. On simulera, aussi, les fuites à travers les joints d'étanchéité en utilisant des approches numériques. La comparaison des trois approches (expérimentale, théorique et numérique) permettra de valider nos résultats et de fournir à l'industrie spécialisée des guides concernant la conception des presse-étoupes.

La méthodologie utilisée pour atteindre nos objectifs est donnée par les éléments suivants. Les fuites seront mesurées dans un premier temps à l'aide de plusieurs techniques développées spécifiquement dans le cadre de ce projet. Plusieurs modèles analytiques basés sur l'écoulement des fluides à travers les milieux poreux tels que les joints d'étanchéité seront développés par la suite en utilisant la base de données expérimentale ainsi produite. Les modèles numériques par la méthode des éléments finis seront élaborés en parallèle sur le

module CFX du logiciel ANSYS. Enfin, la comparaison de ces différentes approches entre-elles permet la validation de notre approche théorique qui à son tour pourrait aider les industriels à développer des nouveaux produits d'étanchéité.

Il s'ensuit que la maitrise des fuites à l'aide de modèles de prédiction fidèles permet d'améliorer la fiabilité et la sécurité des assemblages pressurisés, d'augmenter le niveau de la production et minimiser les temps d'immobilisation et de réduire les frais de maintenance et de prévention. Enfin ce projet rentre dans le cadre de la réduction des émissions fugitives et la diminution du risque d'accident induit dans les installations industrielles des produits chimiques et raffinerie de pétrole.

Mots Clés : Valve avec presse-étoupe, micro et nano fluides dans les milieux poreux, expérimentale, théorique et numérique

Prediction of gas and liquid leak rates in compression packing at room temperature

Ali Salah Omar AWEIMER

ABSTRACT

Packing rings are the most sensitive element in pressurized mechanical assemblies such as valves and compressors. An incorrect choice or improper procedure of packing ring installation could affect the sealing performance and lead the system to leak. Moreover, leakage from valves can be potentially harmful to humans and the environment. Among the equipment requiring sealing compliance in the petrochemical industry, valves are reported as being the number one component that has leakage problems. Very often, the compression packing is the main element to blame. Unfortunately, the situation is made worse with the lack of a standard procedure for the design of packed stuffing boxes and standard test procedures for compression packing rings.

In practice, there are only few experimental, theoretical and numerical studies that are conducted to characterise the flow through packing rings to be able to predict gas and liquid leak rates in valves at room and elevated temperatures. From this standpoint, the need to design a new test rig to test packing rings is essential to be able to predict leakage and reduce fugitive emissions to a minimum level.

Therefore, the objective of this work is to carry out experimental tests on different types of packing rings to be able to characterise their sealing properties for the purpose of developing suitable theoretical models to predict their gaseous and liquid leakage. The work focuses specifically on experimental leak measurements of few packing ring materials to characterise their porosity parameters in order to be used in the developed theoretical fluid flow models to predict the leak rates. Leaks through the porous packing material are also simulated through numerical approaches using Ansys CFX. A comparison between the developed analytical models and the experimental and numerical approaches was conducted to validate their accuracy.

The methodology of this work is to measure initially the leaks through different packing ring materials using the pressure rise and the mass spectrometry leak detection techniques under different conditions of gland stress and fluid pressure. A referenced gas such as helium is first used to characterise the pores size and their number. The developed analytical models based on Navier–Stokes equations are then used to predict the gaseous and liquid leaks in the wide range of 10^{-1} to 10^{-6} mg/s. Different molecule size of gas such as Argon, Nitrogen and air and liquids such as water and Kerosene are tested in the experiment to verify the developed analytical models. Finally, a special numerical model developed in Ansys CFX software is used to support the analytical models. A comparison of these approaches has allowed us to state that the prediction of leakage through packing rings is possible and can be conducted with reasonable accuracy.

X

Finally, the control of leakage in packed stuffing boxes, using accurate prediction models, can improve the reliability of valves, increase the level of production, reduce maintenance costs and minimize fugitive emissions.

TABLE OF CONTENTS

LIST OF TABLES

LIST OF FIGURES

Page

LIST OF ABREVIATIONS

ANSI	American National Standard Institute
API	American Petroleum Institute
ASME	American Society of Mechanical Engineering
CA	Compressed Asbestos
CF	Carbon Fiber
CFX	High Performance Computational Fluid Dynamics
CFD	Computational Fluid Dynamics
EPA	United States Environmental Protection Agency
ESA	European Sealing Association
FCI	Fluid Controls Institute
FSA	Fluid Sealing Association
FEM	Finite Element Method
FG	Flexible Graphite
LVDT	Linear Variable Differential Transformer
PTFE	Polytetrafluoroethylene
PVP	Pressure Vessel and Piping
PVT	Pressure Vessel Technology
ROTT	Room temperature Operational Tightness Test
UPR	Universal Packing Rig
VDI	The Association of German Engineers (In German)
VOC	Volatile Organic Compounds

LIST OF UNITS

MASS

kg	Kilogram

MASS RATE

ppm	Parts per million
mg/s	Milligram per second
ml/s	Milliliters per second

Length/Displacement

m	Meter
mm	milimeters
μs	Micro strain
inch	Inches

TEMPERATURE

C	Centigrade
F	Fahrenheit
K	Kelvin

TIME

S	Second
H	Hours

Pressure/Stress

MPa	Mega Pascal
bars	Bars (0.1 MPa)
psi	Pounds per square inches

INTRODUCTION

The purpose of studying fluid flow through porous materials is fundamental to predict the penetration of gases and liquids in many multidisciplinary engineering component applications. Micro-electro-mechanical systems (MEMS), gas extraction from shale reservoirs, artificial organs, sealing of bolted joints and valves, porous membranes and filters constitute a few of many examples that can be cited. Another significant challenge often faced is the prediction of the leak rate through packing rings when designing valves. With the ubiquitous increase in the environmental regulations and safety protection laws on fugitive emissions, it is becoming an urgent matter to develop and implement leakage tightness based-design methods for packed stuffing boxes, as was done for bolted flange gasketed joints in North America, Europe and Japan. Although a variety of valves exists in the industry, their external sealing mechanisms are composed of almost the same components as illustrated in Figure 0.1, as valves are generally designed to seal internally and externally.

The internal sealing is related to the control of the fluid flow, including the shut-off mechanism. The external sealing, on the other hand, is related to stem sealing and is achieved using packing seals to prevent fluid escape to the outside threshold of the valve system. This thesis focuses on the stem sealing and investigates the tightness behavior of packing rings in stuffing boxes. However, there are many parameters that can control the leakage performance of valves such as: the packing rings material, the amount of radial contact pressures between the packing rings and contact surfaces and the type of liquid or gas that is controlled by the valve. The main criterion for the selection of a compression packing seal is its capacity to produce a minimum allowable leakage rate. Therefore, the optimal use of packing seals in valves, to produce a minimum leak, can be achieved through an adequate design scheme, a suitable material selection and a proper installation procedure. This study will shed light on two major hypotheses: the leak prediction and the leak quantity in packed stuffing box and bolted flange joints. First, we will explain the packed stuffing box system, and then we will present the bolted flange joints system. A packed stuffing box consists of a specific number of packing rings, which are inserted into an annular space between the stem and the housing. The general

working principle of packing seals can be explained as follows: referring to Figure 0.2, the packing rings are compressed downward by the gland, using the studs and nuts, to produce an axial stress and renders them tight. The applied axial stress induces a radial compression of the rings, creating a lateral contact pressure in the interface between the stuffing box and the stem, which generates a perfect seal. Figure 0.2 shows the location of a packed stuffing box in a gate valve.
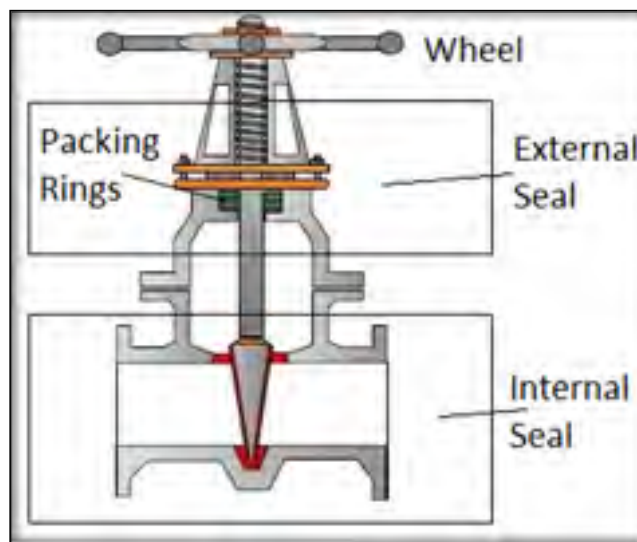
Figure 0.1 Valves Sealing Details
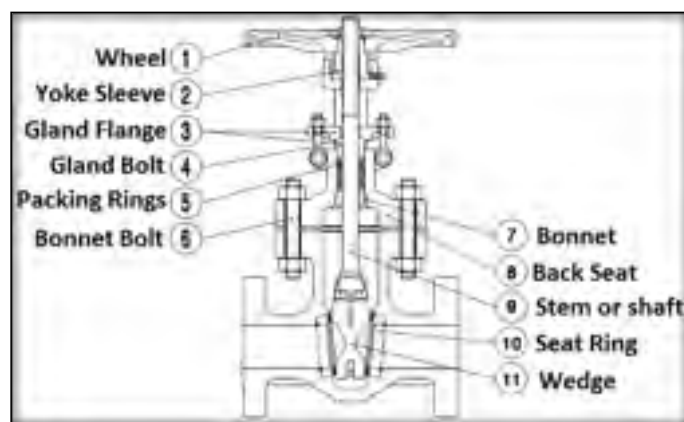
Figure 0.2 Gate valve details

In addition, the packing rings are axially compressed by a gland to create lateral contact pressure with the stem and housing, confining the pressurized fluid and preventing it from escaping to the outer boundary. It is crucial for the packed stuffing box to maintain a threshold amount of contact pressure during the entire service operation of the valve. Valves are used to control fluids circulations in nuclear, chemical and petrochemical process plants. Due to various environments, fluid systems, and system conditions, in which flows must be controlled, a vast amount of diversified designs for valves has been developed. They are designed to carry out two primary sealing duties: the control of the fluid flow in pipes (including shut-off mechanism), and the prevention of fluid leakage. They have a major role in terms of fluid process control and safety in industrial plants (Bartonicek et al., 2001).

Despite the wide use of packed stuffing boxes to seal valves, there are no criteria for their design, no standard test procedures to qualify packing ring leakage and no methodology to determine the required number of packing rings needed for a specific application. Therefore, the choice of a valve to compress packing to prevent stem leakage is made by trial and error. Packing rings must be properly compressed to prevent displacements, escapes of the fluids to the outer boundary and damages to the valve stem. If packing rings are not properly tightened, the valve may leak causing significant safety hazard. If packing rings are too tight, it impairs movement and possibly increases the risks of damages of the stem. From this standpoint, it is important to optimize the tightening of the packing rings based on the *EPA* compliance and the maximum allowable leak rate, while ensuring durability and minimum maintenance.

There are two types of leaks of packing rings and gaskets. The first type is the porous leak that takes place through the packing material, depending on the level of porosity of the material. The second type is the surface leak that occurs at the interface between the packing material and the housing or stem. These two types of leaks are highly difficult to measure or predict separately and their relative proportion depends on the level of the gland stress. Therefore, the developed analytical models related to packing leakage prediction available in the literature do not consider interfacial surface leaks and the leakage flow taking place through the porous structure. From the design viewpoint, stem surface finishes are actually smooth to avoid flow

through serrations and softer packing materials sufficiently seat at low stresses. However, according to (Masi, Bouzid et Derenne, 1998) the *EPA* regulation imposing the 500 ppm leakage limit, is a level that is difficult to comply with and a high stress is often required.

Packed stuffing-boxes in valve applications

The packed stuffing box is an imperative sealing solution for valves to prevent fluids leakage and ensure their safe operation. Most valves use packing seals to prevent stem leakage to the outer boundary. Valve packing rings must be properly compressed to prevent fluid escapes to the outer boundary and damages to the valve stem. Leakage through packed stuffing boxes in valves is a considerable challenge, because there are no standard design procedures that can be used. It is important to optimize their design, while minimizing the leak rate by selecting appropriate packing materials, conducting proper installation and applying adequate gland stress. Figure 0.3 shows a packed stuffing box with all the details. The selection of packing rings for a valve must be done by considering the relevant parameters divided into categories, as shown in table 0.1.

Table 0.1 Packing rings parameters

Major Parameters	Minor Parameters
Temperature of process fluid	Sealing performance
Characteristics of fluid	Low friction
Working pressure	wide range of use

There is a significant lack of data concerning the mechanical properties of packing seals and their behavior under different experimental conditions. In fact, there is no standard procedure to characterize packing seal leakage under different conditions of internal pressure and gland stress. It is only recently that *API 622* standard was developed to test the performance of packing ring under specific conditions. To solve this issue, a methodology, using a robust strategy, was developed to achieve reliable results. A comprehensive study of the literature on packed stuffing box sealing systems in valves has been carried out and used as the basis for the development and the design of a new test rig for packing seals. As a start, leak rate tests

under different working conditions such as temperatures, materials, fluid mediums, pressures and compression levels, are to be conducted experimentally to both investigate the mechanical behavior and the leakage prediction of packing seals.
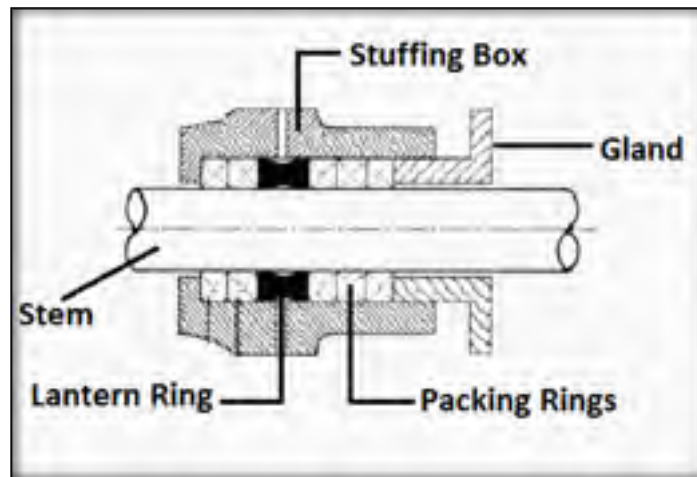
Figure 0.3 Packing seal and stuffing
box in gate valve

Packing seals

Compression packing is the sealing element used inside a stuffing box to seal the valve stem as the stem slides up and down and turns through it. Compression packing rings are the most common valve stem seal used in the industry, because they provide cost effective sealing, even in critical applications. A packing ring is usually defined as a sealing component, which prevents leaks from passing between the stem and the valve bonnet, when pressurized fluids (liquid, vapor or gas) circulate through the valves. The compression yarned packing rings are the simplest and the most common type of packing seal.

The packing rings require to be compressed volumetrically using an external force, typically achieved by a packing gland. The axial force generates a radial force to create a perfect seal. Packing rings usually have a square cross section. However, V-packing or chevron packing are also used, because they require a low external force to generate higher radial forces to produce the seal. An increase in the pressure inlet also increases the force at the sealing edge of the

packing ring. As demonstrated in Figure 0.4, packing rings can be made of various materials: flexible graphite, carbon fiber, inorganic fiber, PTFE (Teflon) and metalloid-plastic, to name a few.

Figure 0.4 Packing ring a) PTFE b) Flexible graphite

Type of packing materials

Although packing materials are numerous and can vary from soft to relatively rigid materials or a combination of both, there are two types of packing materials that will be tested in the development of this thesis:

1. Polytetrafluoroethylene (PTFE)

Because of its mechanical properties, PTFE (polytetrafluoroethylene) is a valuable material to use in the fabrication of packing rings, PTFE-based packing rings have a superior resistance to chemical reactions and a remarkably low permeation and friction coefficient. Due to these properties, PTFE materials are widely used in industrial valve sealing applications.

2. Flexible graphite (FG)

Flexible graphite yarn packing is mainly made from exfoliated high purity crystalline mineral graphite. In general, this type of material maintains all characteristics of mineral graphite such as: chemical resistance, resilience, lubrication and thermal conductivity. Flexible Graphite is a

favorable sealing material for gaskets and a valuable option for compression packing applications, operating at high temperature.

Functions of packing seals

The functions of packing seals in valves are to:
- Control the fluid flow to a preferred location;
- Prevent the escape of fluids;
- Minimize contamination;
- Prevent the ingress of dirt;
- Prevent fugitive emissions.

Bolted flange joints

The reduction of fugitive emissions is an extensive operation to preserve the environment, and even the humankind. However, there are two types of emissions created from industrial factories. The first type is generated by the industrial processes and applications. The second type (considered as undesirable) is produced by leakage of faulty equipment, requiring tightness compliance. Bolted flange joints are frequently used in different industrial applications, specifically for connecting pressure vessels and piping systems together. These pressurized systems contain distinctive type of fluids operating at different pressures and temperatures. The design of bolted joints is conducted according to the *ASME Boiler and Pressure Vessel Code in North America*. Several other codes exist worldwide, in the design of bolted flange joints, such as the *BS5500 JIS* and the *European standard EN 1591*. In the design of bolted flange joints, the structural integrity and the leakage tightness are the two design criteria that must be satisfied.

The bolted joints, with gaskets is an application used in most industrial fields. However, this study will have a limited part in explaining the types of leaks that exist in the static sealing of bolted joints, under different conditions and in the none-relative movement, between the contact surfaces of the bolted joints. Bolted joints with gaskets ensure the confinement of a

pressurized fluid within the joints. The mechanical properties of the flanges of a bolted joint with gaskets are imperative in leak rates performances.

As mentioned above, the discussion or identification of the numerous factors, affecting the leak rates measurements (interfacial and permeation leak) as shown in figure 0.5, are limited in this study. This extensive analysis can be achieved through an experimental approach with different applied pressures and compression stresses. The main idea is to characterize the leakage behavior of gaskets in bolted joints. To prevent leakage in bolted joints assemblies, flanges are designed so that the minimum gasket stress is adequate to seal the joints tightly. Also, during pre-load process it is primordial to verify that the bolt stresses do not exceed the allowable limits.
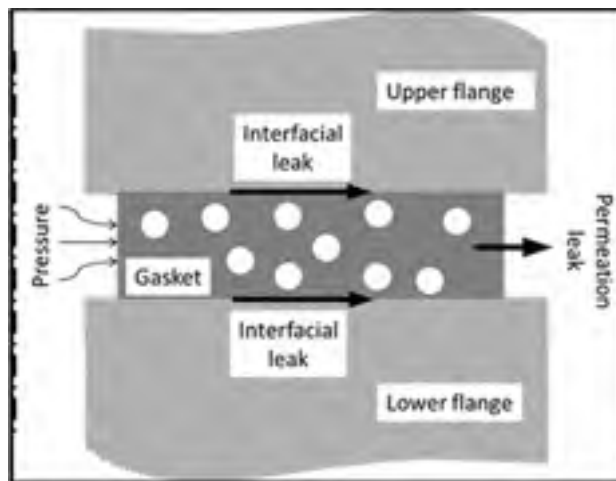
Figure 0.5 Flanges assembly with gasket

Gaskets

A gasket is the main part (core) of a bolted joint assembly. The function of a gasket is to create and maintain a static seal between two flanges. Gaskets are designed to contain various types of fluids (compressible and incompressible). The gasket should sustain a high contact pressure to keep the joint leak-free, even under extreme conditions.

Gaskets can be classified into three categories: soft non-metallic, semi-metallic and metallic gaskets.

1. Soft non-metallic gaskets are cut from sheet materials made of compressed fibre, flexible graphite, PTFE, etc…;

2. Semi-metallic gaskets are made with a combination of a metallic core and a soft material sealing element. Spiral wound, Corrugated metals and double jacketed belong to this category;

3. Metallic gaskets are made out of ring metals such as aluminum, copper and steel and include API ring joints, lens rings and rings in general.

The knowledge of the material properties is a vital requirement for the analysis of any structural system component. The strength and rigidity of a material are two aspects needed for fabrication of a product and sealing materials are no exception. These material properties are often described adequately by the stress versus strain for any kind of material. In this thesis, however, the focus will be on non-metallic gaskets.
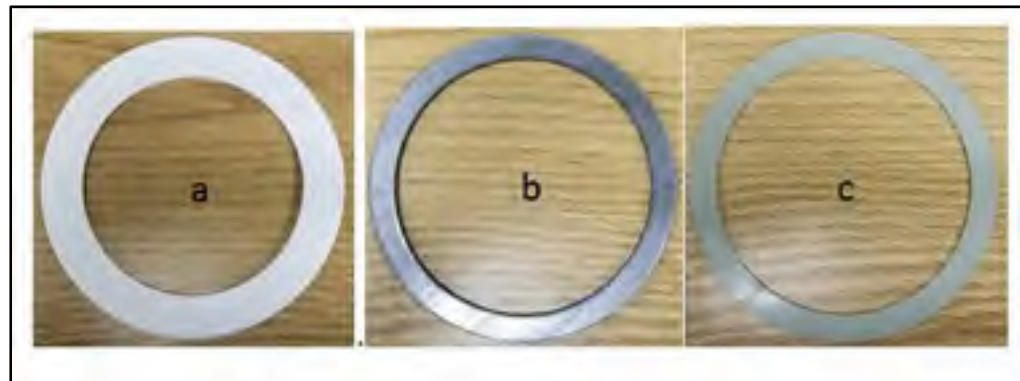
Figure 0.6 Gaskets a) PTFE b) Flexible graphite c) Compressed fibre

For the soft non-metallic gaskets, the three materials shown in figure 0.6 above are part of this investigation have good sealing properties and are often used in bolted flange connections.

PTFE (polytetrafluoroethylene) gaskets are made of a chemically stable material, and therefore are a key example for chemical resistance. In addition, they are used in applications that require high leak and corrosive resistance.

Graphite gaskets are perfect for high temperature and pressure applications. They offer a decent aging and creep resistance. These kinds of gasket are designed to produce an adequate seal for bolted joints exposed to high temperatures.

Compressed fibre non-asbestos provides an excellent capacity to seal at high temperature, retain load and to resist heat and are a good alternative to asbestos. These gaskets are manufactured to perform applications involving air, water, steam and most chemicals fluids.

Fugitive emissions and industrial impact

The constraints and limits documented by the standards developed by the industry, point to the reduction of the amount of fugitive dangerous gases and liquids because of the growing concerns people have for the environment and the humans. Furthermore, this assertion is very much applicable to the issue of climate change, which is one of the most critical environmental concerns. Scientific studies discovered that global warming is attributed predominantly to human endeavors. Considering the overall debate on the amount of hazardous pollutants in the atmosphere and their damages to the environment, stricter regulations on fugitive emissions are currently being legislated.

Recently, in order to adjust the quality of the industries to these regulations, quite a few experimental, numerical and theoretical studies have been conducted to characterize the gas and liquid leak rate through the packing seal in valves at room and high temperatures. The current research project is within the scope of the continuity and ongoing work currently in place, to ensure leakage reduction in the involved applications. The development of a model to predict the actual behavior of packed stuffing boxes at room temperatures is therefore necessary. This work development could be used as a mean to improve valve safety, to predict their behavior and to prevent their leakage failure during service. Therefore, this study can be

extended to examine how to minimize problems related to fugitive emissions and how to avoid possible accidents. Presently, the major concerns for end users of valves are financial losses and pollution through hazardous emissions.

This thesis contributes to the development of leak prediction methodologies by means of characterization tests of packing seals. Particular attention is paid to the future implementation of the methodology in the design of stuffing boxes and the development of leak prediction models that can be used to optimize the sealing performance of their applications. In addition, the results obtained can be used to minimize fugitive emissions in the chemical and petrochemical sectors of Canadian industries. The impact from this research can offer assistance to joint manufacturers in the development, assessment and certification of their products. Having improved leak predictions models, will improved the level of production, and reduced downtime, and maintenance and prevention costs. However, the selection and the proper use of packing seals in valves should be considered as part of an environmental responsibility by protecting the environment from contamination and fugitive emissions. According to the *ESA*, fugitive emissions from European refineries are estimated to be higher than 10,000 tons per year and an estimated of 300,000 tons per year is produced by US power plants. From the mentioned amount of emissions, about 50 to 60 percent are attributed to leakage from valves (Bayreuther, 2012) as shown in figure 0.7.

The *API 622* is considered as a standard test procedure with an arrangement for monitoring leakage from a packed stuffing box. The objectives of the *API 622* are to promote the continuation of operations of compression packing rings, for at least three years, the increase of operational reliability, and the simplification of the maintenance. The standard test procedure gives an indication of the quantity of leak rate expected but does not yet allow the prediction of a leak under specific operating conditions. More investigations through research are required for this aspect (API-622, 2011). The *API 622* standards consider that valve packing leakage may be affected by different operating conditions such as temperatures, pressures and types of gases. Therefore, in order to improve the sealing performance of packed stuffing boxes, it is essential to study their leakage behavior under the influence of these

parameters. The contribution of other parameters, such as contact pressure, lubrication, surface finish, material type, housing and stem are also, not known. It is with a lot of interest that this work will contribute to the understanding of the leakage behavior of stuffing packing boxes under different operating conditions including pressure, compression stress and types of fluids based on real industrial needs.
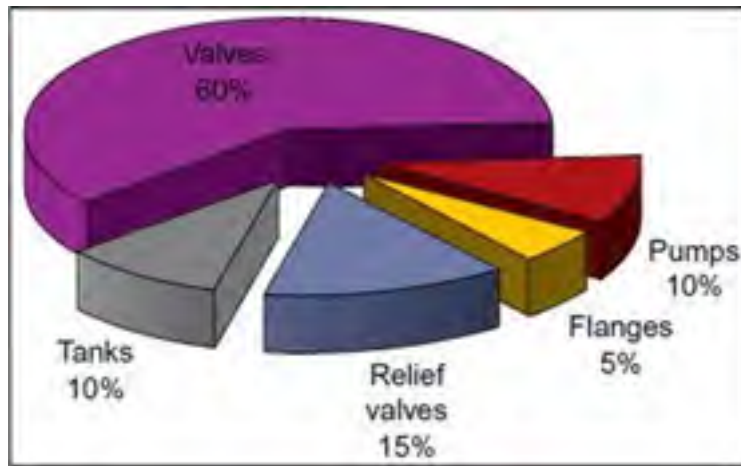
Figure 0.7 Percentage of fugitive emission from refineries (EPA)

Problem definition

Considering the need of sealing development for valves and pumps and specifically in a packed stuffing-box, the development of a comprehensive leakage test program is a considerable challenge. The need for a proper understanding of the different properties of common packing materials is fundamental. For example; gland stress, pressure levels, fluid media, lateral pressure coefficients, friction, surface finish, tolerances, wears and tightness have significant impacts on the sealing performance of compression packing.

The flow of a fluid through porous media has been studied intensively by several research laboratories. It has been the subject of a number of theoretical and numerical models, with less attention to practical experimentation and sealing materials. Based on previous studies, the leakage failure of valves is related to the effects of type of fluids and predictions, which are not considered in the design of packed stuffing boxes.

The challenges to overcome for the designers and end users are listed below:

- First, there is no clear procedure or specific steps to follow for testing packing rings in stuffing boxes. Furthermore, there are no enumerated experimental test conditions for packing rings for specific applications such as those of high pressure and high temperature.

- Second, there is no standard calculation procedure or code used for the design of packed stuffing boxes. Among the inadequate existing models or documentation proposed in the literature, none considers the effect of load, pressure, or type of fluid on the leakage behavior. The quantification of porous and interfacial leak between contact surfaces are not addressed.

- Third, while the development of new packing ring materials and their compliance with new EPA and other international regulation on fugitive emission is of actuality, the qualification tools are not available. Although gaskets and compression packing are sealing elements, there is a big gap between their respective qualification technologies.

- Fourth, the experimental results obtained on packing materials have not been reproduced analytically or numerically because of the lack of data on the packing material properties.

- Fifth, the design of a test rig, to measure these properties, is costly, difficult to achieve, and not straightforward to orchestrate, especially for liquid leaks.

CHAPITRE 1

LITERATURE REVIEW

1.1 Introduction

A handful of studies have been conducted on the prediction of leak rates and the characterisation of mechanical properties of packing seals, at both room and high temperature. The existing studies focus on the following three fundamental aspects: experimental, analytical and numerical (Finite Element).

This chapter is divided into eight sections. The first section is the general introduction, the second section is related to the description of existing standards, criteria and documented codes related to packed stuffing boxes. The third section is a review of the literature on experimental investigations of packed stuffing boxes and existing test rigs. The fourth section is a presentation of numerical models of fluid flow through seals. The fifth section is a discussion on existing analytical models used to predict the leak rates through porous materials. The sixth section is an introduction to compressible flow regimes. Section seven is a note on incompressible flows. The last section presents the thesis objectives.

1.2 Standards and codes on packed stuffing boxes

Few researchers have addressed the design of packed stuffing boxes of valves in details. It is worth noting that there is no specific standard design procedure currently available for the design engineers, end users or manufacturers who deal with packed stuffing boxes for valves.

Despite a great enhancement in sealing technology, there are no specific ASTM like standard test procedures or codes design procedure for packed stuffing boxes. Sealing elements such as compression packing of valves shown in figure 1.1 play an important role in preventing fluid escape to the valve outer boundary and in preventing fugitive emissions to the environment. The new *EPA* rules on fugitive emissions and the new equipment sealing regulations are

serious requirements that the petrochemical industries have to conform with. Jim Drago (June 2010) presented a study on volatile emissions caused by valve stem packing leaks and concluded that a lot of research is required to improve the design of packed stuffing boxes. A study on equipment requiring fugitive emission conformity showed that 60% of volatile organic compounds (VOCs) and hazardous air pollutants (HAPs) released by the chemical process industries (CPI) comes from valves. Therefore, to reduce fugitive emissions of valves, standard test procedures to certify compression packing and design procedure of packed stuffing boxes are essential. Due to the environmental protection and the strict legislation on fugitive emissions, several standard codes, regarding leakage rates of valves, have recently been introduced. However, no specific design methodology for valves have been proposed. The initiative to develop new standards is pressing for the environmental protection and health safety.
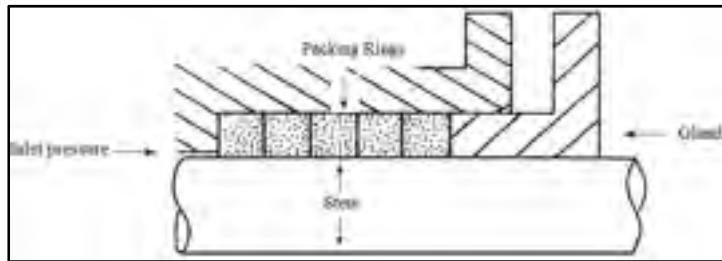
Figure 1.1 Stem packing valve assembly

In North America, manufacturers need to abide by the *EPA*'s strict regulations especially towards the fugitive emission restrictions. The valve production must be qualified and certificated by the *EPA*. Valve stem packing assemblies are considered as the main source of fugitive emissions. Therefore, it is necessary to develop new standards related to the design and the testing of valve stem packing assemblies. Standard organizations have implemented a number of standards to qualify valves and packing with low-emission, such as *ANSI/ISA-93.00.01-1999, VDI 2440, Shell MESC SPE 77/312* and *Environmental Protection Agency (EPA) Method 21*(Luft, 2007).

A standard test procedure for valves has been issued by the *American National Standard Institute (ANSI/ISA-93.00.01-1999)*. It is entitled "standard method for evaluation of external leakage of manual and automated on-off valves". This standard involves the classification of valve designs and the delivery methods for testing valve stems and body seals. However, this standard does not deal with the production testing and the quality control of valves. The scope of this standard is to create a technical procedure assuring that manual and automated on-off valves are tested using specific methods. The compliance with volatile organic compounds (VOC) based on fugitive emissions restrictions is also covered. The test conditions related to this standard are as follows:

- The test is repeated, based on the valve classification;
- The tests can be conducted at temperatures of -50 ºC, 25 ºC, 177 ºC and 399 ºC;
- The leak rate limits are specified based on valve classification and are 50 PPM, 100 PPM and 500 PPM.

A standard test procedure for valves entitled "Flexible graphite packing system for rising stem steel valve (design requirements)" has been developed by the Manufacturers Standardization Society of the Valve and Fittings Industry (MSS SP-120 (2017), but now, it is under the American National Standards Institute (ANSI). The scope of this standard is to qualify flexible graphite packing stem sealing in the valves, to achieve low fugitive emissions. In addition, this standard gives dimensions and tolerances of packed stuffing boxes to certify ASME B16.34 type gate, globe, and angle valves designed with rotating/rising and non-rotating/rising stems. These valves use flexible graphite packing, as the first choice material and they include a lantern ring.

Currently, some important standards and test procedures related to valve fugitive emissions are being implemented. Two standards have been adopted recently: *The Measurement Test and Qualification Procedures for Packing, API 622*, and a valve qualification test, *API 624. The International Standards Organization (ISO)* issued *ISO-15848-1 and 2*. These two parts collect a wide range of data from different industries all over the world. (Harrison, 2006) studied *ISO-*

15848 standard with a special focus on industrial valves, fugitive emissions, measurement tests and qualification procedures.

ISO 15848 - Part 1 (2006-2015) entitled "Classification system and qualification procedures for type test of valve assemblies", tests valves using vacuum or siphoning method to evaluate the external leakage of stem packing rings. The test fluids are either helium or methane. The used test rig for Parts 1 and 2 is shown in Figure 1.2 and Figure 1.3. The test leak detection used is as per *EPA* method 21. However, the categorization for stem packing leakage for both helium and methane gases are classified as A, B, C and D, with A being the lowest one, and increasing in alphabetical order. The range of test temperatures is between -196 ºC and 400 ºC. The criteria for the leakage failure is specified by the manufactures (Davis, 2012).

Figure 1.2 Test rig for ISO, (Davis, 2012)

ISO 15848 - Part 2 (2003-2015) entitled "Production acceptance test of valve assemblies, on–off valves", is a guideline for production certification and quality assurance when testing valves. It is a quality assurance test method used at the manufacturer's site to ensure the production quality of the valves tested in part 1. The testing conditions can be briefly described as follow; firstly, the test is implemented at room temperature, secondly, the gas fluid is helium, and thirdly, the pressure test should be applied at 6 bars. Also, the percentage tested of the total produced valves should be mentioned in this document for inspection purpose (Davis, 2012).

The American Petroleum Industries (API) issued few standards (Harrison, 2004) for the testing of process valve packing, for fugitive emissions: the first one is *API-622*, the second one is *API-624*, the third one is *API 623*, and the fourth one is *API 598*. The first edition for the *API-622 (2011)* was issued to cover the testing of valve packing for fugitive emissions only, but currently, it allows testing an entire assembled valve system. The test bench for *API-622* is shown in Figure 1.3. The test requires certain conditions to be followed: firstly, the testing gas should be methane, secondly, the temperature range should start from ambient temperature up to 260 ºC when five thermal cycles are applied, and thirdly, 1510 mechanical cycles related to the opening and closing of the valve should be conducted.

Also, this standard contains packing material corrosion guidelines. It defines the limits of oxidation to be 15 percent in 24 hours as described in the procedure of *FSA-G-604-07*, method B. The leakage failure restriction in this standard is limited to 500 particles per millions (ppm) as in compliance with the *U.S. Environmental Protection Agency*, but an important revision made in leakage restriction in 2011 now limits it to 100 (ppm).

Figure 1.3 Test rig for API-622, (Davis, 2012)

The second *API-624 (2014)* standard is related to the rotation and the translation of the valve stem. A typical test bench for this procedure is shown in figure 1.4. This standard is a comparative test of leak measured using *EPA* method 21. The test uses methane gas and limits the leak to 100 ppm. The temperature range is -29 ºC to 538 ºC. In addition, the test procedure involves 310 mechanical cycles and three thermal cycles. Finally, the packing materials need to be photographed after the valve is disassembled to record any faultiness introduced during the disassembly, such as changes in the surface finish and any reduction in packing thickness.

The third *API-623 (2013)* standard is entitled: "Steel Globe Valves – Flanged and Butt – welding Ends, Bolted Bonnets". This standard covers all types of valves, which are exposed to corrosion, erosion having large stem diameters and heavy wall sections. It should be noted that this standard procedure can be followed after the *API 624* is executed.

The fourth *API-598 (2016)* is entitled "Valve Inspection and Testing". The objective of this standard is to inspect, examine and implement pressure tests, which are required for certain types of valves such as gate, globe, plug, ball, check, and butterfly valves.

Figure 1.4 Test rig for API-624, (Davis, 2012)

In Germany and some other European countries, the *TA-Luft* is the adopted standard procedure for stem sealing (Luft, 2007). The extension of this standard is to decrease the amount of fugitive emissions and to define the allowable leakage limits for different systems such as stuffing box and bolted joints. The inspection regulations are according to *VDI4 2440*.

Finally, it is important to keep in mind the preservation of a good environment, because it is a planetary issue. The weakest link in a valve, is identified as the packing ring. Therefore, the selected packing rings must be able to work under extreme conditions in order to meet environmental regulations. The standards require implementing many efforts to reduce the leak rates from these kinds of rings to achieve a decrease in the fugitive emissions.

1.3 Experimental methods

A deep understanding in the mechanical characterization of stuffing boxes is required, because it promotes the reduction of the packing valve leakage to the minimum level under extreme operating conditions. The experimental investigation of mechanical characteristics of stuffing boxes such as: contact stress distribution, material compression behaviour and lateral pressure coefficient are essential to enhance the performance of the valve system. Chapter 5, will clearly demonstratre that the contact stress distribution in stuffing boxes affects leakage considerably.

1.3.1 Mechanical characteristics of packing seals

Hayashi et Hirasata (1989) developed the experimental test rig shown in figure 1.5 to determine the amount of axial gland load required to get a sufficient lateral contact pressure to seal packing rings. They concluded that the theoretical contact stress is close to the experimental results when the axial gland stress is substantially high. They also discovered that lateral pressure coefficients $K_h = K_s$ and friction coefficients $\mu_h = \mu_s$ when packing width is significantly thin or when the stem diameter is significantly large. As mentioned, the material behaviours of packing rings are important; (Aikin, 1994) focused on the determination of suitable packing rings materials in the nuclear field and established qualification tests to investigate phenomena like: compression strength, chemical behaviour and corrosion.

Veiga, Girão et Cipolatti (2009), conducted experiments to measure several mechanical characteristics such as: load relaxation, axial force transmitted to the bottom end of the stuffing box, stem torque and sealability. They found that when the number of packing rings increases, the friction force increases. The results show a fluctuation in the ability of the materials to transfer the axial force into a radial force. Finally, they established that the load relaxation decreases as the applied gland stress increases.
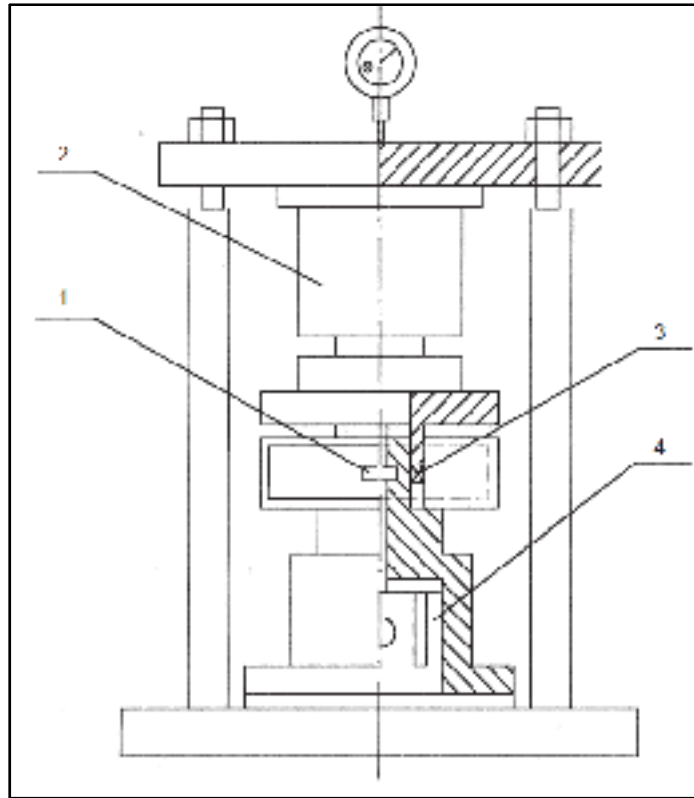
Figure 1.5 Test apparatus designed by (Hayashi et
Hirasata, 1989). 1- Strain gauges, 2- Load Cell, 3-
Packing, 4- Load Cell

Vasse (2009), studied the mechanical properties of compressed expanded graphite (CEG)
packing rings using two methods: experimentation and finite element analysis. Both techniques
are used to estimate the friction force between the stem and the CEG seal material. Vasse
concluded that the mechanical behaviour of CEG packing seals can be represented correctly
by the *Cam Clay model*. The model can be used to evaluate the contact pressure at the interfaces
between the stem, housing and packing rings. The results obtained from FEM are in logical
agreement with experimental results and thus confirm the validity of the developed model.
Diany et Bouzid (2011), studied the mechanical characteristics of packing seals based on
hybrid experimental-numerical techniques to obtain lateral pressure coefficients for two types
of packing materials; Teflon and flexible graphite. They also determined the leak rates for both
packing materials. They concluded that Teflon packing requires a smaller load to seal than
flexible graphite packing. The lateral pressure coefficient of Teflon and flexible graphite were

resulted at 0.62 and 0.87, respectively. In addition, (Diany et Bouzid, 2012) also presented a study on the creep and relaxation behavior of packed stuffing boxes. A constitutive law for creep was developed for different types of braided packing materials (flexible graphite, carbon fiber and PTFE (Teflon)). This work involves a comparison between the three methods of study: analytical, finite element and experimental methods. The analytical approach is based on the equations of viscoelastic materials with time-dependent variables. The finite element approach is used to evaluate the contact pressure between the stem housing and the packing to predict the relaxation that will arise in time. The experimental work is conducted on a test bench that measures the axial gland force and strain deformations, along with the axial length of the housing with 20 strain gauges bounded to the outer surface. The strain measurements, through time, gave an indication on the relaxation behaviour of the stuffing box packing after the application of the gland load. Based on the comparison of the results obtained, the finite element approach was validated. The relaxation is higher for materials having a limited lateral pressure coefficient under room temperature conditions. Zahorulko (2015), determined the surface roughness and the mechanical properties of stuffing box packing made from polytetrafluoroethylene fibrous yarn, through experimental techniques, while a numerical software was used to investigate the effect of surface roughness. The test rig details are shown in figure 1.6 below. He concluded that threaded packing rings have a viscoelastic behavior and the material hardens when the load is increased. The changes of geometric dimensions of the flexible packing inside the slot and the groove are measured to determine the mechanical characteristics of the packing seal.
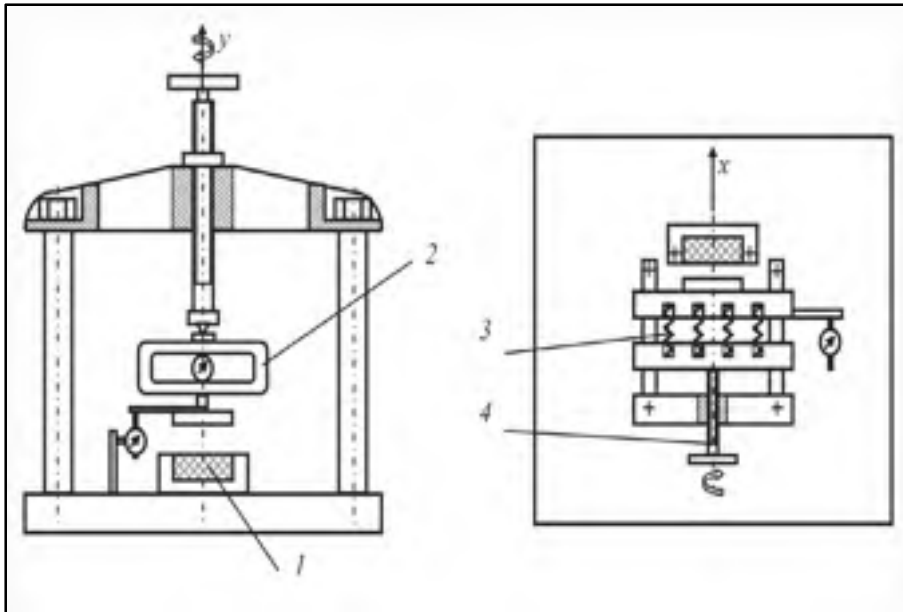
Figure 1.6 The test-rig for determining the mechanical
properties of stuffing box packing front view (a) and top view
(b), [The packing (1), the dynamometer (2), the springs (3)
and the screw (4)].

1.3.2   Leak rates through seals (packing and gasket)

In this part of the literature review, this thesis presents previous studies about leaks through packing and gasket at a micro and a nano level. In general, the amount of leaks through seals varies based on several mechanical and thermodynamic properties. From this standpoint, the most influential factors are the type of the flow regime, fluid (compressible or incompressible), the compression stress, the temperature range, the tolerances and the applied pressure. However, other factors such as surface finish and shape of striations (phonographic) and friction should also be considered.

The major problem in a stuffing box is the leakage through the packing seals. (Thomson, 1961) investigated the leak rate of different yarned packing's and the factors affecting their amount. The results revealed that the leak rate could be reduced when an adequate amount of initial tightening is applied. (Tashiro et Yoshida, Jun 1991) conducted an experimental investigation on two packing seal materials used in packed stuffing boxes. These are; asbestos and flexible

graphite. The experiment was conducted with incompressible fluid (water); the main purpose from this work was to investigate the factors affecting leak rates, such as: the level of compression stress, the number of packing rings and the fluid pressure. Pogodin et al. (1995) carried an experimental investigation based on a test bench with a real industrial valve. The experiment was executed under extreme conditions of high pressures and high temperatures. The leak rates remained constant for flexible graphite materials under the various conditions, while it varied drastically with asbestos, under the same conditions. Schaaf et al. (2005a) experimentally tested a new nowoven material of packing rings. These kinds of materials demonstrated the capibility to sustain high temperatures up to 280 ºC. The main findings of this study were that the amount of leaks did not vary with the change in cross section density as compared to the PTFE and the flexible graphite materials. Thereafter, (Kockelmann et al., 2009) designed a test bench to test different types of packing materials such as flexible graphite and braided PTFE yarn under different types of fluids (liquid and gas). The measurements were conducted at high temperatures. Their focus was to investigate the effect of radial stress on the leak rate and the effect of the axial stress on the frictional forces between the stem and the packing seal. They found that flexible graphite material has a low leak rate with water and steam, and a high leak rate with air. The braided PTFE yarn has a low frictional force compared to flexible graphite. However, the stem frictional forces for the braided PTFE yarn material are lower with water than with air. In another study, (Ottens et al., 2010) conducted tests on a stem valve packing after applying a special coating material such as graphite adhesive on the valve stem. They concluded that the leak rate value varies, based on the coating material used. Diany et Bouzid (2012) presented a study on the leak rate behavior of packed stuffing boxes. Experimental tests with helium, for different types of braided packing materials such as flexible graphite and PTFE, were conducted. A special test bench that measures the leak rates was designed for this study. Based on the results obtained, the leak rates with PTFE are smaller than that with flexible graphite. The leak rate of two packing seals is higher than four packing seals under the same conditions. Finally, (Kazeminia et Bouzid, 2018) presented an experimental-based methodology to accurately predict and correlate the leak rates through porous braided packing seals.

The leakage performance of a sealing material is affected by two major parameters, which are the load compressive stress and the internal pressure of the fluid. The effect of the internal pressure and the gasket contact stress level on the leakage performance of bolted flange joints was investigated by (Gu, 1999) and (Wang, 2000) using capillary flow models for soft porous gasket materials. In a bolted gasketed joint, there are two types of leaks; the leak through the porous gasket material and the interfacial leak that is produced between the gasket material and the flange contact surfaces. The effect of surface roughness on the gasket leakage behavior is recognized by (Haruyama et al., 2013) when testing gasket with helium gas. The results showed that at the lowest stress level, the change in the load causes a significant change in the leak rate. Finally, (Zhang et al., 2018) conducted an experimental investigation to study the effect of surface finish on fluidic leak rates through sealing materials. The results show that the surface topography has a significant role in leak rate values while fluid pressure has a insignificant role when the amount of leakage is very small.

1.3.3   Porous media modeling and permeability

A porous medium of packing ring with several connected pores (which allows the circulation of the fluids) is called "open porosity". The latter can lead to leaks. The leak performance of a stuffing box varies depending on different parameters such as the size of the pores, the number of channels, the size of the voids and the pressure of the fluids. However, the permeability can be considered as one of the most important features related to leaks through packing rings. Amyx, Bass et Whiting (1960a) measured the permeability phenomenon by investigating the capacity of a porous agent to let a fluid flow through. Permeability is a property used to define the flow capacity in a porous material. Henry Darcy is one of the early scientists who studied this phenomenon. The challenge was to measure the permeability based on physical properties such as the porosity and the grain size. The complexity involved in establishing an analytical relationship between them led to the necessity to evaluate the permeability through an experimental approach.

In 1856, Henry Darcy determined the permeability by measuring the amount of water flowing through sand, which is governed by equation (1.1):

$$Q = -\frac{K\,A}{\mu l}\Delta P$$

(1.1)

Q : Volumetric flow rate;

K : Permeability;

μ : Absolute viscosity;

A : Cross section area;

l : Length;

ΔP : Pressure variation between upstream and downstream.

Klinkenberg, in 1941, found that the permeability measurements are not constant when gases are used as a working vehicle instead of liquids. He discovered that permeability changes with the average pressure change. This led to the development of the following expression for gas permeability:

$$K_g = K_l\left(1 + b/\bar{p}\right)$$

(1.2)

K_g : Apparent permeability of porous medium obtained from gas flow tests;

K_ℓ : Absolute permeability of the medium;

$\bar{p}$: Average of the upstream and downstream pressures of the fluid measured in atmospheres;

b : Klinkenberg's coefficient, a constant for a specific gas in a specific porous medium.

This apparent permeability is dependent on the pore size of the porous material and the type of gas used. Klinkenberg's coefficient can be calculated from the slope of equation (1.2).

Hellström et Lundström (2006) proved that Darcy law can be used in leak prediction in applications with flow passing through seals with a low Reynold number. Lv et al. (2013) studied the effect of slippage in laboratory and in source gas production. They investigated the differences between Klinkenberg's corrected permeability and apparent permeability, in tight gas sands, through experimental measurements.

Kazeminia et Bouzid (2015) presented an experimental-based methodology to accurately predict and correlate the leak rates through porous braided packing seals. Their approach is based on the Darcy-Klinkenberg model with an effective diffusion. The leak rates for different gases (helium, nitrogen and argon) were measured experimentally. Helium was used as a reference gas and the leak rate measurements were used to characterize the porosity parameters of the packing ring. The modified Darcy's equation used by the authors is presented below:

$$\nabla P = - \frac{\mu}{K_\infty} V + \rho \, D_{eff} V \tag{1.3}$$

∇P : Variation in the pressures;

μ : Viscosity;

K_∞ : Intrinsic permeability;

ρ : Density;

D_{eff} : Effective diffusion;

V : Velocity.

Figure 1.7 shows the predictions of helium gas leak rates based on the modified Darcy's approach. They concluded that, based on the comparison between the predicted and the measured leak rates, the modified Darcy model is robust for the range of leak rates measured as shown in figure 1.7. The developed methodology is a valuable approach to assert the porosity and the diffusivity of the parameters under the conditions in which the developed equations are functions of stress, pressure and type of gas.
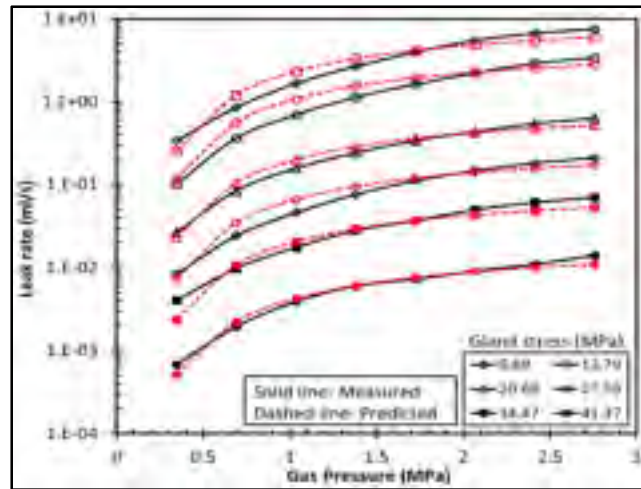
Figure 1.7 Measured and predicted leak rate
with helium (Kazeminia et Bouzid, 2015)
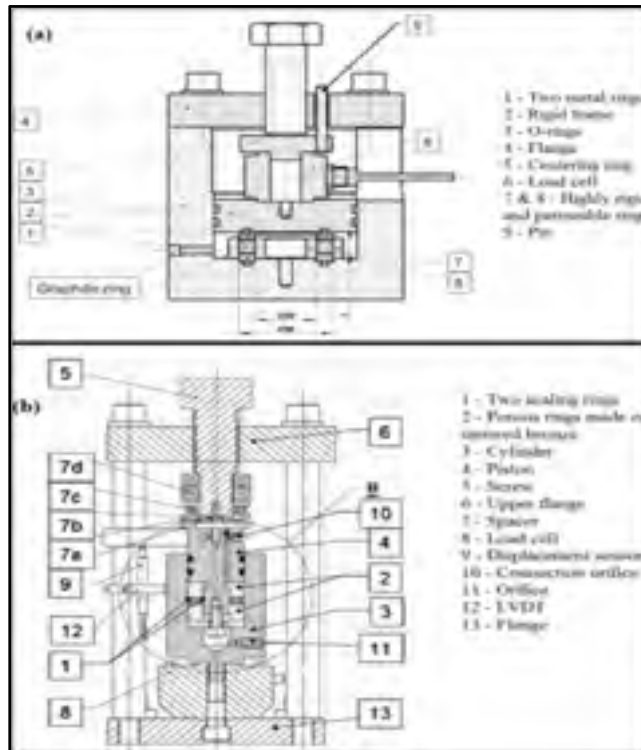
Figure 1.8 Test rigs used to determine the
(a) radial and, (b) axial permeability and
Klinkenberg's effect (Lasseux et al., 2011)

Lasseux et al. (2011) studied the specification of permeability for die-formed exfoliated graphite packing. They also measured the total leak rate during experimental tests, in order to evaluate permeability and Klinkenberg's coefficients in the radial and axial directions. The experimental test rig details are shown in figure 1.8. In the axial direction, if the stress is doubled, the permeability decreases by a factor close to 2, when the Klinkenberg factor value in the radial direction is higher than 1. Furthermore, in the radial direction, when the axial compression stress is increased by a factor of 2, the permeability decreased by a factor of 2.

1.4   Numerical approaches

Gaft, Krivonogov et Petushkov (1989) studied the actual contact zone between packing rings and the stem using FEM. A comparison between the experimental and the numerical approach was performed. The contact pressure calculations used to analyze the functioning of a packing ring were coherent with the experimental results. Adler, Jacquin et Quiblier (1990b) conducted an experimental test on Fontainebleau sandstones (porous medium) to characterize the permeability and the pore size parameters. Furthermore, they also attempted to construct a new simulation for porous medium for the material. Their model is based on a three-dimensional random porous channel, with a given porosity and a given correlation function. They concluded that there is a basic difference between the numerical model and the real experiment test results. Their simulation model was inherently flawed; the average statistical properties of the samples behaved in different ways with the two approaches. Also, the parameters used in the model were too scarce and too insufficient. Gauvin et al. (1996) investigated the accuracy of permeability values for several reinforcements and for mold filling simulations. They were able to validate the results obtained from the simulations by comparing them with the experimental measurements of permeability. They observed a significant difference between the two approaches. Theses are explained by a variety of different raisons: nature of the fluid, pressure and cavity stiffness. Nield et Bejan (1999b) studied the effect of porous medium properties and inlet velocity on the pressure drop, mass flowrate and cross-sectional average velocity at the center of a porous medium zone. They gave a comparison between mathematical and simulation (CFD) results. Based on the results obtained, the model developed with CFD

is found to be consistent with the theoretical results. The prediction of the permeability of tangible porous medium is a long-term problem for imperative practical purposes. Determining permeability is arduous for many reasons. It is indeed difficult to describe the porous medium in a realistic manner. Also, it is a challenging task to apply the solution of flow field, because it can only be done through numerical techniques. Ljung, LUNDSTRÖM et Tano (2006) developed a new model for the dry zone of a travelling grate pelletizing plant. They focused on modeling the velocity and the temperature distribution in the up-draught drying zone through CFX. The velocity distribution is described by the equation of fluid dynamics in a porous medium, while heat transfer (convection) requires two energy equations, since the porous agent region contains both fluid and solid phases. Their simulation shows reasonable convergence for the models of both phenomena. Dongari et Agrawal (2012) developed a new model based on Navier–Stokes equations, with the second order slip boundary condition of high Knudsen numbers, by incorporating the Knudsen diffusion phenomenon in rarefied gases. Their analytical model is based on fixed values of slip coefficients for rectangular and circular capillary shapes. The authors made the comparison between experimental and simulation results for the following parameters: the pressure and the thermal drive of rarefied gas. The simulation results of Boltzmann equations solved using the DSMC method agreed well with the experimental data without requiring any tuning of the slip coefficients. Burnett equations are principally used for higher values of the Knudsen number. Finally, The Computational Fluid Dynamics (CFD) study used by (Tahir, Hallström et Åkermo, 2014) investigates the effect of various parameters of a two-dimensional dual scale fibrous structure model on the overall permeability of packing rings. The difference of the permeability between solid and porous is about 5% to 6%, which indicates a coherence in the results. All references above were useful to establish the basic conception for simulation data on the packing rings as may be seen in the forthcoming chapter.

1.5 Analytical approaches

The first study involving the prediction of leakage through gaskets was done by (Bazergui et Louis, 1987). The gasket material used was asbestos. The flow model describes the porosity

of the gasket material as a set of straight micro capillaries. Nonetheless, the proposed model was limited to a laminar flow regime. The effect of inlet pressure has been studied by (Arkili, 1994); they investigated filtration velocity with slippery boundary conditions using the Navier-Stokes equations. To achieve this, the predicted mass flow rate was compared with the measured flow from the experiments. The latter were conducted with several mass flows through micro channels. Helium was utilized as the reference gas, the inlet pressure ranged from 1.5 to 2.5 atmospheres and the atmospheric pressure conditions were applied at the outlet. From their study, they proposed that slippery perimeters conditions are not an accurate assumption when using substantial Knudsen numbers. Ewart et al. (2006) measured the mass flow rate for a gas flow slip regime via an experimental test, in isothermal steady conditions, through cylindrical micro tubes. The measured values were compared with the results obtained by different approximated analytical solutions based on gas dynamics continuum equations. Through their observation, they concluded that higher Knudsen numbers will deepen the understanding of the reflection/accommodation process at the wall and will extend the awareness of rarefied flows behaviors. Moreover, in a glide regime, the results confirm a significant Kn as a second order effect. Adanhounmè, de Paule Codo et Adomou (2012) proposed the domain decomposition method instead of the nonlinear functional Navier -Stokes equations. They found further continuity with their experiments with the decomposition method. Numerous studies have been conducted on rarefied gas flow in a porous medium. Bahrami, Tamayol et Taheri (2009) developed a model to predict the Poiseuille number of fully developed flow in arbitrary cross sections of micro channels with slip flow regime conditions. They also examined drops in pressures as a function of geometrical parameters. Their model is successfully validated against existing numerical and experimental data from the literature, in which all of the cross sections appear to have an 8% difference. Figure 1.9 shows the shapes of the cross sections featured in this study, specifically: circular, rectangular, trapezoidal, and double-trapezoidal. Agrawal et Dongari (2012) studied Navier-Stokes equations with Knudsen numbers reaching a value of 4. The authors developed an analytical expression and attempted to support it with experimental results.
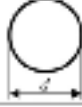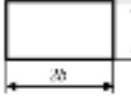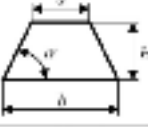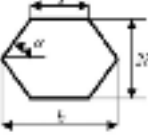
Cross-Section	Area (A)	Perimeter (Γ)	Non-Dimensional Polar Moment of Inertia (I_p^*)	Aspect Ratio (ε)
circle	$\dfrac{\pi d^2}{4}$	πd	$\dfrac{1}{2\pi}$	1
rectangle	$4ab$	$4(a+b)$	$\dfrac{1-\varepsilon^2}{12\varepsilon}$	$\dfrac{a}{b}$
trapezoid	εb^2	$2b\left(a+\sqrt{a^2-\beta\varepsilon^2+1}\right)$	$\dfrac{[\beta\varepsilon^2+2]+\beta[1-3\varepsilon^2]}{3\pi\varepsilon}$	$\dfrac{a+b}{2b}$
hexagon	$2\varepsilon b^2$	$2b\left[\left[2\sqrt{\varepsilon^2-\beta\varepsilon^2+1}\right]+\varepsilon-\dfrac{1}{\tan\alpha}\right]$	$\dfrac{[\beta\varepsilon^2+2]+\beta[1-3\varepsilon^2]}{1\delta\varepsilon}$ $-\dfrac{3}{9\varepsilon}\left(1-\dfrac{1}{\varepsilon\tan\alpha}\right)^2$	$\dfrac{a+b}{2b}$

Figure 1.9 The geometrical characteristics of different
cross sections (Bahrami, Tamayol et Taheri (2009))

The analytical theory rendered these values for slip coefficients: C_1 = 1.3466 and C_2= 0.06, where C_1 is the first-order slip coefficient and C_2 is the second-order slip coefficient. The results from this study indicate that the extension of Navier-Stokes equations for gas flow at the capillary range can reach a Knudsen number of 4.

1.5.1   Leak predictions

(Grine et Bouzid, 2011a) exploited an experimental methodology to estimate the gasket porosity parameters, based on Navier-Stokes equations with first slip flow conditions. The results show a decrease of these parameters as the stress is increased. The diameter of leak paths, the number of micro paths or the void layers depending on the model used decrease with gasket stress. There is a linear relationship between the reciprocal pressure and porosity parameters A1 and A2. The predicted leak rates are anticipated with reasonable accuracy for other gasses over the whole range of Knudsen number. The author used capillary and annular models to predict leaks in gasket sheet materials using equation (1.4) and (1.5) respectively.

$$L = \frac{N\pi R^4 P_o^2 \left(\Pi^2 - 1\right)}{16\mu RT l}\left[1 + 16\frac{2-\sigma}{\sigma}\frac{Kn}{(\Pi+1)}\right] \tag{1.4}$$

$$L = \frac{2N\pi h^3 P_o^2 \left(\Pi^2 - 1\right)}{3\mu RT \ln\frac{r_e}{r_i}}\left[1 + 24\frac{2-\sigma}{\sigma}\frac{Kn}{(\Pi+1)}\right] \tag{1.5}$$

The leak rates for diverse gases are predicted using porosity parameters R and N obtained from experimental tests using helium as a reference gas. Comparisons between the measured and predicted leak rates for different gases (air, argon and nitrogen) were fulfilled. (Grine et Bouzid, 2011b) also treated the prediction of liquid leak rates using a developed model based on Navier-Stokes equations. The authors compared measured and predicted leak rates for different liquids, such as water and kerosene. The prediction was achieved using equation (1.6).

$$L = \frac{NR^4 \pi \rho \left(P_i - P_o\right)}{8\mu l}\left[1 + \frac{4L_s}{R}\right] \tag{1.6}$$

They concluded that the ratio of liquid leak rates depends on the pore size and number, the length of slip in the wall and the pressure variation between the inlet and the outlet. The theoretical liquid leak forecasts are 40–70% higher than the experimental ones. They found that the difference depends on the liquid pressure and the level of stress on the gasket.

(Singh, Dongari et Agrawal, 2014) investigated the accuracy of a new model based on Navier–Stokes equations. They concluded that there is a unity between the experimental results and the analytical solutions obtained.

1.5.2   Stress distribution in valve packing rings

The most critical element in a valve assembly is the compressed braided rings or packing. The packing is compressed axially to produce lateral contact pressure to confine the internal fluid

within the valve body and to prevent it from escaping to the outer boundary. The behavior of packing is outlined by its ability to adhere well to the housing inner surface and the stem outer surface. Many researchers attempted to study the effect of packing material, axial stress and geometrical dimensions on the lateral pressure coefficient K. (Pengyun, Kuangmin et Zongyun, 1997) developed a new theoretical model by observing the relationship between the lateral pressure coefficients K_i (between packing and stem) and K_0 (between packing and housing) in a soft-packed stuffing box seal and obtained their ratio.

$$\frac{K_i}{K_0} = \left(\frac{\mu_0}{\mu_i}\right)\left(1+\frac{2t}{d}\right)\left(\frac{4d+3t}{4d+5t}\right) \tag{1.7}$$

Here, t is the packing width, d is the stem diameter, μ_0 is the coefficient of friction between packing and housing in the axial direction when mounted, μ_i is the coefficient of friction between packing and stem in the axial direction when mounted, K_0 is the coefficient of lateral pressure between packing and housing, and K_i is the coefficient of lateral pressure between packing and stem. The vital highlight from this piece of research is that the theoretical values of the ratio are extremely close to the experimental values. Furthermore, they showed that the ratio between K_0 and K_i is equal to 1 when the packing is narrower or when the stem diameter is larger compared to the width of the packing ring.

Kazeminia et Bouzid (2014a) presented an analytical model used to analyze stress in the different elements of the stuffing box packing. Their analytical approach provides the stress distribution in the packing seal, the stem and the housing. They validated their analytical model by comparing its results to those obtained numerically and experimentally. The experimental tests were based on the assessment of the housing deformation. The numerical FEM model is based on an axisymmetric analysis and the analytical technique is based on thick pressure vessels theory and the theory of beams on elastic foundation. Coherence is observed between the three methods in the evaluation of the stress and strain values.

1.6 Flow regimes (compressible)

Theoretical and applied research in flow, heat, and mass transfer in porous medium has become significant during the past two decades. This is due to the diversified engineering applications, including packing seals. Navier–Stokes equations, based on the continuum approximation, are adequate to model the fluid behavior when the flow is relatively considerable. Continuum approximation shows that the mean free path of the molecules λ of a gas is much more modest than the characteristic length l of the leak path or voids in the porous structure, which leads to low Knudsen number $Kn = \dfrac{\lambda}{l} \ll 1$. However, for a variety of flows, this assumption is not valid when the Knudsen number is within the range of 1. In these flows, the gas is neither completely in the continuum regime nor in the rarefied free molecular flow regime. Therefore, such flows have been categorized as continuum transition or transitional flows. In such cases, the porosity of a packing seal influences the type of flow regime. The type of flow regime is dictated by the Knudsen numbers (Knudsen, 1909b): for values less than 0.001, it is defined as continuum flow regime, for a range between 0.001 and 0.1, the regime is a mixture of continuum and slip flow, for a range between 0.1 and 3, the transitional flow regime predominates, and for values greater than 3, the flow is considered to be in a free molecular regime. Figure 1.10 shows the details for compressible flow regimes. Several parameters can change the value of the Knudsen number. Those parameters demonstrate the type of flow regime in porous medium, such as the inlet gas pressure and type of porous materials. Studies in this domain often apply conditions based on a certain combination of the aforementioned parameters.
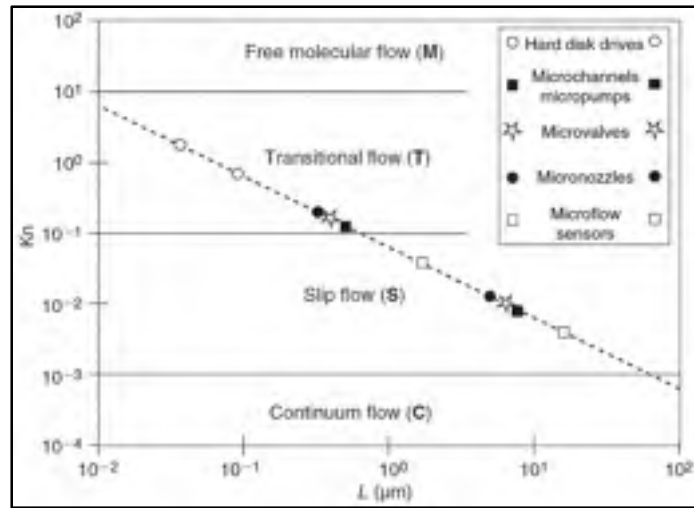
Figure 1.10 Gas flow regimes (Karniadakis,
Beskok et Gad-el-Hak, 2002)

1.6.1 Laminar flow regime

The porous material of a packing ring can be represented by micro capillaries having different size diameter depending on the flow regime. Based on the basic Poiseuille law (Masi, Bouzid et Derenne, 1998), large diameter capillaries have the capability of simulating the gas to flow through the porosity of packing rings at low stress. The viscous laminar flow, in this regime, describes the leak rate through rings, which was derived from the Navier-Stokes equations with no slip condition at the wall except when gas to gas collisions are dominant.

$$L = \frac{\pi N R^4}{16 l} \frac{\left(P_o^2 - P_i^2 \right)}{v^* P^*}$$

(1.8)

1.6.2 Molecular flow regime

The radii of the capillaries are narrow enough to follow Knudsen's law as mentioned in (Masi, Bouzid et Derenne, 1998). In this flow regime, the gas collisions between the molecules are negligible. This flow is dominated by gas to wall collisions. The rate of leakage is proportional to the pressure drop through the length of the capillaries, as given below:

$$L = \frac{8NR^3}{6l}\sqrt{\frac{2\pi M}{RT^*}}\left(P_i - P_o\right)$$

$$(1.9)$$

1.6.3 Intermediate flow regime

According to this flow regime, the porous medium of packing rings consists of a set of micro capillaries with different diameters. Therefore, the flow is mainly considered to be a mix between the laminar and the molecular flow regimes, where the flow is dominated by both gas-wall collisions and gas-gas collisions. The leak rate for this kind of flow regime is given by (Masi, Bouzid et Derenne, 1998):

$$L = \frac{\pi NR^4}{16l}\frac{\left(P_o^2 - P_i^2\right)}{v^* P^*} + \frac{8NR^3}{6l}\sqrt{\frac{2\pi M}{RT^*}}\left(P_i - P_o\right)$$

$$(1.10)$$

1.7 Liquid leak prediction (incompressible)

The liquid micro flow is a singular subject, because few researches have taken the initiative to study it. Based on a surface tension property, the molecules in liquids have uncommon behaviours, because they indicate the interference of the liquid with another fluid. However, for liquids and solids, the contact angle will indicate if the liquid is wet or not. Grine et Bouzid (2011b) predicted the leakage rate for liquids as follows:

$$L = \frac{\pi NR^4}{8\mu l}\left(1 + \frac{4L_s}{R}\right)\left(P_i - P_o\right)$$

$$(1.11)$$

1.8 Objective for this thesis

The main objective of this study is to describe the flow behaviour of compression packing rings made of porous materials and to clarify the complexity of the leakage prediction in stem valve seals. In addition to the above, the methodology to achieve this goal is to determine the porosity parameters from tests with a reference gas at room temperature. The effect of packing

material, surface finish, type of fluid and the different flow regimes (laminar, molecular, intermediate, permeation and interfacial flow) are addressed.

The main objective of this research is to predict gas leaks in packed stuffing boxes at room temperature although liquid leaks are also of consideration. After studying the nature of fluid flow through packing seals, assuming the medium to be porous, attention will be focused on the prediction of leaks in packing rings with several fluids, based on the known behaviour with a reference gas (helium). The experimental test rig is to be modified to study the different flow regimes according to the porosity changes of the packing rings, as a result of mechanical and compressive loads applied by the gland. Finally, this research work will address leakage in compression packing rings with a combination of analytical, experimental and numerical techniques for the purpose understanding packing seal tightness behaviour and meet the requirements of industrial needs.

The sub-objectives are divided into 4 categories. First, to develop analytical models that are capable of predicting leakage through packing rings with liquids and gases. Second, to study the contribution of interfacial leak on sealing systems rely on different experimental conditions. Third, to characterize the porosity parameters of the packing rings for use in the simulation and analytical approaches. Fourth, to validate the results developed from analytical and simulation models with experimental test data.

1.9   Thesis structure

This thesis is presented in six chapters. The first chapter represents a significant literature review on packed stuffing boxes and bolted joints. Also included in this chapter reviews on mechanical properties of packing rings, experimental rigs used in studying the behaviour of fluid flow through porous medium such as packing rings and gaskets, fundamental physical conditions for analytical approaches and numerical simulations in porous medium.

Since this study focuses on analytical models to predict leak rate through packing rings, a verification of these results, through experimental measurements, is conducted. The second

chapter describes the test rig used to produce the results and in particular the test procedure required to characterize the physical parameters under the real conditions. This second chapter details the experimental set-ups and describes the technical procedures for measuring the leak rates though packing rings and gaskets. Tests are performed using the *Universal Packing Rig (UPR)* and the *Room Temperature Tightness Test rig (ROTT)* that accurately reproduces the real leakage behavior of packing rings and gaskets under different stress and pressure conditions.

The third chapter presents diversified analytical models (capillary with second order flow model, diffusion flow model and Ergun model) that predict the leakage of various gases (argon and nitrogen) based on leakage measurements of a reference gas (helium), from which the porosity parameters of the packing seals are characterized. The number and size of the leak paths are established based on leak test for use by the analytical model. The two significant parameters, which affect the leakage prediction, are the compression level and the gas pressure that are applied in the tests at room temperature. This chapter is a copy of the journal paper entitled "Prediction leak rate through valve stem packing in nuclear applications", which was published in the prestigious ASME journal of *Nuclear Engineering and Radiation Science*.

The objective of the fourth chapter is to demonstrate through an experimental technique the contributions of the two different types of leaks: permeation and interfacial leak in both bolted gasketed joints and packed stuffing boxes with helium gas. The amount of the total leak is the summation of the permeation leak through the sealing material and of the interfacial leak generated between the sealing element and the metallic surfaces. Furthermore, this chapter investigates the importance of the pre-compression of packing rings (Teflon and flexible graphite) and gaskets (compressed fiber, Teflon and flexible graphite). This chapter is a copy of the paper entitled "Evaluation of interfacial and permeation leaks in gaskets and compression packing which was also published in the prestigious ASME Journal of *Nuclear Engineering and Radiation Science*.

In the fifth chapter, a comparative study is conducted to predict leaks through soft packing materials with analytical and numerical modeling. The results are compared to the experimental data obtained with different gases (argon, nitrogen and air). The aspiration of

analytical and simulation models is to predict and correlate gaseous leaks under different pressure and stress levels. The analytical prediction is done with a model of fluid flow through capillaries with a varying section and based on Navier-Stokes equations. The simulation modelling is conducted using the Ansys CFX software to estimate the flow through packing rings of different materials using Darcy's law. The porosity parameters are obtained from tests using helium as a reference gas. This chapter is a copy of the paper entitled "Leakage estimate in non-uniformly compressed packing rings", and was submitted in the ASME journal of *Nuclear Engineering and Radiation Science*.

The sixth chapter presents the prediction of leakage using liquids (water and kerosene) and gases (air, nitrogen and argon) as the fluid vehicle. The elaborated analytical model is based on the experimental measurements of micro-gas flows and on the characterization of the internal structure of packing rings. The analytical model for leakage prediction is based on the Navier-Stokes equations. This chapter was shaped in the form of a conference paper entitled "Prediction of liquid and gas leak rates in packed stuffing boxes", which was submitted and accepted for the ASME 2019 *Pressure Vessel and Piping conference*.

This thesis concludes by summarizing the findings and by providing recommendations for future work on packing seal properties under different working conditions.

CHAPITRE 2

EXPERIMENTAL SETUP

2.1   Introduction

This chapter is divided into four sections. The first section is an introduction to the experimentation. The second section deals with the details of the *Universal Packing Rig (UPR)* used to test packing rings. The third section is a concise presentation of the existing *Room Temperature Tightness Test (ROTT)* used to test gaskets. The fourth section handles the presentation of the numerical simulation using Ansys CFX to predict leak rates through packing rings.

In general, the leakage performance of a stuffing box is affected by numerous parameters such as: lateral pressure distribution on stem and housing, type of fluid, applied pressure, porous medium structure, number of packing rings and others (Temperature, aging, corrosion, surface finish, friction, geometry etc….). From this viewpoint, an experimental approach is essential to explore the effects of these parameters on the leakage performance.

The primary function of a packing seal is to create and maintain a seal between the stem and housing in the stuffing box of valves. The ratio between the compression stress and the pressure under different conditions can vary substantially from one assembly to another, depending on the nature and the type of the application that is in cause. In this study, the *UPR* was used for the investigation of the gas and liquid leakage prediction for two types of packing materials specifically, flexible graphite and PTFE. The tests are conducted at room temperature. The *ROTT* was used for the investigation of the nature of the leak in three types of gasket materials, which are flexible graphite, PTFE, and compressed fiber. The tests are also conducted at room temperatures. The goal of this analysis is to validate the theoretical models developed during this research work. The results from these theoretical approaches are thus compared to the experimental results for validation. In order to obtain the experimental results, the two test benches have each a hydraulic tensioner system to apply the load, a gas or liquid pressurization

system to pressurize the sealing element and a sophisticated leak detection system to measure the leakage of the fluid media.

2.2 Universal Packed Rig

The Universal Packing Rig (UPR) which was used in this study, is presented in Figure 2.1. This test rig consists of six parts. The general mechanical assembly #1 simulating a packed stuffing box (stem, gland, packing rings and housing) accommodates up to 6 packing rings of 3/8 of an inch square section for leak detection tests.   A control panel with three major circuits. The first circuit is an electrical board, which supplies power to all instruments and connected to the data acquisition systems and control unit. The second circuit #3 is a pressurizing system, which supplies pressure to the packed stuffing box. The third circuit #2 consists of the leak detection system, which is used to measure leaks with different techniques, depending on the leakage level. The flow meter, the pressure decay, the pressure rise and mass spectrometry are the four methods used in the lab. The pressurization system #3 uses a circuit with four gas bottles (air, helium, argon and nitrogen). These bottles are connected to an electro-pneumatic pressure regulator. The pressure regulator has a PID with a feedback control system connected to the pressure transducer. This system provides the desired level of gas pressure to the packed stuffing box based on the experimental test requirements. The electrical box #4 consists of the electrical circuits from the instrumentation and electrical valves and the power suppliers.

The hydraulic system #5 provides the compressive load on the packing rings, through the gland by a bolt tensioner connected to the stem. This system contains an accumulator, which is used to maintain a constant gland stress on the packing set in the stuffing box. Finally, each system has its own instrumentation to measure the required parameters. These are simultaneously monitored and recorded through a data acquisition system. LabVIEW software acts as an interface program between the data logger and the computer as shown in system 6.
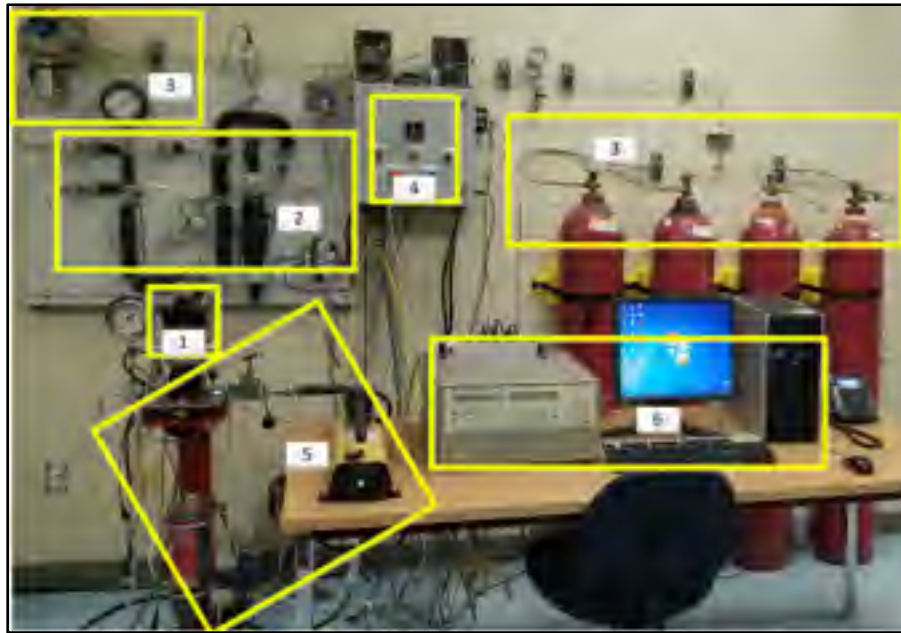
Figure 2.1 Universal Packing Rig test

2.3   Packed stuffing box assembly

The mechanical assembly shown in Figure 2.2 represents a stuffing box at room temperature, which closely mimics the real packed stuffing boxes contained in valves.
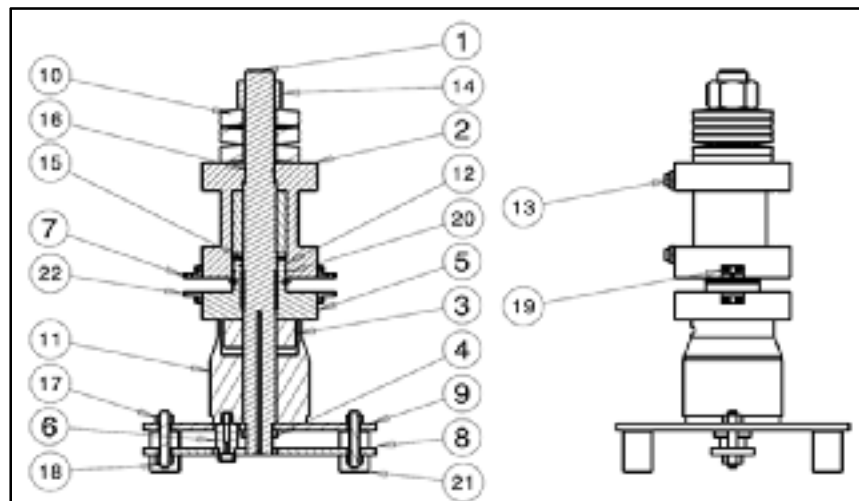
Figure 2.2 Universal Packing Rig with details

In Figure 2.2, the stem is defined as part number 1, and is mainly used to open or close the flow using the wheel. In this study, 3/8 inch diameter of packing rings with a stem of 1-1/8 inch diameter were adopted for all experimental tests. The stem is threaded on both sides (up and down) in order to accommodate the nut on one side and the hydraulic tensioner on the other side. The design of the stem enables the load to be applied through the gland without any additional bolts. Part number 2 is the housing, which contains the packing rings and the stem. Part number 10 is the Belleville washers, which are used as live loads. Part number 13 is the inlet gas pressure. Part number 16 is the circular groove which contains special O-rings which are placed between the stem and housing to confine the leaking gas at room temperature. Part number 15 is the metal ring which is placed between the packing rings and the gland. It is essentially used to distribute the load equally on the packing rings. Part number 5 is the gland which is used to compress the packing rings with the hydraulic tensioner. The hydraulic tensioner is part number 11 and the tensioner nut is part number 3. Parts numbered 19 are the two LVDTs used to measure the axial displacement of the packing rings when compressed as shown in figure 2.3. Parts 22 & 7 are two holders located between the gland and housing and are stabilized by screws.

Figure 2.3 Displacement
measuring system

In order to prevent any circular movements of the stem, when the nut is rotating (part number 14), the stem is fixed by two plates (parts number 9 & 8). Part number 6 is the adapter which is used to connect the high-pressure oil tubing to the manual hydraulic pump and the hydraulic tensioner.

2.4 Fluids and pressure system

The gases used in this study are: helium (He), air, argon (Ar), and nitrogen (N2). In this experiment, the reference gas of choice is helium, because it is a colorless, odorless, tasteless, non-toxic, inert, very stable and monatomic gas, whereas the other gases are used for comparison purposes. The pressurization system in the test bench is optimized, with four gas bottles with different gases connected, to easily deliver the appropriate gas, for the selected experiment. The gas pressure is controlled by a valve fitted with an electronic air operated pressure regulator (PR) and a pressure transducer (PG2) to ensure that a constant gas pressure is supplied to the system. A dial gauge is installed to indicate the pressure that the system is subjected to. For safety purposes, a retention tank, where the gas could be released, was used in case of a wide measured leakage. There is also one Relief Valve (RV) and Manual Valve (MV) installed, to purge the system. The pressurization system details are demonstrated in Figure 2.4. The molecular weight and the mean free path of the four gases used in this experimental study, are presented in table 2.1.

Table 2.1 The physical values of molecular weight and mean free
path of gases

Gas	Molecular weight (g/mol)	Mean free path $(*10^{-10})$
Helium	4.003	17.65
Argon	39.94	6.441
Nitrogen	28.01	6.044
Air	28.97	6.111
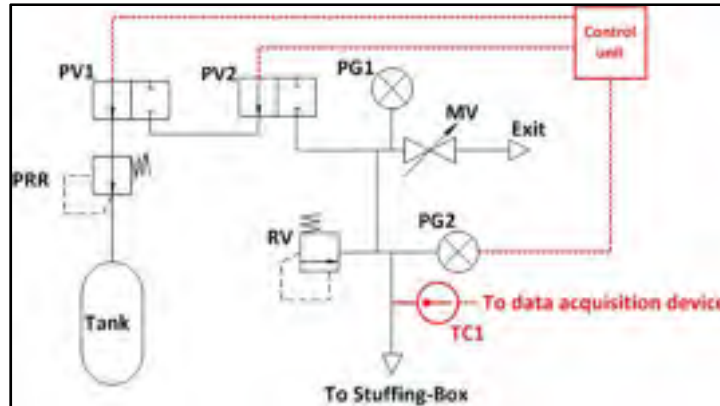
Figure 2.4 Pressurization system details in (UPR)

2.5   Hydraulic system

The compressive load on the gland is applied by the bolt tensioner with a hydraulic system. The hydraulic system is capable of providing a maximum pressure amount of up to 10,000 psi. A manual hydraulic pump is used to apply the desired pressure to the packed stuffing boxes. A hydraulic accumulator is employed to keep the pressure constant during the test. The amount of gland load applied to the system is measured by a Wheatstone bridge strain gauge, which is attached to the stem. Figure 2.5 shows the schematic of the hydraulic system of the Universal Packing Rig.

2.6   Leakage detection techniques

This test bench utilizes five leak detection measuring techniques. The suitable measuring technique was selected in terms of the amount of leak rate produced under the specified conditions. In general, the five leak rate detection techniques are composed of two main categories: the pressure decay technique and the pressure rise technique. The details of each technique are briefly described in the following sections, and the valve sequence for each method is clearly mention in table 2.2.
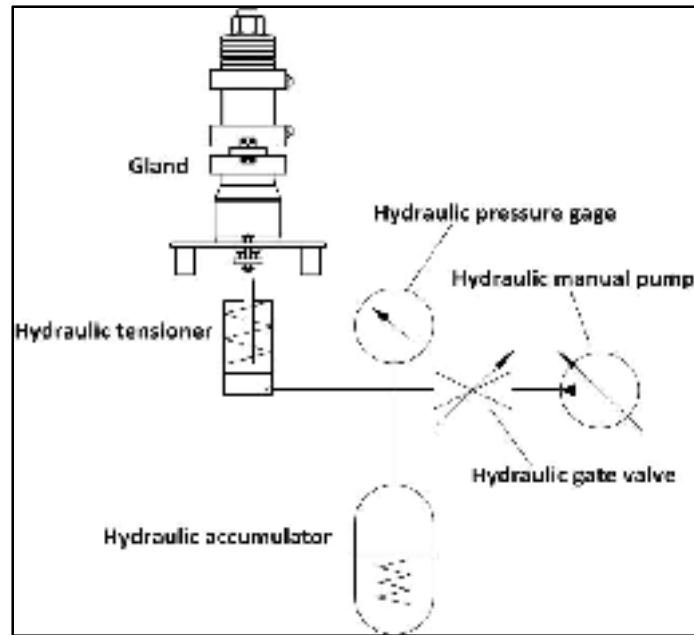
Figure 2.5 Hydraulic system details

Table 2.2 Leaks and the squance of valves (UPR)

Valve Number	V1	V2	V3	V4	V5	V6	V7	V8
Flowmeter	C	C	O	C	C	C	C	O
Pressure Decay leak	C	C	O	C	C	C	O	C
Gross leak	C	C	C	C	C	O	O	C
Small leak	C	C	O	C	C	C	O	O
Spectrometer	C	C	C	O	O	C	O	C

Here, O represents valve Open and C represents valve Closed.

2.6.1 Pressure decay technique

The pressure decay technique was the first noteworthy method. The pressure decay operation is accomplished by filling the system with a desired gas until it reaches the target amount of gas pressure. Then the gas supply is isolated by closing the gas supply valve. The drop of pressure due to leak over time can give the leak rate through the sealing element. The sequence of the valves using this technique is enumerated in table 2.2. Figure 2.6 displays the general

schematic diagram for the pressure decay operation. The variations of pressure and temperature are monitored to calculate the amount of leak rate. The leak rate is calculated with the equation (2.1) using LabVIEW.

$$L = \frac{T_{st}}{P_{st}} \frac{P_v V}{T_v} \left(\frac{1}{P_v} \frac{\partial P}{\partial t} - \frac{1}{T_v} \frac{\partial T}{\partial t} \right)$$

(2.1)

In equation 2.1, T_{st} and P_{st} are the monitored temperature and pressure over time. P_v is the average gas pressure and T_v is the average temperature, where V is the volume of the high pressure side.

2.6.2 Pressure rise method

The pressure rise method is the second relevant method. This approach is the opposite of the previous one mentioned in 2.6.1. A known volume of the leak collection chamber of the UPR is isolated from the gas supply. Then, the gas leak is collected once it passes through the sealing element while the pressure increase and time are monitored continuously. The sequence opening/closing of valves shown in figure 2.7 is given in Table 2.2. The leak rate is calculated based on equation (2.1). The pressure rise technique is divided into two different subtypes of leaks: small and gross leaks.

2.6.2.1 Small leaks

The pressure rise small leak method is used when the leak rate is minor. A special pressure transducer is used to measure the small increase of pressure precisely. Furthermore, the extra volume of the cylinder of 1000 ml, which is used to collect the gas, is not used in this case. The principle of this method is to measure the pressure rise of the collecting chamber of known volume. The leaks are then calculated by applying the law of perfect gases. This method can detect the leakage in the range between 0.1 to 0.001 ml/s. This technique is demonstrated using table 2.1 and figure 2.7.
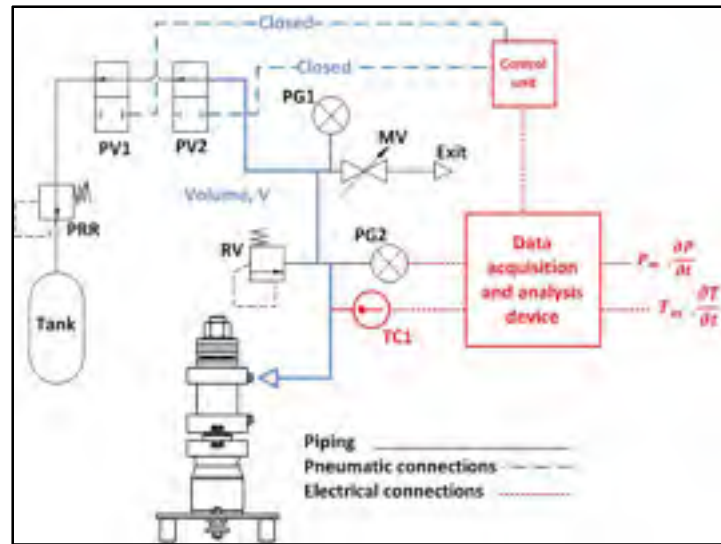
Figure 2.6 Pressure decay leak system
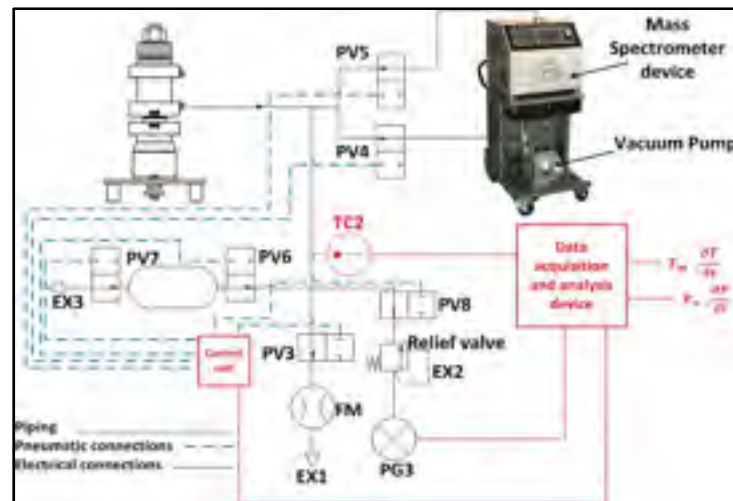
Figure 2.7 Pressure rise methods

2.6.2.2 Gross leaks

The doctrine for the gross leak method is the same as the small leak method, but it is applicable to high rates of gas leakage. A cylinder, with a volume capacity of 1000 ml, is added to the system to reduce the amount at which the pressure grows. The gross leak detection method can detect the leaks between 1 to 0.1 ml/s. The valve opening and closing sequence is shown in Table 2.2.

2.6.3   Leaks by flowmeter

This is the most direct method used in the case of significant leaks (above 1 ml/s). The valve sequences are displayed in table 2.2 for this method. The flowmeter is connected at the outlet of the leak collection chamber in the *UPR*.

2.6.4   Leaks by Mass Spectrometer (ADM142D)

The last method of leakage measurement is conducted using a mass spectrometer, which is also connected to the outlet of the leak collection chamber. The measurement circuit used for small leaks up to 10^{-9} ml/s works under vacuum and is shown in figure 2.7. In this technique, helium is the only gas used. The sequence of valve opening and closing is given in table 2.2. In order to avoid saturation of the mass spectrometer, the maximum leak rate measured with this method is 0.1 ml/s.

2.7   Instrumentation and control

The *UPR* instrumentation and control contains two main categories: the measuring transducers and the control devices. The measuring devices are: strain gauges, LVDTs, thermocouples, pressure transducers and flowmeters.

- Twenty strain gauges are fixed on the external wall of the packed stuffing box to measure the deformation in axial direction;
- Two LVDTs are installed diametrally opposed to measure the axial displacement of the packing rings when it is compressed;
- The thermocouples are installed on the test rig pipes to measure the temperature;
- The pressure transducers measure the applied pressures;
- The flowmeter measures the leaks rates above 1 ml/s.

The control of the valves through the HP Data Acquisition and Control system is essential to define which type of leak detection technique needs to be used, based on the amount of leak rates. Several electro-valves are used to achieve the desired leak measurement method

according to the level of leak rate. In addition, the gas supply bottles are connected to an electro-pneumatic servo-valve ER3000 that control the pressure applied to the stuffing box packing. The rig is also equipped with a PID temperature controller connected to a cartridge heater to be able to run tests at elevated temperatures using a high temperature version of the stuffing box module.

2.8   Data acquisition and control system

The acquisition of data and the control of various devices are carried out through LabVIEW, which makes it possible to record numerous parameters during the experimentation. These parameters are: temperature, pressure, strain, displacement, leakage and time. With this system, it is possible to control the internal gas pressure and temperature while the applied loads to the packing are achieved manually through the hydraulic tensioner and pump. The LabVIEW program is modified based on the new conditions set by the experimental requirements. Section 6 in Figure 2.1 shows the HP Data Acquisition and Control system. Figure 2.8 shows the lab View program used for this study.

2.9   Test procedure

The test procedure used with the universal packing rig, starts with the insertion of the packing rings inside the housing in immaculate condition. The gland is then mounted on the stem first to be placed at the bottom. The LVDTs are then placed on both external sides of the gland. The O-rings for high pressure (on the stem) and low pressure (on the gland) are already in place. The housing, which contains the packing rings, is positioned on the stem. The most crucial factor, at this stage, is that the packing ring should be in direct contact with the gland. The sealing of the high and low-pressure sides of the packed stuffing boxes using the two set of o-rings is of utmost importance to prevent unintended leaks, and thus, the skewing of experimental results. The packed stuffing box in the UPR is designed to accommodate up to six packing rings. Now that the mechanical assembly is complete, the operator needs to turn on the power supply of the panel, then switch on the data acquisition system and finally, run

the LabVIEW program. At the beginning of the test, the reference values on the program for strain gauges, pressure, compressive stress, and LVDTs should be set to zero.

Figure 2.8 Lab View for UPR

The leak detection test for packed stuffing box is controlled through LabVIEW. The operator needs to exercise the desired compression through the hydraulic tensioner, and then applies the desired gas pressure to the system through the regulator valve, as mentioned in section 2.3. The leak measurement in the UPR is always initialized by the flowmeter. Based on the amount of leak rate obtained, the operator will decide the appropriate leak detection method based on the level of leak rate expected. At the end of the test, the gas pressure supply should be cut from the system, and then, the load should be released on the packing rings by opening the purge valve. The test procedure is summarized in table 2.3.

Table 2.3 Test procedures for Universal Packing Rig

Leak detection test
To start any types of leak test 1. Assemble the packed stuffing box with the required number of rings. 2. Inspect the O-rings conditions and change them if needed. 3. Turn the power supply on, and then start the data acquisition system and Lab View program. 4. Adjust LVDT's and record zero the instruments. 5. Apply the load through the hydraulic pump. 6. Apply the desired gas pressure. 7. Verify the appropriate leak detection method after measuring by flowmeter. 8. Wait for leakage stabilization. 9. Record temperature, pressure, strain, displacement leakage and time. **To finish the test** 1. Disassemble packed stuffing box and release gas pressure. 2. Close the data acquisition system and the power supply.

2.10 Liquid leakage measurements

The leak rates in porous braided packing rings, used in valve stuffing boxes for liquids, can be analyzed through two types of packing rings: PTFE and flexible graphite.

The porosity parameters N and R are estimated experimentally by tests conducted with helium used as a reference gas. The packing universal test bench is used to experimentally measure leak rates of packing rings with liquids. Leakage, under different conditions, with liquids such

as water and kerosene, are measured with these two types of packing rings. The choice of these liquids is motivated by different factors. Water is the common liquid employed in most industrial plants. Kerosene possesses different fluid properties and is representative of the oil refinery products with a large spectrum of leakage behavior. For liquid leak predictions, the selection of helium gas is made based on its sizable molecular structure and its ability to define the porosity parameters. For liquid leak tests, the leak collection chamber at the outlet is filled with liquid leaving a small known volume of air of 2 ml to be compressed when leak is present. Any leaks, into the collection chamber, would compress this small air volume and increase its pressure.

Figure 2.9 Liquid leak in UPR

The leak is proportional to the pressure increase and the change of the ambient temperature as suggested by differentiating the perfect gas law with respect to t. In practice, the ambient temperature is kept relatively constant during the measurements by adding isolation when possible

$$\frac{dV}{dt} = V\left(\frac{1}{T}\frac{dT}{dt}\right) - \left(\frac{1}{p}\frac{dp}{dt}\right)$$

(2.2)

Figure 2.9 shows the liquid leak test rig details. More details about liquid leak measurements will be given in chapter 6.

2.11   ROTT test bench

As part of this study, the ROTT test machine was used to detect the leak rate through gaskets to put emphasis on the type of leak present in seals. The objective of the work is to quantify the porous leak and the interfacial leak present in a sealing device that is composed of a porous material compressed between two mating surfaces usually metallic faces having a surface roughness. The test consists of measuring gasket total leak with trying to eliminate interfacial leak by introducing a tight coating while varying the experimental conditions. The ROTT test rig assembly is shown in figure 2.10. The ROTT test bench contains three main parts: the pressurization part, the leak detection part and the hydraulic part as in the UPR. This test rig was used to detect the leak rates through a variety of gasket materials. The permeation and interfacial leaks, through gaskets, are investigated experimentally by ROTT test rig the details of which are described in chapter 4.

Figure 2.10 ROTT test rig

2.12 Packing simulation using CFX

A simulation of leak through porous media is nowadays becoming more and more popular. More and more Software are adding this option in their list of possible analysis. The growing interest to predict leakage in sealing product has fostered the need to do such simulations.

A packing seal, based on geometric matter, can be represented as a three-dimensional cylinder. The simulation models used in this project consider the packing seal as a porous medium. Although limited, in the choice of models, the CFX software offers the possibility to use a model based on Darcy's law and its implementation by Ansys CFD team to predict the mass flowrate or leak through porous materials is a big step in the advancement of knowledge in this field. The procedure for simulating the flow through packing seal, when the phenomenon of a porous medium is applicable, can be done by the following steps in CFX:

- Create the geometry;
- Set the material properties and boundary conditions;
- Combine the domain by meshing;
- Apply the pressure and get the results of mass flowrate (the solution should be convergent).

2.12.1 Geometry

The geometry consists of an inside and outside walls, a porous medium, a pressure inlet and a constant pressure outlet (atmospheric pressure). The length of the porous agent is (L_P), the radius of the packing seals at the outlet is (R_{out}), the radius of the packing seals at the inlet is (R_{in}), the length of the packing seals is (L) and the thickness is (t_{cy}). Figure 2.11 shows the details of the packing seal geometry mesh and indicates the applied boundary conditions (inlet wall, outlet wall, inlet gate, outlet gate and porous medium region in the middle).

- L : Total length of the cylinder: 0.046 (m);
- R_{in} : Radius of the cylinder at the inlet: 0.0143 (m);
- R_{out} : Radius of the cylinder at the outlet: 0.0283 (m);
- L_P : Total length of the porous medium: 0.0481 (m);

- t_{cy} Thickness of the cylinder: 0.014 (m).

2.12.2   Mesh details of the packing seal

Coarse types are used to identify the mesh density of packing seals a factor value of 1.4141.

2.12.3   CFX Physical model

As already pointed out, based on the flow characteristics and CFX options the Darcy model is used to predict the flow through the packing rings.
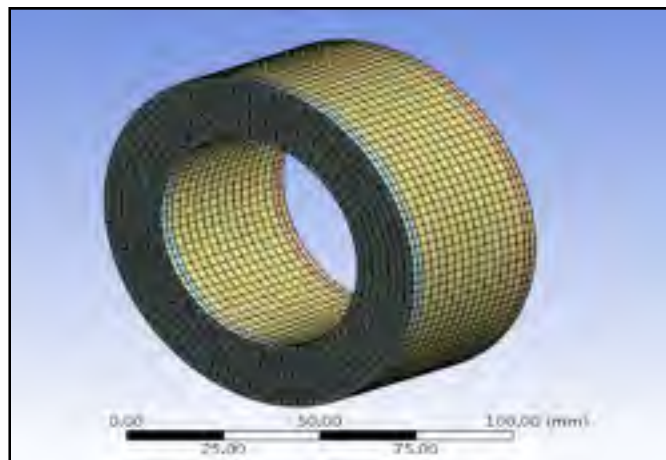
Figure 2.11 Geometry and mesh in CFX Model.

2.12.4   Fluid properties and porous medium material properties

The following properties are required to define both the fluid media and the packing material considered a porous medium or packed bed:

For the fluid:
1) Density;
2) Viscosity.

For the packing:

1) Volume porosity;
2) Permeability;
3) Interfacial area density.

2.12.5   Boundary conditions

The following boundary conditions are applied to the CFX model:

- Inlet pressure with changes from 0.34 to 2.74 MPa.
- Outlet pressure constant at a value of 1 atmosphere.
- Inlet wall and outlet wall are solid at standard condition (the space is at room temperature).
- No - slip condition in the inside wall of the model.

The porous medium region is in the middle, where the inlet and the outlet are located at both ends of the cylinder flat faces shown in Figure 2.11.

2.12.6   Parameters of the simulation

The variation of the pressure values, from the inlet to the outlet, passing through the porous medium region, is shown in figure 2.12. The permeability variation with the length plays a significant role in the mass flowrate results. Figure 2.13 shows the variation of the velocity values from the inlet to the outlet when fluid flow occurs in the porous material. The flow velocity in Darcy's model affects the calculation of mass flowrate or leakage in this case. The pressure, velocity and permeability are the main parameters that have major effect on the fluid flow through the packing rings simulation. Finally, when the solution converged or when the specified number of iterations is met, the value of mass flowrate can be calculated.
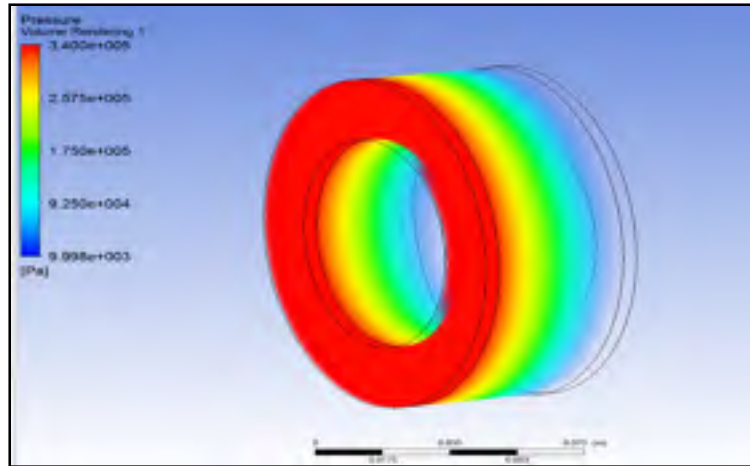
Figure 2.12 Pressure variation at the inlet
and outlet boundary.
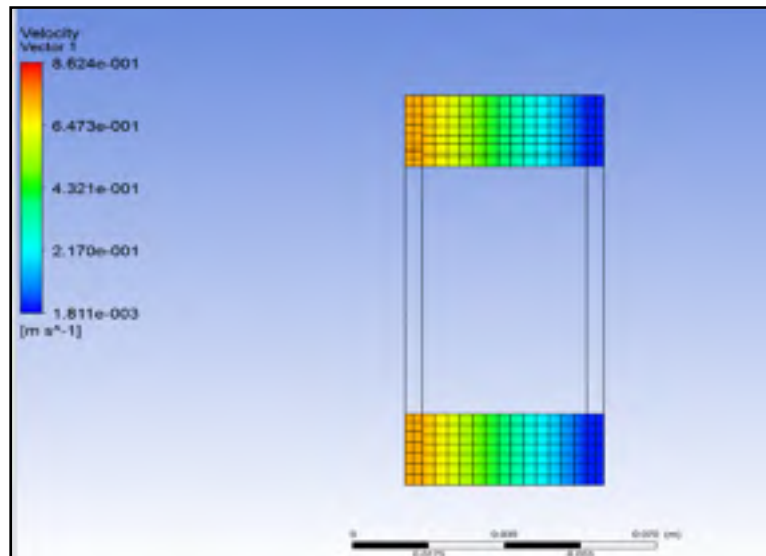
Figure 2.13 The velocity variation at the
inlet and outlet boundary.

CHAPITRE 3

PREDICTION LEAK RATE THROUGH VALVE STEM PACKING IN NUCLEAR APPLICATIONS

[a] Ali Salah Omar Aweimer[1], [b] Abdel-Hakim Bouzid[2], [C]Mehdi Kazeminia[3]

[a] Ph. D. student, Mechanical Engineering Department, École de technologie supérieure, 1100 Notre-Dame St. West, Montreal, Quebec, H3C 1K3
[b] ASME Fellow, Professor, Mechanical Engineering Department, École de technologie supérieure, 1100 Notre-Dame St. West, Montreal, Quebec, H3C 1K3
[C] Graduated Ph. D. student, Mechanical Engineering Department, École de technologie supérieure, 1100 Notre-Dame St. West, Montreal, Quebec, H3C 1K3

3.1   Abstract

Leaking valves has forced shutdown in many nuclear power plants. The myth of zero leakage or adequate sealing must give way to more realistic maximum leak rate criterion in design of nuclear flange joints and valve stem packing. It is well established that the predicting leakage in these pressure vessel components boxes is a major engineering challenge to designers. This is particularly true in nuclear valve due to the different working conditions and material variations. The prediction of the leak rate through packing rings is not a straightforward task to predict. This work presents a study on the ability of micro channel flow models to predict leak rates through packing rings made of flexible graphite. A methodology based on the experimental characterization of the porosity parameters is developed to predict leak rates at different compression stress levels. Three different models are compared to predict the leakage, where the diffusive and second order flow models are derived from Naiver-Stokes equations and incorporate the boundary conditions of an intermediate flow regime to cover the wide range of leak rate levels. The lattice model is based on porous media of packing rings as packing bed (D_p). The flow porosity parameters (N, R) of the micro channels assumed to

simulate the leak paths present in the packing are obtained experimentally. The predicted leak rates from different gasses (He, N_2, Ar) are compared to those measured experimentally, in which the set of packing rings is mainly subjected to different gland stresses and pressures.

NOMENCLATURE

A_c, B_c, D_c	Parameters for capillary second order slip model
A_2	Constant for capillary second order slip model
A_D, B_D	Porosity Parameters for diffusivity model
D_p	Diameter of spherical particles, m
L	Leak rate, kg/s
ℓ	Length of packing, m
N	Number of capillaries
NR^4	Porosity Parameters for capillary and diffusivity models , m^4
P	Pressure, Pa
R	Radius of capillary, m
T	Temperature, K
u	Axial velocity, m/s
z	Capillary axial direction, m

Greek Letters

ε Porosity

φ Sphericity, m

λ Mean free path, m

μ Dynamic viscosity, Pa s

ρ Density, kg/m3

σ Tangential momentum accommodation coefficient $= 1$

$\Re$ Specific gas constant, J/kg K

∇P Pressure difference between upstream and downstream, Pa

Non-Dimensional Number

Kn   knudsen number; $\left(\dfrac{\lambda}{2R} \right)$

Re   Reynolds number; $\left(\dfrac{D_p u \rho}{(1-\varepsilon)\mu} \right)$

Subscripts or Superscripts

b Bulk

c Capillary second order model

D Capillary diffusive model

i Inlet or upstream

66

o	Outlet or downstream
p	Packed beds model
s	Sphere

Acronyms and abbreviations widely used in text and list of references

NSE   Navier-Stokes Equations

3.2   Introduction

Further to the global concern of the amount of hazardous pollutants that is released to the atmosphere and the consequence on the environment, health and safety, stricter regulations on fugitive emissions are legislated. To tune the quality of industrial equipment performance with these regulations, in recent years, research programs that cover experimental, numerical and theoretical studies on gasketed joints and valve stem packing have been launched in North America Europe and Japan recently. The characterization of gas leak rate through valve packing seals at room and high temperatures is the latest. The development of a model to predict the actual behavior of packed stuffing boxes at room and high temperatures represent our major contribution, from this stand point. Theoretical and applied research in flow, heat, and mass transfer in porous media has become an attention during the past two decades. This is due to the importance of this research area in many engineering applications including packing seals which are used in valves. It is important that the mechanism of a packed stuffing box maintains a threshold amount of contact pressure during the operation of a valve. In order to improve the sealing performance of packed stuffing boxes, it is essential to study their leakage behavior, the factors which contribute to leak, and the influence level of the affecting parameters. The purpose of this work is to use theoretical and simulation models to investigate the leakage behavior of packing seals under different operating conditions, such as pressure, stress and type of fluid. Most valves use packing seals to prevent stem leakage. Valve packing must be properly compressed to prevent fluid escape and stem damage. If a packing seal is too

loose, leak occurs between the stem and the packing rings, which is a safety hazard, if it is too tight, it will impair the movement and possibly damage the stem. Furthermore, 60% of fugitive emissions of pressure vessel equipment requiring sealing compliance come from leakage of valve. Therefore, it is important to predict the long term leakage behavior and ensure a long working lifetime and reduce maintenance work of valves. The flow in packing seals can takes place through cracks, serration and porosity. These types of leak are very difficult to measure or predict separately. Therefore, it is very difficult to predict the leak rate using simple analytical approaches. Up until now; there have been few analytical models to simulate gas flow through packing seals, it can be expressed as continuous flow through capillaries or tortuous flow through a porous media. There are different flow regimes that could possibly be used to model the flow in packing rings. The suitability of a model that covers the wide range of leak due to the various applications is a difficult task to achieve. The type of flow regime is dictated by Knudsen number (Knudsen, 1909b); for values greater than 1 the flow is considered to be in the free molecular regime, for a range between 0.01 and 1 the transitional flow regime is present and for values less than 0.01, continuum flow regime is predominant. (Ewart et al., 2006) measured the mass flow rate for a gas flow in slip regime and isotherm steady conditions in cylindrical micro tubes. The measured values were compared to the ones obtained by analytic models based on gas dynamics-continuum equations. They conclude that in a slip regime, there is a significant Kn second order effect. In another study, (Kazeminia et Bouzid, 2016c) used different analytical approaches based on first order slip model and modified Darcy model to predict the leakage through packing seals. Their results show that these flow models have nearly the same accuracy for the level of leak rate above 10-3 mg/s for 28.575 mm (1 1/8 in) stem diameter with 9.525 mm (3/8 in) square packing rings. The effect of inlet pressure has been studied by (Arkilic, Schmidt et Breuer, 1994), where they investigated filtration velocity with slip boundary conditions applied to Navier-Stokes Equations (NSE). They conclude that the slip boundary conditions are not an accurate assumption with a larger Knudsen numbers. Adanhounmè, Codo et Adomou (2012) found better agreement with their experiments results when using the domain decomposition method instead of the nonlinear functional NSE. Numerous studies have been conducted on rarefied gas flow in porous media. Hong, Asako et Lee (2009) developed a methodology to estimate the gaseous leak flow rates in a narrow crack

for a wide range of flow conditions, using Darcy's friction factor and the Reynolds number. They validated the predicted leak flow rates by comparing them with both numerical results and available experimental data. Diany et Bouzid (2011) determined the leak rate for two packing types, where they found that Teflon required smaller compression stresses to seal than flexible graphite. Agrawal et Dongari (2012) estimated the mass flow rate using NSE with a Knudsen number equal to four. They found an agreement with experimental measurements. In another study conducted by (Dongari, Agrawal et Agrawal, 2007), the microscale gas flow was characterized by NSE with second order slip boundary condition. They employed a generalized form of the second-order slip model, earlier developed by (Sreekanth, 1969) and solved the integral form of the NSE retaining the inertia terms. The solution obtained for long micro-channel gave satisfactory results up to a Knudsen number value of 2. Singh, Dongari et Agrawal (2014) investigated the leakage behavior in low-speed isotherm micro scale gas conditions obtained good results up to a Knudsen Number of 2.2. Amyx, Bass et Whiting (1960a) measured the permeability phenomenon by investigating the capacity of fluid flow through rock samples. In the macroscale regime, the diffusion model based on wall adsorption prevails. Dongari, Sharma et Durst (2009) developed a theoretical treatment for mass flow rate through a micro-channel using NSE and including the diffusion effect caused by density and temperature gradients. The theoretical predictions using the modified NSE are found to be in good agreement with the available experimental data, while ignoring wall-slip boundary conditions.

In parallel a lot research has been dedicated to the flow through porous media. The use of Brinkman–Forchheimer-extended Darcy or the more generalized model is suitable for an extensive variety of engineering applications, including flows through packed beds, packing seals, and gaskets. The porosity in terms of the size and shape of pores has a significance effect on the flow properties using Ergun equation, (Handley et Heggs, 1968) investigated the effect of cylindrical and spherical pore shapes. Macdonald et al. (1979) studied impact on flow of the porosity range between $0.36 < \varepsilon < 0.92$. Zou et Yu (1996) proposed an empirical equation to quantify the relationship between the porosity and sphericity of cylindrical particles in dense random packing using an experimental approach. They found that the formulated relations

obtained demonstrate to be useful in characterizing porosity prediction of non-spherical particle mixtures. Parkhouse et Kelly (1995) investigated the relationship between the length to diameter ratio of the bed using a statistical approach on the distribution of the pores in the stacks. The model agrees with experimental results. Liu, Afacan et Masliyah (1994) focused on the fundamentals of flow through porous materials, and attempted to include a factor to account for the wall effect. They discovered that the total length of the leak paths varies with the void ratio. The materials used in this study were spherical glass beads of varying diameters, with a porosity ranging from 36-44%. The Ergun equation was only valid for Reynolds number less than 1000. With a modification to the Ergun equation, (Jones et Krier, 1983) extended its validity up to a Reynolds number of 76000.

The aim of this paper is to shed light on the underlying phenomenon of packing seals leakage prediction by examining different analytical models to describe leakage behavior in packing seals. Experiment validation is conduct to verify the suitability of the analytical models. A set of four flexible graphite based packing rings is tested under three types of gasses; namely nitrogen, argon, and helium at different gland stress levels and internal pressures. The need to predict leakage through different materials in the multidisciplinary engineering applications including rocks gas extraction from shale reservoirs and pressurized equipment has fostered a lot of research in the field of gas flow through porous materials. The different studies are conducted at the micro and nano-levels depending on the range of flow or leak to be considered.

3.3 Physical flow models

3.3.1 Capillary model with second order slip condition

The analytical solution of the NSE with the second order velocity slip condition in circular channels is employed to evaluate the mass leak rate through a set of porous packing rings. The model implemented in the present work is already exploited in micro channels within known dimensions for different types of geometry such as circular (Tison, 1993), rectangular (Maurer et al., 2003), triangular and trapezoidal (Araki et al., 2002). The leak paths that fluid particles

follow through the porous the packing material such as flexible graphite used in this study are modelled as circular channels oriented in the axial direction. Therefore a set of N_c parallel capillaries of uniform radius R_c with the second order slip condition shown in figure 3.1.
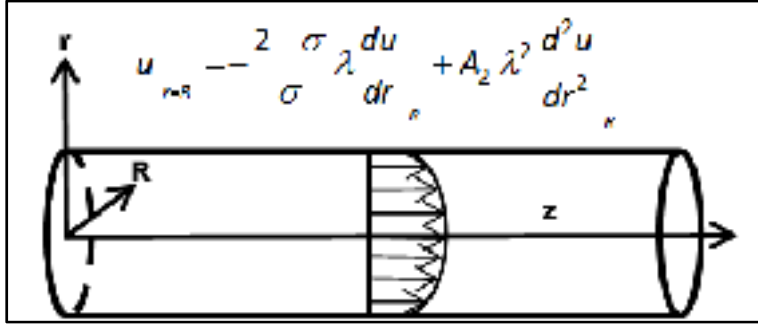
Figure 3.1 Capillary model with second order slip flow

The equation of conservation of momentum in cylindrical coordinates for an ideal gas, without taking into account the effect of inertia at low Reynolds number and large $l/2R_c$, reduces to (Grine et Bouzid, 2011b):

$$\frac{1}{r}\frac{d}{dr}\left(r\frac{du}{dr}\right) = \frac{1}{\mu}\frac{dP}{dz} \qquad (3.1)$$

In the case of isothermal flow without displacement of the wall of a micro tube of circular section, the first and second boundary conditions are:

$$\left.\frac{du}{dr}\right|_{r=0} = 0 \qquad (3.2)$$

$$u\Big|_{r=R} = -\frac{2-\sigma}{\sigma}\lambda\left.\frac{du}{dr}\right|_{r=R} + A_2\lambda^2\left.\frac{d^2u}{dr^2}\right|_{r=R} \qquad (3.3)$$

σ is the tangential momentum accommodation coefficient taken as 1 for simplicity and λ is the mean free path. Integrating equation (3.1) twice and applying the above boundary conditions gives the solution for the velocity in the z direction as a function of the radial position such that:

$$u\left(r,z\right) = \frac{1}{\mu}\frac{dP}{dz}\left[\frac{r^2}{4} - \frac{R^4}{4} - \frac{2-\sigma}{\sigma}\lambda\frac{R}{2} + A_2\,\lambda^2\,\frac{1}{2}\right] \qquad (3.4)$$

The Leak rate from N number of capillaries can be obtained by integrating the velocity through the area as:

$$L = N\,\rho\int\limits_{0}^{R} 2\,\pi\,r\,u\left(r,z\right)dr \qquad (3.5)$$

Substituting for the velocity and using the ideal gas law give the leak rate as:

$$L = \frac{N\pi R^4 P_o^2\left(\Pi^2 - 1\right)}{16\mu RT l}\left[1 + 16\frac{2-\sigma}{\sigma}\frac{Kn}{\left(\Pi+1\right)} - 32\,A_2\,Kn^2\,\frac{In\left(\Pi\right)}{\left(\Pi^2 - 1\right)}\right] \qquad (3.6)$$

Where Kn is the Knudsen number defined as:

$$Kn = \frac{l}{2R} \qquad (3.7)$$

And Π is the pressure ratio such that:

$$\Pi = \frac{P_i}{P_o} \qquad (3.8)$$

And λ is the mean free path:

$$\lambda = \frac{16\,\mu}{5\,P_o}\sqrt{\frac{RT}{2\,\pi}}$$

(3.9)

3.3.2   Diffusive flow model

The analytic solution of the NSE with the diffusive conditions in circular channels is employed to evaluate the mass leak rate (Dongari, Sharma et Durst, 2009) in the simple case of an isotherm flow and without displacement of the wall. The first and second order boundary conditions are:

$$\left.\frac{du}{dr}\right|_{r=0} = 0$$

(3.10)

And

$$\left.u\right|_{r=R} = -\frac{\mu}{\rho P}\frac{dP}{dz}$$

(3.11)

Neglecting the temperature gradient in the z direction Soret's term has no contribution to the diffusion velocity and only Fick's term contributes by following equation (3.11). Given the expression for the velocity:

$$u\left(r,z\right) = -\frac{1}{2\mu}\frac{dP}{dz}\left(R^4 - r^2\right) - \left(\frac{\mu}{\rho P}\frac{dP}{dz}\right)$$

(3.12)

Integrating the velocity over the area using equation (3.5) gives the mass flow rate as:

$$L = \frac{N \pi R^4 P_o^2 \left(\Pi^2 - 1\right)}{16 \mu R T l}\left(1 + \frac{16 \mu^2 R T}{R^2 P_o^2}\frac{In\left(\Pi\right)}{\left(\Pi^2 - 1\right)}\right) \tag{3.13}$$

3.3.3   Ergun model for a porous media

The Ergun model is often used to predict the leak rate through porous materials (Ergun, 1952). Based on the Forchheimer's Law, the flow through packed beds of spheres is given by Ergun equation such that:

$$f_p = \frac{150}{Re_p} + 1.75 \tag{3.14}$$

Where f_p is the friction factor for packed beds and Re_p is the Reynolds number for packed beds, $(150, 1.75)$ are values found experimentally (Ergun, 1952). f_p and Re_p can be expressed as:

$$f_p = \frac{\Delta P}{l}\frac{D_p}{\rho u^2}\frac{\varepsilon^3}{\left(1 - \varepsilon\right)} \tag{3.15}$$

$$Re_p = \frac{D_p u \rho}{\left(1 - \varepsilon\right)\mu} \tag{3.16}$$

The pressure drop $\nabla P = P_i - P_o$ through a randomly packed bed of spheres is given by:

$$\nabla P = \frac{150 \mu u l}{\varphi^2 D_p^2}\frac{\left(1 - \varepsilon\right)^2}{\varepsilon^3} + \frac{1.75 \rho u^2 l}{\varphi D_p}\frac{\left(1 - \varepsilon\right)}{\varepsilon^3} \tag{3.17}$$

This model can be applied to packing seals simulated as a material made with particles of diameter D_p and having a porosity, ε. The porosity ε of the material can be defined through the relationship between bulk density ρ_b and solid density ρ_s, where experimentally the values at each stress level are obtained as:

$$\varepsilon = 1 - \frac{\rho_b}{\rho_s}$$
(3.18)

The porosity is an indication of the closeness of the packing, with a smaller void ratio indicating a tighter packing. For the flexible graphite packing material tested, the values of the porosity at the different gland stresses are presented in table 3.1. For the case of non-spherical particles a correction or shape factor known as sphericity φ and defined in (Carman, 1956) is frequently used. It is the ratio of the surface area of spheres with the same volume the particles over the surface area of particles. This is used to obtain the equivalent sphere diameter, where in the case of sphere particles a sphericity of 1 applies, while in our case the equivalent diameter is estimated to 0.9.

Table 3.1 Flexible graphite packing porosity

Stress (MPa)	7	14	28	41
Porosity	0.44	0.4	0.3	0.2

3.4 Experimental set up

The experimental leak measurement tests are conducted on the stuffing box test bench shown in figure 3.2.

Figure 3.2 General configuration of the
test bench for leak detection test

This test bench has three main systems: a hydraulic tensioner system with a manual pump and accumulator, a pressurization system composed of different gasses and a leak detection system. Every system has its own instrumentation and controls connected to a data acquisition system using LabView software as an interface program between the data logger and the computer. The housing of a total length of 104.775 mm (4.125 inches) in height can accommodate up to 5 packing rings of 9.525 mm (3/8 inch) square section. A set of four packing rings were used for the purpose of the current test study. The stuffing box housing has an outside diameter of 79.375 mm (3.125 inches) and an inside diameter of 47.625mm (1.875 inches). The stem is made of steel with a diameter of 28.575 mm (1.125 inches). Depending on the leak rate, four different leak measurement techniques can be used: flow meter, pressure decay, pressurized rise and spectrometry, with the latter being able to detect down to 10^{-10} ml/s. For this study, only the flowmeter and pressure rise methods were used to measure the leak rates. A gland stress ranging from 6.9 to 41.1 MPa (1000 to 6000 psi) in steps of 7, 14, 28 and 41 MPs is applied by using the hydraulic tensioner. The gland stress is deduced from the measurement of the load through a Wheatstone bridge strain gage placed on the stem. For every gland stress level, pressures ranging from 0.34 to 2.76 MPa (50 to 400 psi) in steps with 0.34 MPa are applied to the packed stuffing box. Three gasses, Nitrogen, Argon, and Helium, were used in the experiment. The physical values of molecular weight and mean free path of gasses used in the experimental investigation of this study are presented in Table 3.2. Using the pressurized

method to measure leak and taking into consideration that the uncertainties of pressure, temperature, volume and time as 7×10^{-4}, 3.36×10^{-3}, 3.18×10^{-6} and 6.67×10^{-4} respectively, the uncertainties of helium, argon and nitrogen leak rate are showed in Table 3.3.

Table 3.2 Physical properties of the gasses used in experimental investigations

Gas type	Density (g/l)	Viscosity (Pa.s) X 10^{-5}	specific gas constant (J/kg.K)	Molecular Weight (g/mol)	mean free path (nm)
Helium	0.179	1.94	2077	4.003	17.65
Argon	1.632	2.217	208.2	39.94	64.41
Nitrogen	1.251	1.8	296.8	28.01	60.44

Table 3.3 Uncertainties for lowest and highest mass leak rate

Gas type	Uncertainty of low leak rates (mg/s)	Uncertainty of high leak rates (mg/s)
Helium	$1.217 \times 10^{-4} \pm 5.8 \times 10^{-7}$	1.341 ± 0.011
Argon	$9.792 \times 10^{-4} \pm 4.6 \times 10^{-6}$	7.752 ± 0.037
Nitrogen	$8.757 \times 10^{-4} \pm 4.1 \times 10^{-6}$	7.716 ± 0.036

3.5 Porosity parameters evaluation

3.5.1 Capillary model with second slip velocity

The mass flow rate equation can be written in the following form:

$$A_c = NR^4 \left[1 + B_c \frac{1}{(\Pi + 1)} - D_c \frac{In(\Pi)}{(\Pi^2 - 1)} \right] \qquad (3.19)$$

Where

$$A_c = \frac{16 L \mu R T l}{\pi P_0^2 (\Pi^2 - 1)} \qquad (3.20)$$

$$B_c = 16 \frac{2 - \sigma}{\sigma} Kn \qquad (3.21)$$

$$D_c = 32 A_2 Kn^2 \qquad (3.22)$$

The porosity parameters N and R can be obtained from a curve fit of the data obtained with tests using helium as a reference gas and equation (3.19) that expresses A_c as a function of the pressure ratio Π .

3.5.2   Capillary model with diffusive velocity

The mass flow rate equation can be written in the following:

$$A_D = NR^4 \left[1 + B_D \frac{\ln(\Pi)}{(\Pi^2 - 1)} \right] \qquad (3.23)$$

Where

$$A_D = \frac{16 L \mu R T l}{\pi P_o^2 (\Pi^2 - 1)} \qquad (3.24)$$

$$B_D = \frac{16\,\mu^2 R\,T}{R^2\,P_o^2}$$
(3.25)

Following the same procedure as with the second order model, the porosity parameters N and R of the diffusivity models are obtained.

3.5.3 Parameters of porous media condition

The leak rate and pressure drop being known for each stress level during the tests with helium, the values of D_p can be obtained and used to predict the leak rate for other gasses such as nitrogen and argon.

3.6 Results and discussion

Helium is used as the reference gas to determine the porosity parameters embedded in each of the analytical models. Figure 3.3 shows the leak rate measurements versus helium pressure at different 4 different gland stresses. Using the data from these tests and a curve fitting of a plot of A_c versus the pressure ratio Π the porosity parameters N and R are obtained for the second order and diffusion models. Figure 3.4 gives a plot of NR^4 as a function of the gland stress. The two curves given by the second order slip and diffusion models are very similar. The porosity parameter values from the two models are close to each other at the low and intermediate stresses. However, for the high stress the second order slip model predicts smaller values of the porosity parameter.
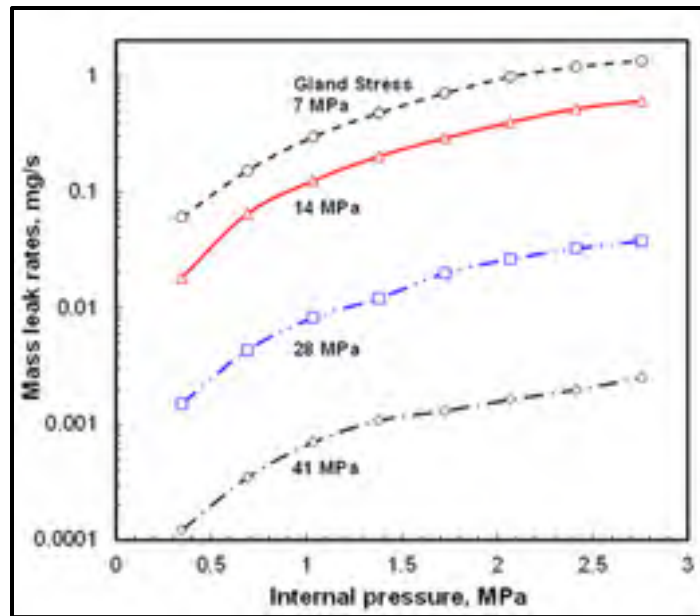
Figure 3.3 Measured leak rates using helium
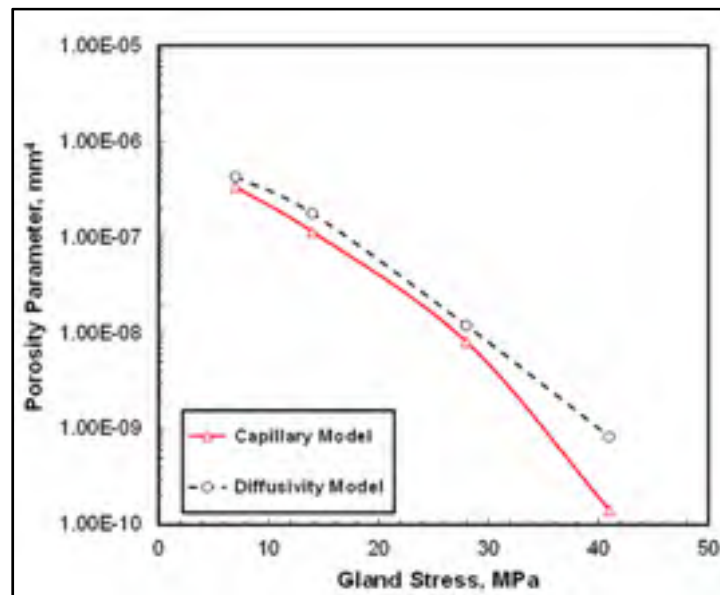
Figure 3.4 Porosity parameter NR^4 for second
order & diffusivity models

The porosity and the Ergun model solid phase sphere size D_p are plotted against the gland stress in figure 3.5. As the stress increases both parameters decrease. In addition the sphere

size decreases with pressure increase although the effect is comparatively small as shown in figure 3.6. The porosity parameters and the other constants obtained from data curve fitting have been used to predict the leak rate for other types of gasses namely nitrogen and Argon. For the second order and diffusivity models the number and radius of capillary obtained from Helium tests were incorporated in equations (3.6) and (3.13) respectively while the diameter of particles is used in equation (3.17) to predict the leak rate for other gasses.
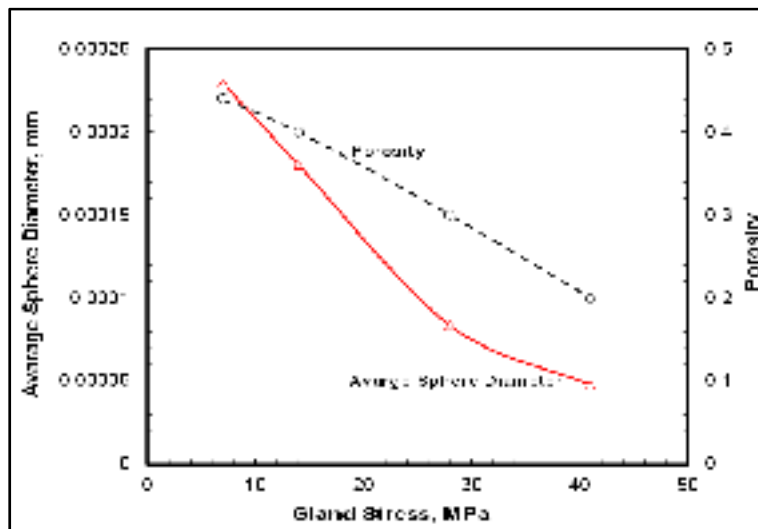
Figure 3.5 Average sphere diameter D_p and porosity ε

In parallel tests were conducted with these two gasses in order to compare the results with all three models. The measured leak rates are conducted at four stress levels varying from 7 to 41 MPa and eight different gas pressures ranging from 0.34 to 2.7 MPa. As general, the theoretical leak predictions are slightly higher than the experimental leak measurements depending on the gas pressure and the level of stress on the packing rings. Figures 3.7 and 3.8 present the Nitrogen gas results for 7, 14, 28 and 41 MPa gland stresses respectively. The second order slip model is show to predict leak better than the diffusivity and Ergun models with the latter showing less accuracy. In addition as the gland stress is increased the leak becomes smaller and the diffusivity and Ergun model curves separate from the measured curve indicating the flow does not obey the porous media and diffusive flow regimes. The capillary flow with the second order slip model predicts better results in this case.
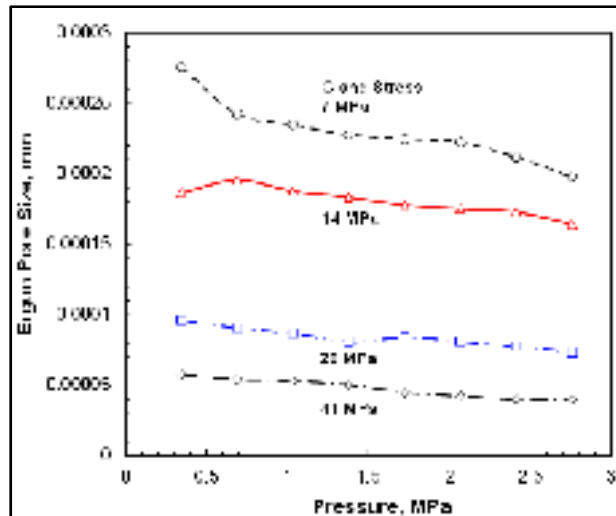
Figure 3.6 Ergun pore size D_p vs
pressure at different stress levels
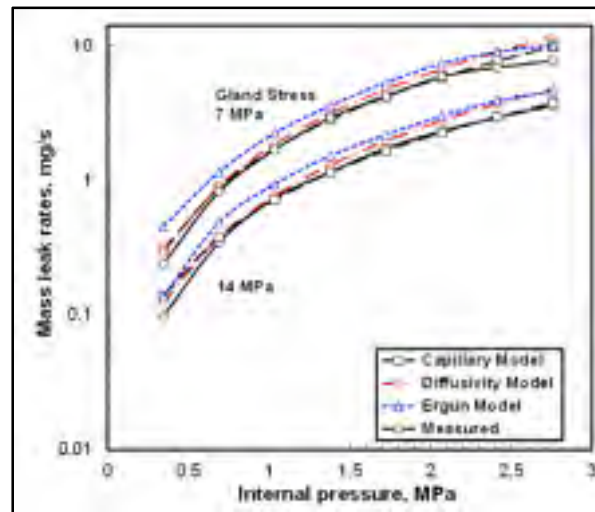
Figure 3.7 Comparison of leak rates of
Nitrogen at 7 and 14 MPa gland stress

Figures 3.9 and 3.10 present the Argon gas results for 7, 14, 28 and 41 MPa gland stresses respectively. Although all models predicts leak rates with acceptable error margin, the second order slip model gives a better agreement with experimental data for all pressure values of Argon gas. The gap between the experimental curves and the diffusion and Ergun models is relatively large for higher gland stress values indicating a larger percentage difference even in

a log scale. Therefore the second order slip model simulates better the leakage behavior of flexible graphite packing seals over a wide range of flow 0.0001 to 1 mg/s of helium. Tighter packing seals are the subject of future studies. It is suspected that the second order slip model could still be used to predict even leak rates up to 10^{-6} mg/s where the molecular flow prevails.

3.7   Conclusion

This study investigates the suitability of capillary and porous media models to predict gaseous leaks in flexible graphite packing rings of valve stuffing boxes. The packing rings are a homogeneously distributed porous media with disordered porosity. In the slip and diffusive flow models, the porous media was hypothetically constructed with micro-tubes in the direction of the fluid flow. While in the Ergun model, the porous media was assumed to be a packed bed made of spheres. Helium was used as the reference gas to determine the porosity parameters of the different models. These parameters were then used to predict the leak rate for other types of gases.
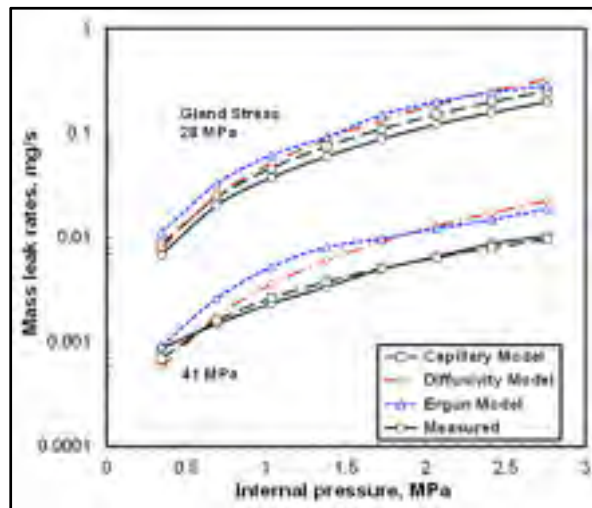
Figure 3.8 Comparison of leak rates of
Nitrogen at 28 and 41 MPa gland stress
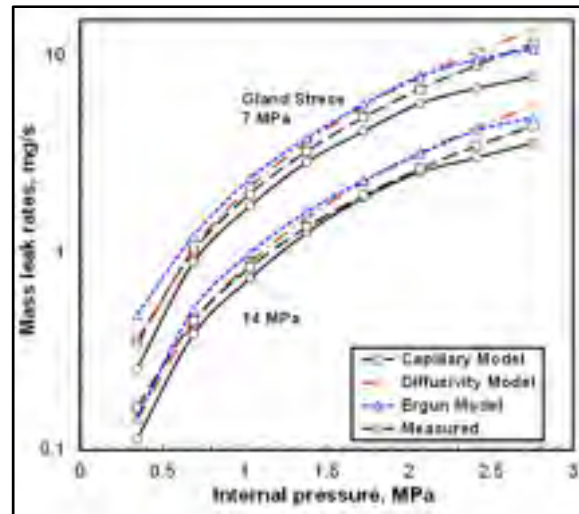
Figure 3.9 Comparison of leak rates of
Argon at 7 and 14 MPa gland stress
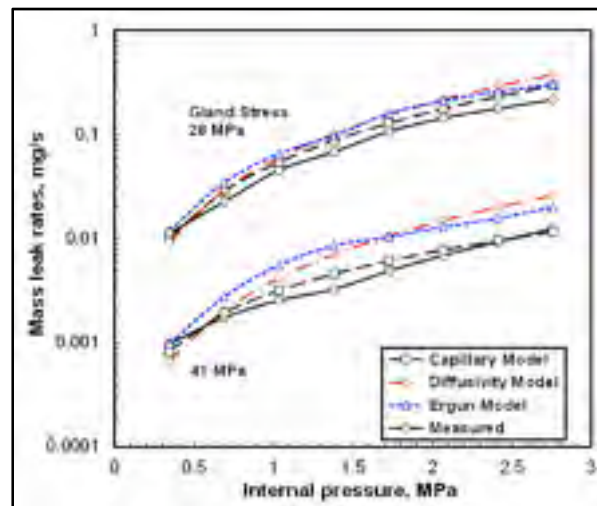
Figure 3.10 Comparison of leak rates for
Argon at 28 and 41 MPa gland stress

In general, the results showed a good agreement between the predicted leak rates and those measured experimentally. However the second order slip model showed a better agreement over the four decade range of leak rates from 0.0001 to 1 mg/s with helium. This model is currently being tested for other tighter packings such as those made of PTFE and other materials.

CHAPITRE 4

**EVALUATION OF INTERFACIAL AND PERMEATION LEAKS IN GASKETS
AND COMPRESSION PACKING**

[a] Ali Salah Omar Aweimer[1], [b] Abdel-Hakim Bouzid[2]

[a] Ph. D. student, Mechanical Engineering Department, École de technologie supérieure, 1100
Notre-Dame St. West, Montreal, Quebec, H3C 1K3
[b] ASME Fellow, Professor, Mechanical Engineering Department, École de technologie
supérieure, 1100 Notre-Dame St. West, Montreal, Quebec, H3C 1K3

4.1   Abstract

The quantities of leak rate through sealing systems are subjected to strict regulations because of the global concern on radiative materials. The maximum tolerated leak is becoming a design criterion in pressure vessel design codes, and the leak rate for an application under specific conditions is required to be estimated with reasonable accuracy. In this respect, experimental and theoretical studies are conducted to characterize gasket and packing materials to predict leakage. The amount of the total leak is the summation of the permeation leak through the sealing material and the interfacial leak generated between the sealing element and it's mating surfaces. Unfortunately, existing models used to predict leakage do not separate these two types of leaks.

This paper deals with a study based on experimental testing that quantifies the amount of these two types of leaks in bolted gasketed joints and packed stuffing boxes. It shows the contribution of interfacial leak for low and high contact surface stresses and the influence of the surface finish of 0.8 and 6.3 μm (32 and 250 micro-inch) resulting from phonographic grooves in the case of a bolted flange joint. The results indicate that most leakage is interfacial reaching 99% at the low stress while interfacial leak is of the same order of magnitude of permeation leak at

86

high stresses reaching 10^{-6} and 10^{-8} mg/s in both packing and gaskets, respectively. Finally, particular focus is put on the technique of pre-compression to improve material sealing tightness.

Acronyms and abbreviations widely used in text and list of references

ASTM	American Society for Testing and Materials
CF	Compressed Fiber
EN	European Normalization
FEM	Finite Element Method
FG	Flexible Graphite
NPS	Nominal Pipe Sizes
KTA	Kerntechnischer Ausschuss (German Nuclear Code)
PTFE	Polytetrafluoroethylene
RAAH	Roughness Arithmetic Average Height
ROTT	ROom Temperature Tightness
UPR	Universal Packing Rig

4.2   Introduction

The motivation behind studying fluid flow through porous materials is the need to predict the penetration of gases and liquids in many multidisciplinary engineering material applications. Micro-electro-mechanical systems, gas extraction from shale reservoirs, artificial organs,

sealing of bolted joints and valves, porous membranes and filters are to name a few. Nowadays, the prediction of leak rates through packing rings and gaskets is a significant challenge when designing sealing systems such as stuffing boxes and bolted flange joints. With the global implementation of the strict environmental regulations and safety protection laws against the release of radioactive materials and fugitive emissions, it became an urgent need to develop leakage criteria based designs for pressure vessels and piping systems to insure that pressure equipment comply with these new rules. Therefore, sealing products together with design and assembly methods of packed stuffing boxes and bolted flange joints should evolve to meet the new standards and regulations. It is well established that improving the sealing compliance of gasketed joints and packed stuffing boxes is a big challenge for the nuclear and petrochemical industries. The main criteria for the selection of compression packing rings or gaskets are their capacity to produce a minimum allowable leakage rate. Consequently, in order to optimize the utilization of a seal to produce an acceptable minimum leak rate, a selection scheme based on material properties and a proper assembly procedure are the key solution.

A packed stuffing box consists of a number of packing rings inserted into an annular space between the stem and the housing. The general working principle of packing seals is relatively simple. A packing gland or follower is pushed downward using studs and nuts generating both axial and lateral forces to produce a volumetric compression of the yarned packing rings. The applied axial stress on the yarned packing rings produces a radial expansion creating a lateral pressure on the sides of the stuffing box and the stem to close the axial leak paths in the material and mating surfaces. Bolted flange joints uses a similar technique that consists of compressing a circular gasket between two flanges in the axial direction by means of studs and nuts to close the material pores and leak paths in the radial direction to produce a tight seal. The packing seal in a stuffing box prevents leaks between the stem and the bonnet whereas the gasket prevents leakage between the flange facings. As shown in figure 4.1, in addition to the interfacial leak between contact surfaces there is permeation leak through the sealing material itself that affects the amount of the total leak rate in a sealing devise.
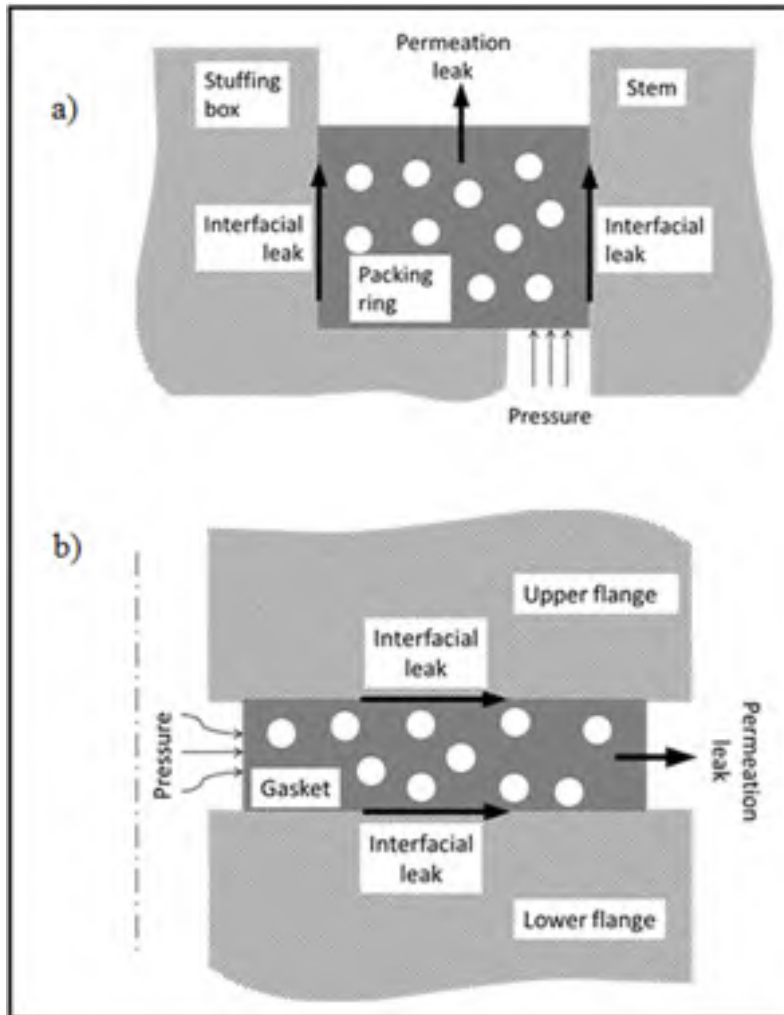
Figure 4.1 Permeation and interfacial leaks a)
Packing Ring b) Gasket

Very few papers deal with the quantification of these two types of leaks. Lasseux et al. (2011) conducted an experimental approach to measure permeability and Klinkenberg Slippage of flexible graphite packing rings in both axial and radial directions. The die-formed exfoliated graphite packing rings were tested in a special test rig designed by the authors. The results showed clearly that the leak rate in the axial direction is one order of magnitude larger than that of the radial direction. Schaaf et al. (2005b) tested different packing materials (flexible graphite, Polytetrafluoroethylene (PTFE) and nonwoven) with special focus on axial deformation, relaxation and leak rate. The author tested packing seals under different conditions of stress and temperature using different gas types. The conclusions drawn are:

firstly, nonwoven packing rings have less leak rate and show better tightness performance compared to PTFE and Flexible graphite materials, and, secondly, smoother contact surfaces with packing rings reduce the amount of leak rate at the interfaces. Ueda et Fujiwara (1997) measured the amount of leak rate in a reciprocating valve with packing seals made of flexible graphite subjected to helium at different pressures and stem cycles. The leak range measured was between 0.25 ml/min after 100 cycles to 0.55 ml/min after 500 cycles. They concluded that the packing material porosity is important to reduce the permeation of gases. Kockelmann et al. (2009) tested different packing materials with different liquids and gases at elevated temperature. The results indicate that at high stresses, leakage with gases is higher than with liquids, which points to the significant contribution of interfacial leakage in the case of gas. Kazeminia et Bouzid (2016b) measured leakage through packing rings experimentally using helium as a reference gas and used the results to predict leakage using analytical models for other gases like Argon and Nitrogen. The results show that the modified Darcy's model can be as accurate as the capillary first order slip model under the conditions of testing utilized. The surface roughness between the contact surfaces in a stuffing box plays a significant role in the interfacial leak and tightness of packing rings. Roe et Torrance (2008) investigated the friction and the wear of graphite packing in a sliding stem configuration under atmospheric pressure experimentally and using FEM (Finite element method) and obtained good agreement between the two approaches. They found that reducing friction decreases wear considerably. The stress distribution in gasket and packing seals has been the subject of many studies. Bouzid, Derenne et El-Rich (2004) studied the impact of stress distribution due to flange rotation on leakage in gasketed joints. Ochoński (1988) investigated the distribution of the radial contact stresses in soft packed stuffing-boxes experimentally. The results showed that the lateral contact pressure generated by the gland stress decreases due to friction. Denny (1957) studied the lateral pressure coefficient and found that it is constant and independent of the magnitude of gland axial pressure.

The leak rate through gaskets and packing seals is a combination of two leaks: an interfacial leak, which takes place through the surface leak paths and a porous leak, which in essence is permeation. Geoffroy et Prat (2004) looked into the radial and circumferential leaks modelled

by diffusive and viscous flows in transition regime of a spiral-groove metallic static ring gasket. The authors concluded that the predictions are better for higher loads for which the pores and leak paths are small. Saeed et al. (2008) and (Yanagisawa et al., 1990) investigated the interfacial leak in solid metal gaskets and concluded that the leakage performance could be improved considerably by adding soft metal coatings. Pérez-Ràfols, Larsson et Almqvist (2016) developed a model to predicate liquid leak rates for both spiral groove and metal to metal seals. They found good agreement with the experiment results obtained from the literature. Boqin, Ye et Dasheng (2007) developed a model to predict the leak rates through non-metallic gaskets. They found that leakage is proportional to the square difference of the inlet and outlet pressures. Kockelmann et Hahn (2006) conducted leakage measurement with different gases including helium, methane and ethane. A comparison between the pressure rise and mass spectrometry was conducted. The authors found a good agreement between the two methods. Arghavani, Derenne et Marchand (2003) investigated the effect of surface finish on the leakage performance of different gasket materials. Grine et Bouzid (2011a) predicted leak rates with a reasonable accuracy using capillary and parallel plate first order slip models in flat sheet gaskets. Schaaf, Schoeckle et Bartonicek (2008) evaluated the leak tightness of gasket products both numerically and experimentally according KTA 3211.2 and EN 1591-1 standards for compliance in nuclear power plants in Germany and Europe, respectively.

Unfortunately, neither all conducted tests nor models in the literature quantified the interfacial and porous leaks separately from the total leak. In this paper, the interfacial and porous leak rate through packing rings and gaskets are quantified experimentally. The amounts of interfacial and porous leaks from the total leak are estimated using an experimental technique that consists of eliminating one type of leak and measuring the other type of leak. Two different test benches are used to experimentally measure the leak rates of packing rings and gaskets. Leakage under different conditions of helium gas pressure and contact stress is measured on PTFE and flexible graphite based packing rings and on flexible graphite, compressed fiber and PTFE based gaskets. The experimental tests are conducted with helium gas. The important contribution of interfacial leak at the low stress is acknowledged. Finally, the effect of surface roughness and pre-compression on the leak rates is also investigated.

4.3   Experimental set up

The experimental leak tests with yarned packing rings and gaskets are conducted on the Universal Packing test Rig (UPR) and the Room Temperature Tightness (ROTT) test rig shown in figure 4.2. The universal packing rig has three fluid circuits; a hydraulic tensioner system, a gas pressure system and a leak detection system. Every system has its own instrumentation monitored through a data acquisition system and an interface program written under LabView software. The housing of a total length of 105 mm (4.125 inches) in height can accommodate up to 5 packing rings of 9.5 mm (0.375 inches) square section. Only a set of two packing rings were used for the purpose of the current study. The stuffing-box housing has an outside diameter of 79.4 mm (3.125 inches) and inside diameter of 47.6 mm (1.875 inches). The stem is made of ASTM A193 Grade B7 steel with a diameter of 28.6 mm (1.125 inches). The leak measurements were taken with a helium mass spectrometer only with a sensitivity of 10^{-10} ml/s. The gland stress is applied through a hydraulic tensioner fixed to the stem. The stress is deduced from the measurement of the load through a Whinstone bridged strain gages bounded to the stem. For every gland stress level, helium gas pressures were applied in steps and leak rate was measured at 10 minutes intervals until stabilization is reached. All tests were conducted under controlled room temperature (24°C).

Table 4.1 UPR test conditions and materials

Gas pressure (MPa)	0.345,0.69, 1.38, 2.76, and 4.14
Gland stress (MPa)	6.9, 13.8, 27.6 and 41.4
Packing materials	100% flexible graphite sheet, Expanded PTFE

Figure 4.2 a) Gasket ROTT test rig and b)
universal packing test rig

Table 4.2 ROTT test conditions and materials

Gas pressure (MPa)	0.69, 1.38, 2.76, 4.14 and 5.52
Stress gasket (MPa)	13.8, 27.6, 55.2, 82.8 and 110.3
Surface Finish (μm)	0.8 and 6.3
Gasket materials	Compressed fiber sheet,100% flexible graphite sheet, Expanded PTFE

In addition, to avoid any effect of temperature variation on the leak measurements, the pressurization and leak detection tubing systems are thermally isolated. The UPR test conditions are presented in table 4.1.

The ROTT test rig is specially designed to measure small leak rates with the pressure decay method and mass spectrometry. The main parameters such as gasket stress and pressure are controlled while monitoring small leaks down to 10^{-10} mg/s. The pressurization and leak detection tubing systems are also thermally isolated to avoid temperature effects. The joint assembly consisting of two Nominal Pipe Sizes (NPS) 4 class 900 welding neck flanges provides a uniform contact stress distribution of the force across the gasket width. Flat sheet gaskets of ROTT dimensions 124 × 150 mm (4.875 × 5.875 inches) made of polytetrafluoroethylene (PTFE), compressed fiber and flexible graphite 3.2 mm (0.125 inches) thick are compressed between two flanges. Hydraulic load tensioners are used to tighten simultaneously the eight bolts with a total load capacity of 1.8 GN (400,000 lbs). The main measured parameters are bolt load, internal pressure, gasket displacement, mass leak rate and time. The test sequence used is similar to that followed by (Grine et Bouzid, 2011a). The leak rates of helium gas were measured at different stresses and gas pressures. The test conditions used in the ROTT test rig are summarized in Table 4.2. The quantities of leaks measured consists of a combination of permeation leak that passes through the sealing element porous material and interface leak that takes place between the sealing element and the joint metal contact surfaces. In the latter, the surface roughness plays a major role as may be appreciated from the tests that are conducted on the ROTT with phonographic flange surface finish of 0.8 and 6.3 μm (32 and 250 micro-inch) RAAH Roughness Arithmetic Average Height). In order to quantify the two types of leaks, the contact surface between the sealing elements and the metallic flange faces were once free of coating and once covered with a special coating based on a nitrocellulose compound, which after polymerization becomes leak tight and prevents most of the interfacial leak.

4.4 Results and discussion

The leak test measurements using helium gas under different pressures and stresses applied to the packing rings and gaskets were conducted with the mass spectrometer. The compression stresses applied to the packing rings were from 6.9 to 41.4 MPa, while the gas pressure range was between 0.34 and 4.14 MPa.
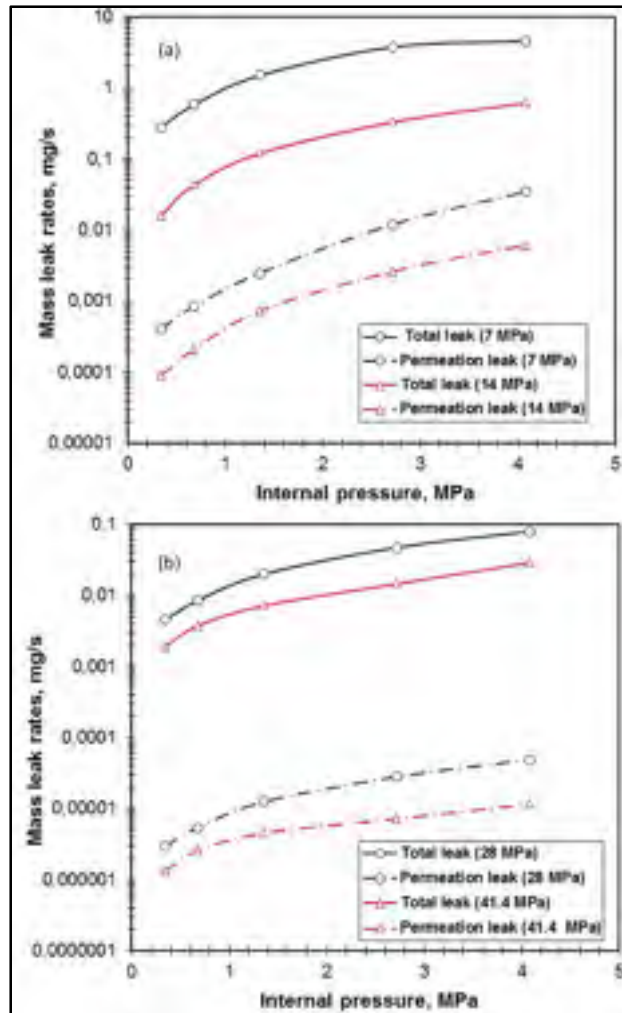
Figure 4.3 Permeation and total leak of FG
packing at a) 7 and 14 MPa b) 28 and 41.4 MPa

For the test with coating to eliminate the interfacial leaks, the nitrocellulose compound was applied to the stem and housing contact surfaces with the packing rings. The gasket was subjected to stresses ranging from 13.8 to 110 MPa while the pressures applied were from 0.69 to 5.52 MPa.
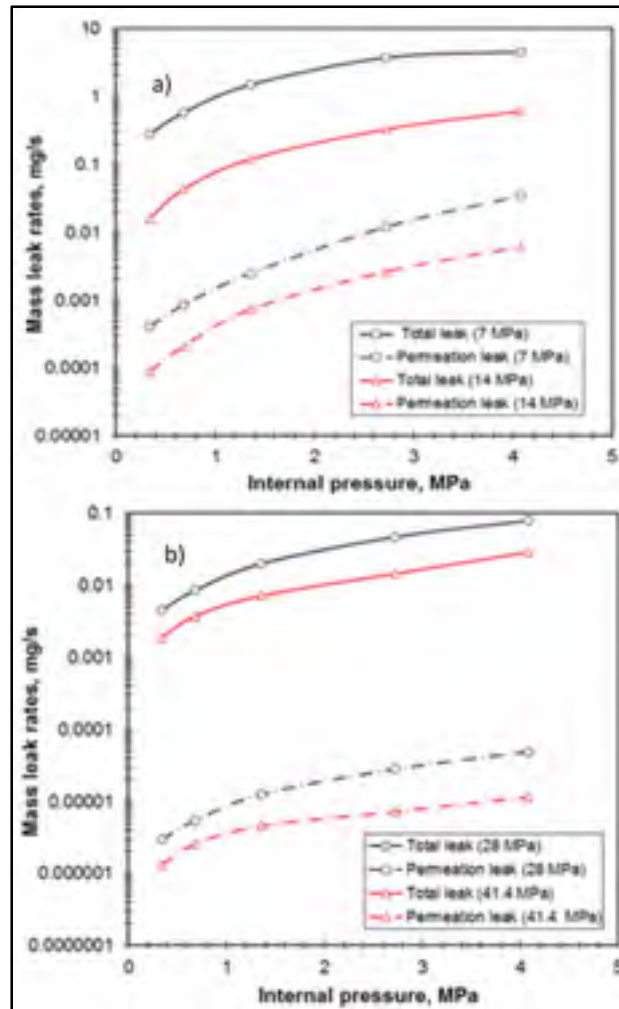
Figure 4.4 Permeation and total leak of PTFE
packing at a) 7 and 14 MPa b) 28 and 41.4 MPa

For the test with no interfacial leaks, the coating was applied to both flange mating surfaces. Figures 4.3 and 4.4 show the total and permeation leak rates of flexible graphite and PTFE packing rings. The contribution of the permeation leaks was found to be very low as compared to that of interfacial leaks.
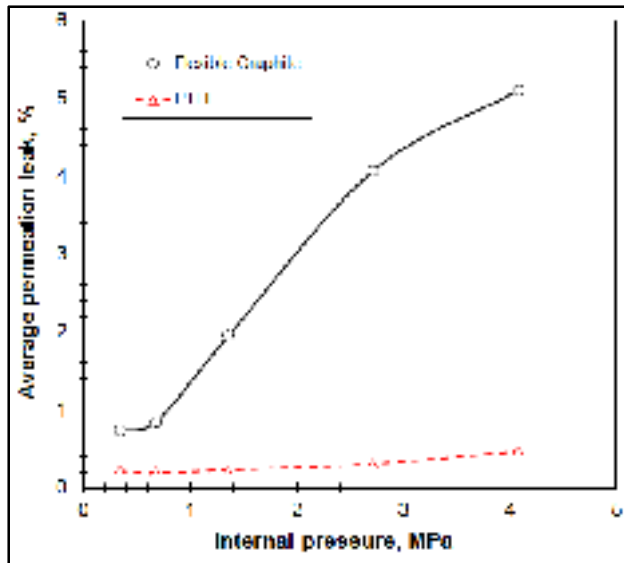
Figure 4.5 Average of Permeation leak over
total leak of FG and PTFE packing rings
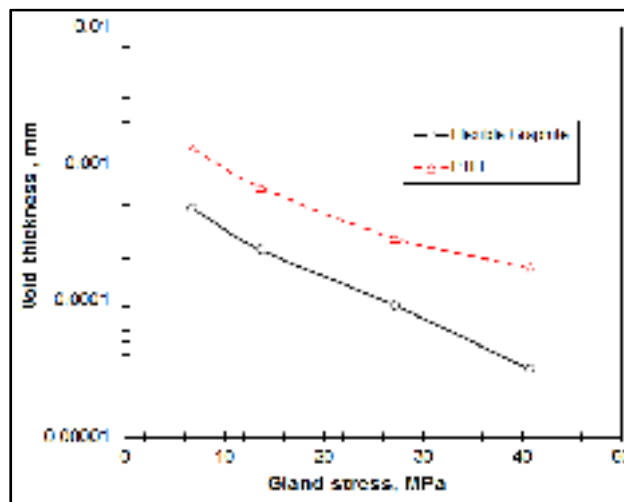
Figure 4.6 Equivalent void thicknesses of FG
and PTFE packing rings at different gland
stresses
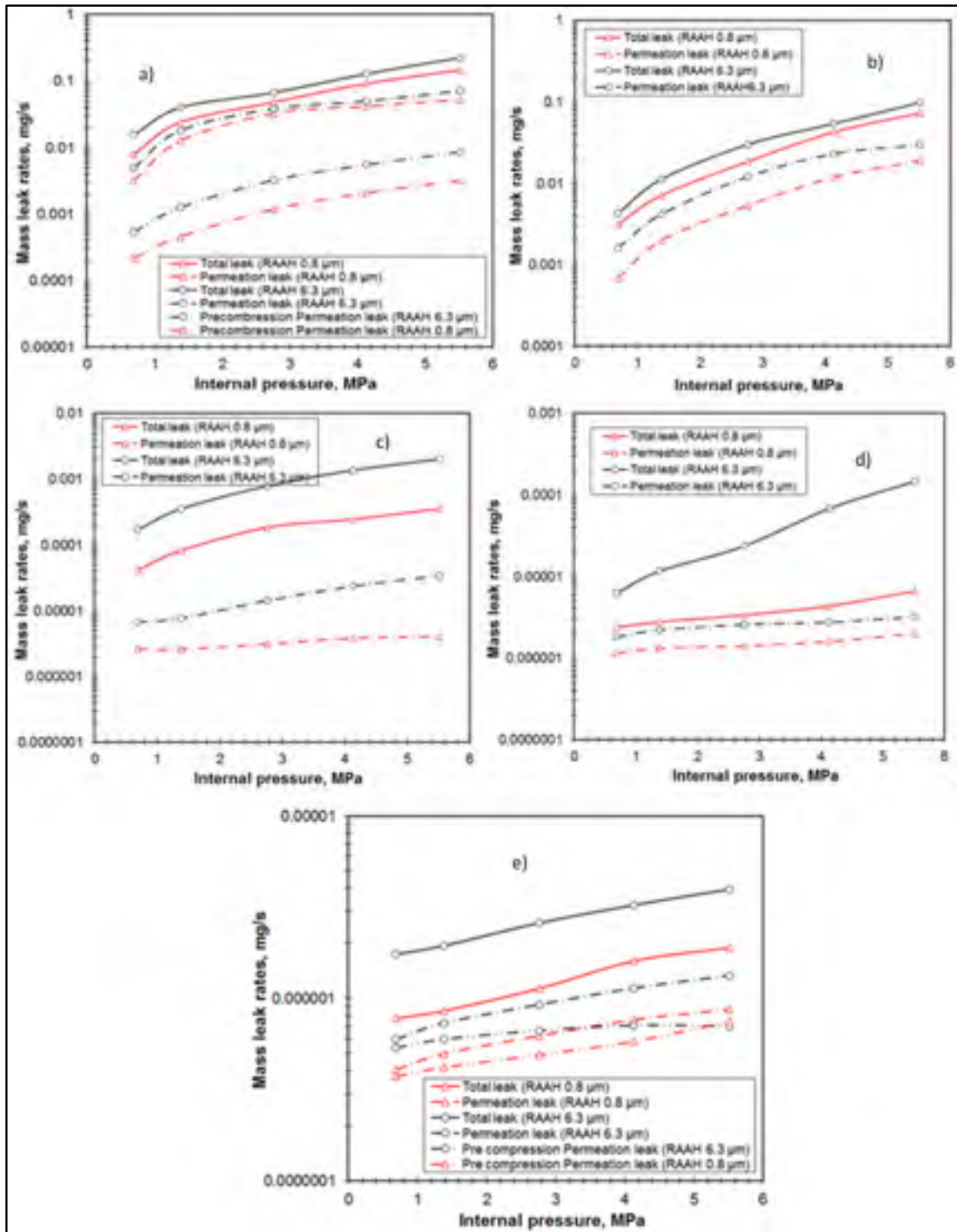
Figure 4.7 Leak rates of CF gasket at a) 14 MPa b) 28 MPa c) 55.2 MPa
d) 83 MPa e) 110.3 MPa

There are two to three decades between the total and permeation leaks with a higher difference at the high stress level. This is observed with both FG (Flexible Graphite) and PTFE packings. The coating deposited at the packing stem and packing housing interfaces fills the surface leak paths and prevents helium gas from leaking at the interface. The stem and housing have a smooth surface finish. Figure 4.5 shows the average percentage of permeation leak over the range of gland stress applied to PTFE and FG packing rings at different internal pressures. Once again, the low percentage of permeation leak indicates that most leaks are interfacial. However, the percentage of permeation increases with pressure more with FG than PTFE packing rings. Figure 4.6 shows the equivalent thickness of the gap between the packings rings and the stem and the housing if the interfacial leak is modelled to flow through two parallel cylinders (Kazeminia et Bouzid, 2016b). This interfacial gap decreases clearly with the gland stress, however it is smaller with flexible graphite indicating that the latter is a material that penetrates easier in the flange surface serrations and valleys produced by machining, which concretely constitute leak paths. This is confirmed by the lower leaks at the low stress when coating is applied. Similar tests were conducted with CF (Compressed Fiber), FG and PTFE gaskets with a standard phonographic surface finish of 6.3 µm and a smooth surface finish of 0.8 µm. It can be seen from figures 4.7, 4.8 and 4.9 that for the case of CF, FG and PTFE, the difference in the leak rates between the smooth and standard surface finish is relatively small except with the CF gasket where the difference is low at low gasket contact stress but somewhat high at higher gasket contact stresses. Indeed, the difference is nearly a decade at high gasket contact stress levels. The application of coating to reduce the interfacial leak to a minimum has demonstrated that the contribution of the latter is definitely important and in particular with CF and FG. The leak curves of figures 4.8 to 4.12, 4.14 to 4.18 and 4.20 to 4.24 show the permeation leaks in dotted lines and the total leaks in solid lines. The difference is very pronounced with all gaskets except PTFE at the high stress suggesting that permeation leak is of the same level as interfacial leak but in overall remains small.
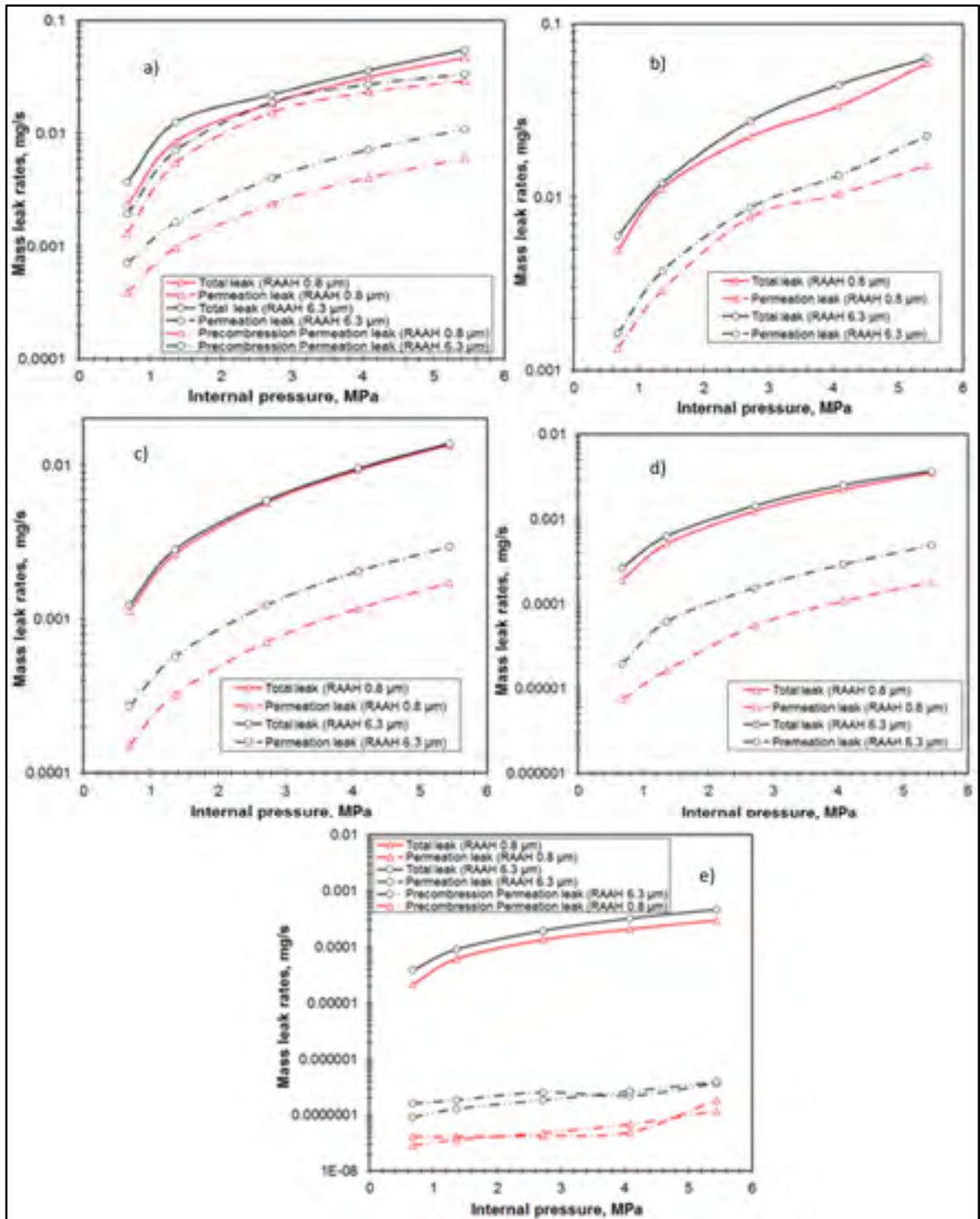
Figure 4.8 Leak rates of FG gasket at a) 14 MPa b) 28 MPa c)
55.2 MPa d) 83 MPa e) 110.3 MPa
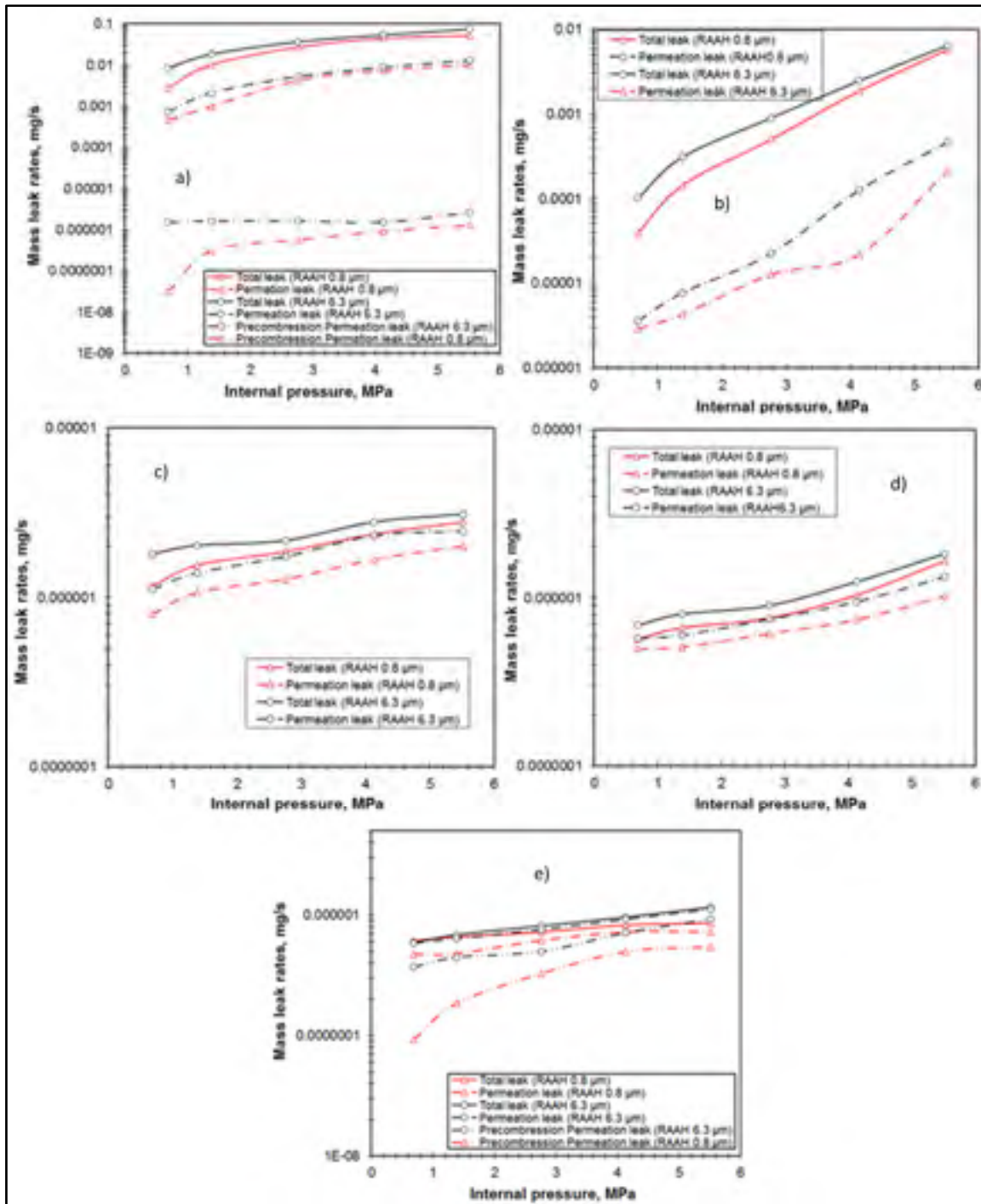
Figure 4.9 Leak rates of PTFE gasket at a) 14 MPa b) 28 MPa c) 55.2 MPa d) 83 MPa
e) 110.3 MPa
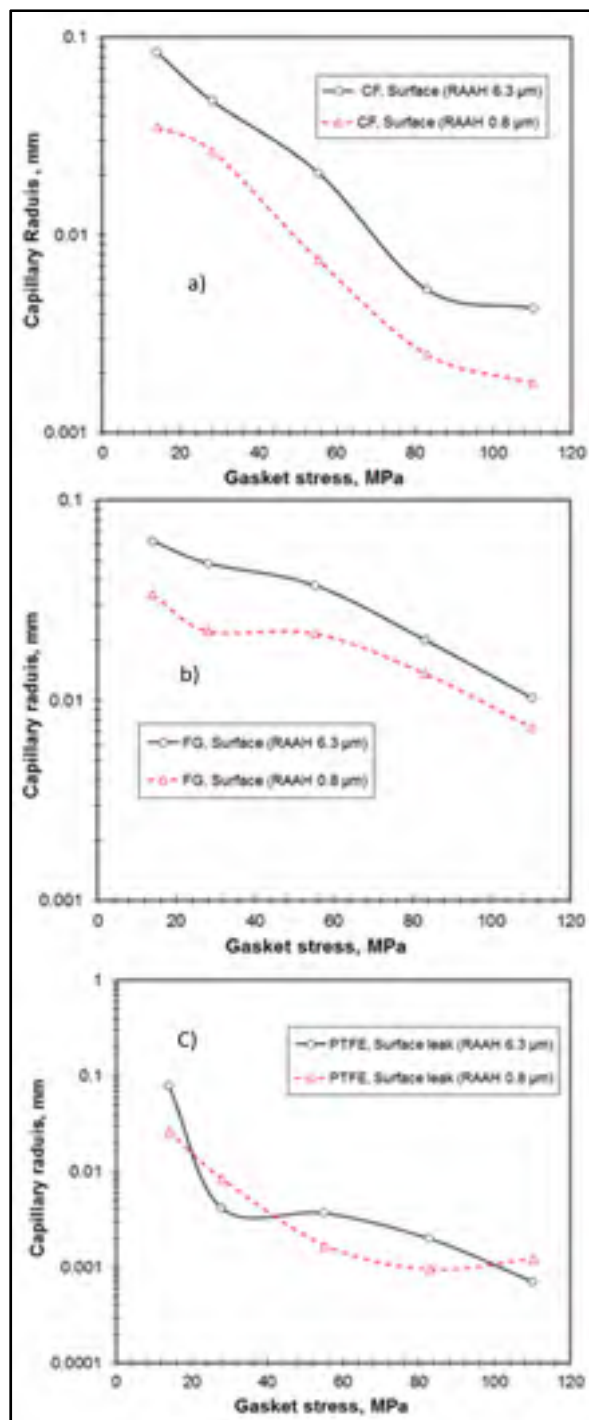
Figure 4.10 Radius of the capillary
generated by the phonographic finish with
a) CF gasket b) FG gasket c) PTFE gasket

However FG gasket shows a huge difference between total and permeation leaks at the high stress level suggesting that interfacial leak is predominant and the ability of flexible graphite to fill the surface leak paths and serrations is less than that of PTFE at the high stress level. In theory, the curves of permeation leaks for both surface finishes of all graphs of the same material should superimpose because interfacial leak is eliminated by the application of coating. Unfortunately, this is not the case because of a few considerations; firstly, the repeatability of a gasket material is known to be hard to obtain in terms of leak rate measurement especially at low level of leak, secondly the coating is not completely leak proof and also can penetrate inside the material to block partially permeation leak. Nonetheless the results give a good indication on the contribution of the interfacial leak in these gaskets under the specified test conditions.

Figure 4.10 shows the size of the capillary radius enrolled as a spiral groove made by the phonographic finish obtained with a lathe machine. The interfacial leak is assumed to flow in the circumferential direction inside this capillary. Reference (KAZEMINIA ET BOUZID, 2016B) was used to obtain the curves of figure 4.10. These curves show a net decrease of this radius with an increase of gasket contact stress. Depending on the gasket material and the applied gasket contact stress the capillary radius is between 0.1 mm and 0.001 mm. The radius is smaller for the smaller surface finish while the difference between the two is smaller for PTFE because of its ability to fill-in the serrations.

Figure 4.11 shows the contribution of interfacial leak expressed in percentage with respect to the total leak. The interfacial leak is averaged over the range of pressures and is given for the different gasket contact stresses. While the average contribution is somewhat constant over the range of stress, it would appear that the interfacial leak contributes around 80% for CF and FG while it is more or less equal to the permeation leak for PTFE with the interfacial leak at just less than 50%. This observation is valid for both surface finishes. Finally, the effect of pre-compression is shown in figures 4.12a and 4.13a. In figure 4.12 the PTFE gasket with coating is pre-compressed to 41 MPa before the stress is released to 7 MPa. Similarly, the FG packing rings with coatings are subjected to the same loading history.
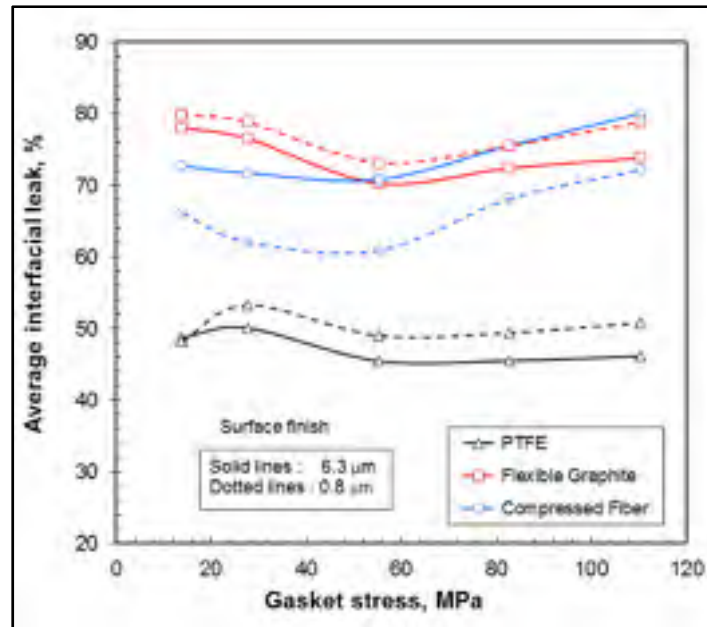
Figure 4.11 Contribution of permeation leak rates

It is clear that pre-compression decreased the leak rate by a least a decade. This is attributed to the fact that the more the load is higher the more the materials penetrate the serrations and closes the leak paths at the interface. The recompression back to 41 MPa shows that the leak rate returns back to the level it was before the stress was brought down to 7 MPa as may be seen in figures 4.12b and 4.13b.

4.5 Conclusion

This experimental work investigated the contribution of the interfacial and permeation leaks present in valve stem packing and sheet gaskets. The gaskets were made of CF, FG and PTFE sheet materials while the packing rings were made of FG and PTFE yarned materials. Interfacial leak is predominant in valve stem packing ring with over 95% as shown in this study.
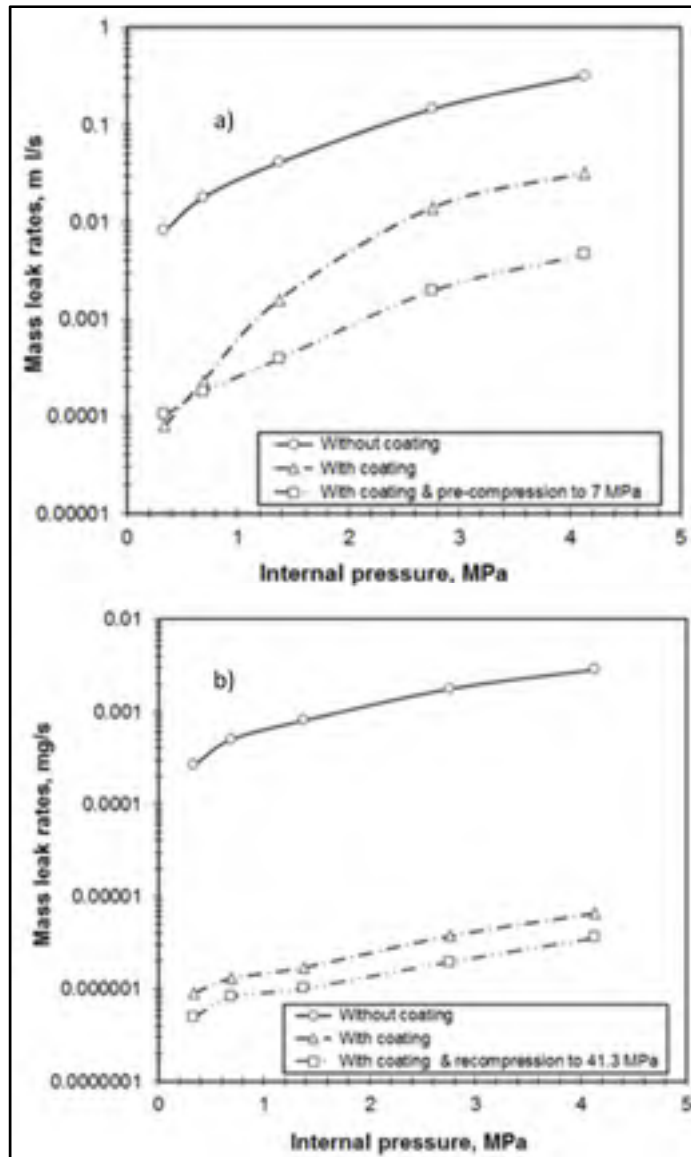
Figure 4.12 Pre-compression of PTFE packing to
41.3 MPa a) Leaks at 7 MPa b) Leaks at 41.3 MPa

The results for gaskets show that at low stress interfacial leak is predominant with low and high surface finish. As expected the ability of PTFE to reduce interfacial leak to a minimum is demonstrated especially at high stress. The surface finish has very little effect on leak with interfacial leak predominant for CF material at higher stress levels especially with rough surfaces.
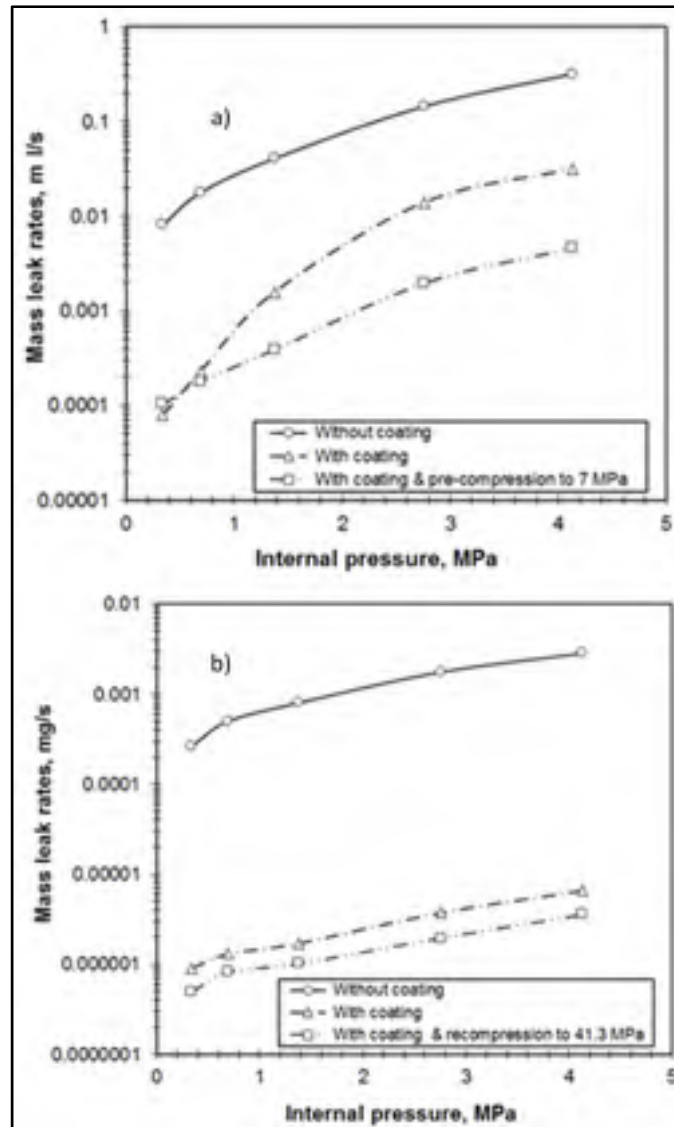
CF and FG gaskets showed a major contribution of interfacial leak with an average of 80% with respect to the total leak while PTFE showed on average a little less than 50%. Pre-compression of sealing materials is beneficial to tightness if it can be achieved in practice. This is particularly true for harder materials such as fiber reinforced materials.

CHAPITRE 5

LEAKAGE ESTIMATE IN NON-UNIFORMALY COMPRESSED PACKING RINGS

[a] Ali Salah Omar Aweimer[1], [b] Abdel-Hakim Bouzid[2], [C] Zijian Zhao[3]

[a] Ph. D. student, Mechanical Engineering Department, École de technologie supérieure, 1100 Notre-Dame St. West, Montreal, Quebec, H3C 1K3
[b] ASME Fellow, Professor, Mechanical Engineering Department, École de technologie supérieure, 1100 Notre-Dame St. West, Montreal, Quebec, H3C 1K3
[C] Ph.D. student, Mechanical Engineering Department, École de technologie supérieure, 1100 Notre-Dame St. West, Montreal, Quebec, H3C 1K3

5.1   Abstract

Characterizing the permeation performance of nano-porous material is an initial step towards predicting micro-flows and achieving acceptable designs in sealing and filtration applications. The present study deals with analytical, numerical, and experimental studies of gaseous leaks through soft packing materials subjected to non-uniform axial compression in valve stuffing boxes.

A new analytical model that accurately predicts gaseous leak rates through nano-porous packing materials assumed made of capillaries having an exponentially varying section. Based on Navier-Stokes equations with the first order velocity slip condition for tapered cylinder capillaries, the analytical model is used to estimate gas flow through soft packing materials. In addition, computational fluid dynamic modelling using CFX software is used to test its capacity to estimate the permeation of compression packing ring materials assuming the fluid flow to follow Darcy's law. Helium gas is used as a reference gas in the experiments to characterize the porosity parameters. The analytical and CFX numerical leak predictions are compared to leak rates measured experimentally using different gas types (Helium, Nitrogen,

Air, and Argon) at different pressures and gland stresses. The packing ring set is subjected to different axial compression in order to change the porosity with the stem axial distance.

Keywords: Valve compression packing, gland stress, leakage prediction, tapered capillary.

NOMENCLATURE

d	Inlet diameter of packing rings, m
k	Stem lateral pressure coefficient
D	Outlet diameter of packing rings, m
L	Leak rate, kg/s
ℓ	Length of packing, m
N	Number of capillaries
NR_g^4	Porosity Parameters for tapered capillary, m^4
P	Pressure, Pa
R	Pore radius at outlet near the gland, m
R_g	Pore radius at outlet near the gland, m
r	Radial direction, m
T	Temperature, K
u	Axial velocity, m/s
z	Capillary axial direction, m

Greek Letters

β Packing ring coefficient

λ Mean free path, m

μ Dynamic viscosity, Pa s

ρ Density, kg/m3

σ Tangential momentum accommodation coefficient = 1

σ_g Gland Stress, MPa

σ_z Axial gland stress, MPa

$\Re$ Specific gas constant, J/kg K

∇P Pressure difference between upstream and downstream, Pa

Non-Dimensional Number

Kn   knudsen number; $\left(\dfrac{\lambda}{2R}\right)$

Subscripts or Superscripts

i Inlet or upstream

o Outlet or downstream

h   Refers to housing

s   Refers to stem

g   Refers to gland

5.2   Introduction

Valves, which contain external and internal seals, are used to control fluid circulation in nuclear and petrochemical process plants. The stem seal prevents leakage from the inside to the atmosphere. The stuffing box contains usually compressed yarned packing rings, which are used to minimize leak and reduce the release of fugitive emissions to the atmosphere. This important component of the packed stuffing box and together with the gland is designed to maintain a threshold amount of contact pressure during the operation of a valve to guarantee a tight seal. The porosity of the compression packing can be optimized to minimize the leak. This optimization can be achieved experimentally, analytically, and through various simulation approaches.

The industry and researchers strive to improve the sealability of gaskets and compression packing materials to prevent leakage failure during service. However, this cannot be achieved without a thorough development of analytical and numerical tools to facilitate the prediction of the actual leakage behavior under the various working conditions. The selection of a suitable packing material depends on several parameters. Pressure, temperature, initial compression, aging and fluid compatibility are to name a few. Nevertheless, the maximum allowable leak rate level remains one of the most critical parameters to consider in most modern valve designs. In addition to the lessons-learned, health and safety issues, cost and maintenance for over decades of use, the new strict regulations enforced by government organization worldwide have triggered a lot of research to improve the performance of sealing materials.

Based on (Flitney, 2011) report, more than 60% of equipment requiring sealing compliance are attributed to valves. In view of this statistic, it is necessary to improve the design of packed stuffing boxes and enhance valve-stem sealing performance. The literature review on packed stuffing-boxes focuses on their mechanical behavior under different working conditions but very little research is dedicated to their leakage behavior and leak rate prediction. Schaaf et Schoeckle (2009b) conducted leakage tests of compression packings for the purpose of compliance with TA-Luft with the standard test VDI-2440. They found that several packing

materials that pass the TA-luft test in the laboratory have high leak rates in the field. They recommended the use of simultaneous hydraulic tensioners and the pre-deformation of packing rings with higher loads to improve the leak performance.

The control of the valve packing stem can be achieved under different circumstances. Veiga et al. (2008b) developed a packing design procedure that determines the required seating stress to achieve a target level of leakage rate during operation. They adopted the philosophy of the new rule for the design of gasketed flange joints (Bouzid et Beghoul, 2003) to packed stuffing boxes and concluded that gaseous emissions could be reduced by applying a predetermined seating gland stress on packing rings. Leakage in a compression packing can be simulated as a micro-flow through capillaries or micro-channels. The flow regime through a porous material is dictated by the interaction between gas molecules and the walls of the pores. It depends on the gland load and Knudsen number (Knudsen, 1909a). For values of the latter less than 0.001, continuum flow regime is predominant. For the range between 0.001 and 0.01, slip flow regime is present. For the range between 0.1 and 3, transitional flow regime takes place and, for values greater than 3, the flow is considered to be in the free molecular regime.

The analytical models in micro-channels are numerous. There are those that are based on capillary models (Beskok, Karniadakis et Trimmer, 1996; Tison, 1993), first order models (Arkilic, Schmidt et Breuer, 1997) and second order models (Aweimer, Bouzid et Kazeminia, 2017) . The effect of tortuosity is considered (Vallabh, Banks-Lee et Seyam, 2010). While most research focused on the different cross sections of the microchannel including circular square and triangular shape very few papers treat tapered shape models in case of liquid flow (Kumar et Kumar, 2009). There are few reported studies focusing on the prediction of gaseous flow through compression packing rings using CFD simulation. The simulation of fluid flow through porous packed stuffing materials is usually based on permeability. Using Darcy's Law, the prediction of leak rate of gases can realistically give reasonable results provided the permeability parameters are determined experimentally using a reference gas. Amyx, Bass et Whiting (1960b) measured permeability of rock samples. Adler, Jacquin et Quiblier (1990a) tested Fontainebleau sandstones for permeability and determined their pore size. They

simulated the stone material as a porous media and compared their predictions with real experimental data. Furthermore, (Gauvin et al., 1996) compared permeability based simulated results with experimental flow measurements on Continuous Fiber Reinforced Polymer Composites and concluded that there is significant difference due to the nature of the flow regime present in polymer composites. Finally, (Nield et Bejan, 1999a) studied the effect of porosity and inlet velocity on the pressure drop, mass flow, and cross-sectional average velocity at the center zone of porous materials. Analytical and numerical simulation results are compared together to highlight the virtues of the numerical simulations.

The aim of this paper is to shed light on the underlying phenomena for the prediction of gas flow in compression packing rings. This is done by developing an analytical capillary model with an exponential varying section dictated by the axial stress distribution in the packing rings. A numerical simulation using CFX and experimental testing are used to validate the model. The experimental tests are conducted using four gas types: air, nitrogen, argon, and helium. All tests and simulation models are conducted at the ambient temperature. Based on Navier-Stokes equations, the exponential varying section with the first slip order velocity at the walls is adopted in the analytical approach. The results show that the capillary with an exponential varying section is representative of flow through compression packing rings. The model can be used to predict gaseous leak in packed stuffing boxes.

5.2.1   Capillary flow model

The Navier-Stokes equations with the first order velocity slip condition for tapered cylinder capillaries is used to develop the capillary model with varying section to evaluate the leak rate through porous packing materials. The leakage prediction requires the porosity parameters to be known. This is achieved by calibration of the model experimentally with a reference gas; helium in this case. The flow is assumed to be fully developed locally, permanent, and isothermal. Because the capillary section is small relative to its length, the velocity in the radial direction is neglected and only the velocity in the axial direction is taken into account (Guo, 1998). Figure 5.1 shows a cut section of an idealized packing material showing capillaries of

a varying section through the length. The analytical model derivation start with fluid flow velocity obtained from the momentum conservation equation to which the boundary conditions are applied to obtain the mass flow rate through the micro tapered capillaries. This model considers a one-dimensional flow due to the axisymmetric flow assumption where the r dependency is neglected because of the simplified consideration of the flow profile that is lumped by the introduction of the momentum correction factor. Therefore, the only explicit dependency of the flow is the z direction (Munson-McGee, 2002).
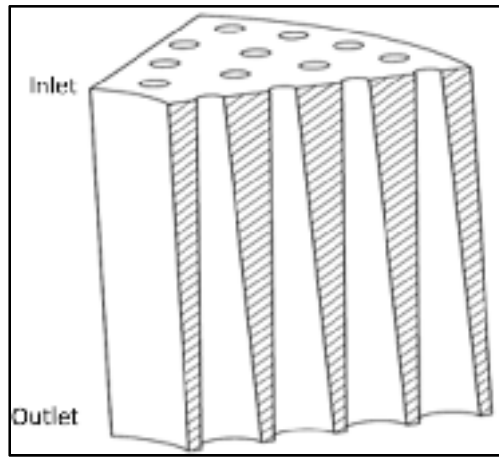
Figure 5.1Tapered capillary model
with first order slip flow

The correlation between velocity and pressure for a capillary model based on the conservation of momentum is (Colin, 2006):

$$\frac{1}{r}\frac{d}{dr}\left(r\frac{du}{dr}\right) = \frac{1}{\mu}\frac{dP}{dz} \tag{5.1}$$

Assuming a fully developed and isothermal flow is present in the tube, the boundary condition at the middle of tube would be:

$$\left. \frac{du(r)}{dr} \right|_{r=0} = 0 \tag{5.2}$$

The boundary condition at the wall, based on a first-order slip model is:

$$u(r,z) = -\frac{2-\sigma}{\sigma} \lambda \left. \frac{du}{dr} \right|_{r=R} \tag{5.3}$$

Integrating equation (5.1) twice and applying the above boundary conditions gives the solution for the velocity in the z direction as a function of the radial position such that:

$$u(r,z) = \frac{1}{\mu} \frac{dp}{dz} \left[\frac{r^2}{4} - \frac{R^2}{4} - \frac{2-\sigma}{\sigma} \lambda \frac{R}{2} \right] \tag{5.4}$$

The leak rate from N number of capillaries can be obtained by integrating the velocity through the capillary area such that:

$$L = N \int_0^R \rho \, 2\pi r \cdot u(r,z) \, dr \tag{5.5}$$

The cross section of the capillary changes with the axial length in the z direction because in a yarned packing the compressive stress changes with axial position on the stem. To obtain this variation it is assumed that the cross section is inversely proportional to the radial stress and hence the axial stress involving the lateral pressure coefficient. The axial stress distribution in the packing rings is given by an exponential form developed in (Diany et Bouzid, 2009) such that:

$$\sigma_x = \sigma_g \, e^{-\beta z} \tag{5.6}$$

The relationship between the capillary external radius and the axial position is therefore given by:

$$\frac{R^2(z)}{R_g^2} = \frac{\sigma_g}{\sigma_z} = \frac{\sigma_g}{\sigma_g e^{-\beta z}} = e^{\beta z}$$

$$R(z) = R_g e^{\frac{\beta z}{2}}$$

(5.7)

Where R_g is the capillary radius near the gland and σ_g is the gland stress. β is given by a rigorous calculation of the moment about the stem axis produced by the axial packing stress and friction forces at the walls neglecting the radial shear stress (Diany et Bouzid, 2006) such that:

$$\beta = \frac{6\left(\mu_h K_h D^2 + \mu_s K_s d^2\right)}{\left(D^3 - d^3\right)}$$

(5.8)

Where D is the inside diameter of the stuffing box, d is the stem diameter, k is the lateral pressure coefficient ratio and μ is the friction coefficient assumed equal at both wall. Substituting for u from equation (5.4) and R from equation (5.7) into equation (5.5) gives:

$$L = \frac{N \pi R_g^4 e^{2\beta z}}{4 \mu R T}\left[\frac{1}{2} p \frac{dp}{dz} + 16 \frac{2-\sigma}{\sigma} Kn \ p \frac{dp}{dz}\right]$$

(5.9)

It is to be noted that the quantity Kn_p is constant for an isothermal flow and can be written as a function of the outlet conditions such that Kn_p equals $K_o n_{po}$. Bearing in mind that the leak rate is constant and is independent of z, the integration with respect to z and p between the inlet and outlet gives the total leak rate passing through all capillaries such that:

$$L = \frac{N \pi \beta R_g^4 p_o^2 \left(\Pi^2 - 1 \right)}{8 \mu R T \left(1 - e^{-2\beta l} \right)} \left[1 + 16 \frac{2 - \sigma}{\sigma} \frac{Kn_o}{(\Pi + 1)} \right]$$ (5.10)

Where Kn is the Knudsen number defined as:

$$Kn = \frac{\lambda}{2R}$$ (5.11)

And Π is the pressure ratio and is given as follows:

$$\Pi = \frac{P_i}{P_o}$$ (5.12)

And λ is the mean free path given by:

$$\lambda = \frac{16 \mu}{5 P_o} \sqrt{\frac{RT}{2\pi}}$$ (5.13)

Equation (5.10) is dependent on the inlet to outlet pressure ratio Π and the two porosity parameters, namely the number and radius of capillaries N and R_g. As a general technique for the calculation of these parameters, a nonlinear regression approach is performed. The packing porosity parameters expressed as a function of packing stress, using helium as the reference gas are obtained by a curve fitting and are then used to predict the mass leak rate for other gases.

5.3 Experimental set up

An experimental stuffing box test bench is designed to measure the gas flowrate for yarned packing rings at room temperature as shown in figure 5.2 & 5.3. The stuffing box is composed

of four parts: the housing, the stem, the gland, and the yarned packing rings. The housing is 100 mm in height and can accommodate up to 6 packing rings of 3/8 inch square section (9.5 x 9.5 mm). A set of five packing rings was used for this study. The stuffing-box housing has an outside diameter of 80 mm inches and an inside diameter of 47.6 mm. The stem is made of steel with a diameter of 28.6 mm. The rig has three fluid systems. The pressurization system composed mainly with 4 different gas bottles, a gas valve switch system, an electro pneumatic pressure regulator, a pressure gage and a pressure transducer. The hydraulic system is composed of a hydraulic tensioner mounted on the stem to apply the load, an accumulator, a hand pump, a high pressure valve and a pressure gage. The leak detection system uses four different techniques: flowmeter, pressure decay, pressurized rise, and mass spectrometry, with the latter being able to detect down to 10^{-10} ml/s. A system of circuitry and valves is used to automatically direct the leak collection depending on the measuring technique. For this study, only the flowmeter and pressure rise were used to measure the leak rates. The rig is equipped with various sophisticated instruments: A strain gaged Wheatstone bridge to measure gland load, two LVDTs to pick up packing compression, a low and a high pressure transducers and thermocouples. The test rig is controlled by a computer and through a data acquisition and control unit using LABVIEW software. The data is recorded at regular intervals. Four gases, namely helium, argon, air, and nitrogen, are used in the experiment. The physical properties of gases are presented in Table 5.1. All tests are conducted under controlled room temperature. In addition, to avoid any effect of temperature variations on the leak measurements, the tubing systems are insulated. Finally, the test conditions related to gland stress and gas pressure are summarized in Table 5.2.

Table 5.1 Physical properties of gases

Gas type	Molecular Weight (g/mol)	mean free path m x10^{-9}	Density (mg/ml)	Viscosity (Pa,s) m x10^{-5}	Specific Gas Constant (J/Kg,K)
He	4.003	17.65	0.179	1.941	2077
Ar	39.94	6.441	1.632	2.217	208.172
N$_2$	28.01	6.044	1.251	1.8	296.8
Air	28.95	1.205	1.293	1.85	287

Table 5.2 Experimental testing conditions

Gas pressure (MPa)	0.34, 0.69, 1.38, 2.76 & 4.14
Stress gasket (MPa)	7, 14, 20.7 & 27.6
Packing rings	flexible graphite

Figure 5.2 Universal Packing Rig
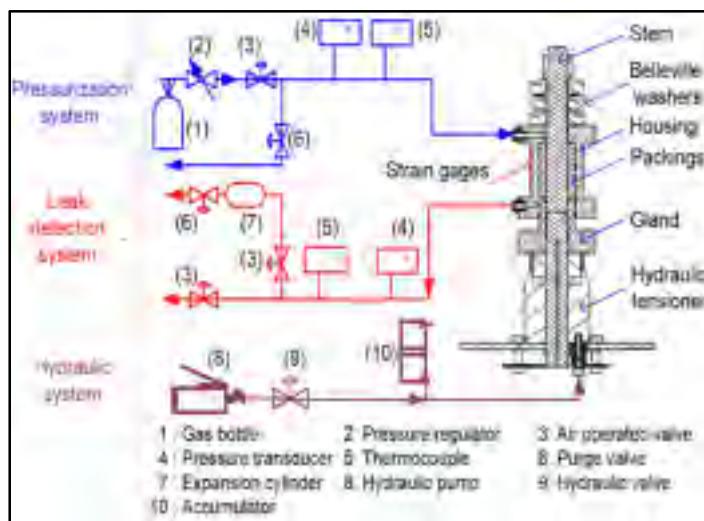
Figure 5.3 Universal Packing Rig Fluid Systems

5.4   Simulation using static structural model & CFX model

In order to further validate the analytical model, a simulation of the flow through the porous packing material is conducted using CFX module of Ansys. The boundary conditions in the simulation are quite simple. The yarded packing rings are modelled as a cylinder core with inside and outside surface walls that have no flow them. The elements are selected to be of the porous type with a gas pressure applied at the inlet bottom flat face ranging from 0.34 to 2.74 MPa, and a constant atmospheric pressure at the outlet top flat faces. The porosity of the element changes with the axial length and the amount of gland stress applied to the top ring. The flow is through the axial length of the porous material, which consists of five packing rings. Figure 5.4 shows the geometry and mesh for the set of the five soft packing rings in static structural model and CFX model. The mesh is refined near the inlet and outlet surfaces to improve the simulation and allows the solver to capture accurately the flow physics under the particular permeability conditions. A mesh refinement criteria of less than 5% change in the flow obtained at the upper output surface was adopted. Based on a low Reynold's number and the required physical and permeation properties, the physical CFX model provides a simulation with Darcy flow. Figure 5.5 illustrates a typical pressure distribution along the axial length of the five compression packing rings.

To obtain the porosity as a function of axial stress, two and five packing FEM static analysis models were carried out separately to obtain the stress distribution under different gland stress levels. The axial stresses in the packing rings were utilized to deduce a relationship between the axial stress and the porosity based on Darcy's model implemented in the CFX module. Extrapolating the results from two packings to 5 packings and calibrating for the leak numerically by that obtained experimentally one can find the relationship between the permeability Kp and packing axial stress and gas pressure as follows:

$$K_p = 0.66\,P^{\,0.02\sigma_z+1.4} \times \sigma_z^{-3.9+0.11P}$$

$$\text{(5.14)}$$
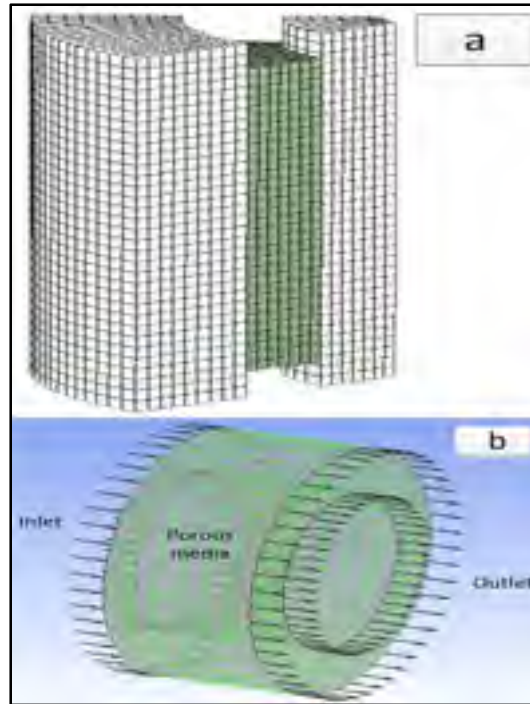
Figure 5.4 a) Static structural model
b) CFX Model

5.5   Results and discussion

Figure 5.6 shows the experimental leak rate measurements of helium gas for 2 and 5 packing rings under different gland stresses and internal pressures. The results are used as data source to determine the porosity parameters N and Rg of flexible graphite packing rings using the curve fitting technique and Eq.(10) in addition to obtain the relationship between permeability stress and pressure. These parameters N and Rg are used to predict leak for other gases, namely air, argon, and nitrogen. Figure 5.7 shows the axial stress distributions along the axial length of the five packing rings at different gland stresses namely 7, 14, 20.7 and 27.6 MPa. In general, as the gland stress increases the axial stress distribution increases. Not with standing, the packing axial stress decreases exponentially with the position on the stuffing box. The analytical results given by Eq.(6) are in good agreement with those obtained numerically using FEM. Figure 5.8 shows the permeability variation with stress and pressure based on an analysis obtained from FEM static analysis and CFX based on Darcy's model.
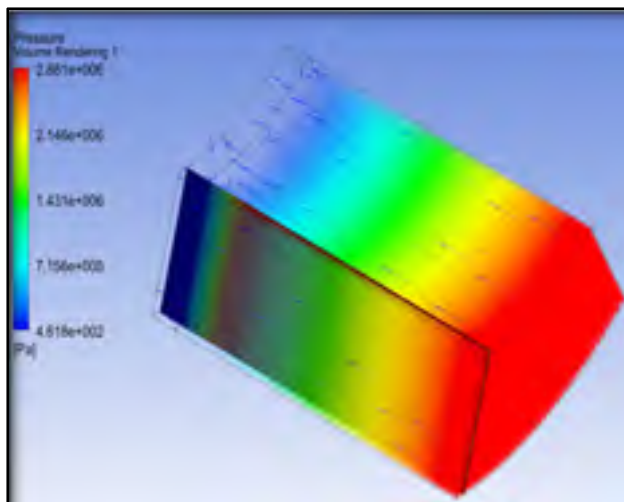
Figure 5.5 Pressure variations at the inlet
and outlet boundary in CFX Model
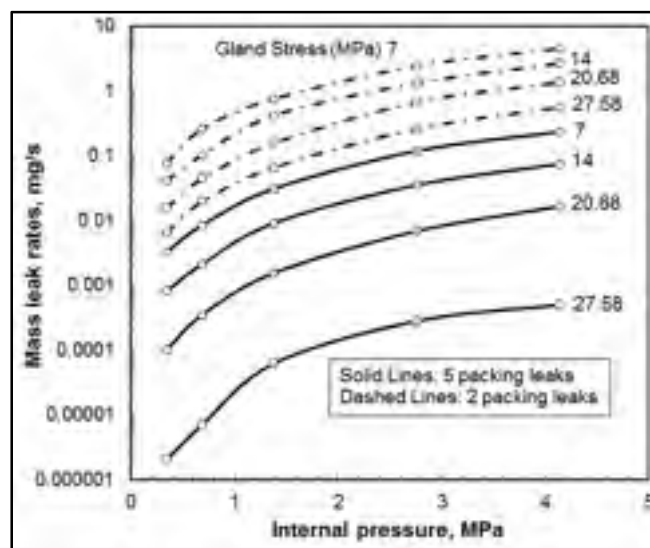
Figure 5.6 Helium leak rates of 2 and 5
packing rings
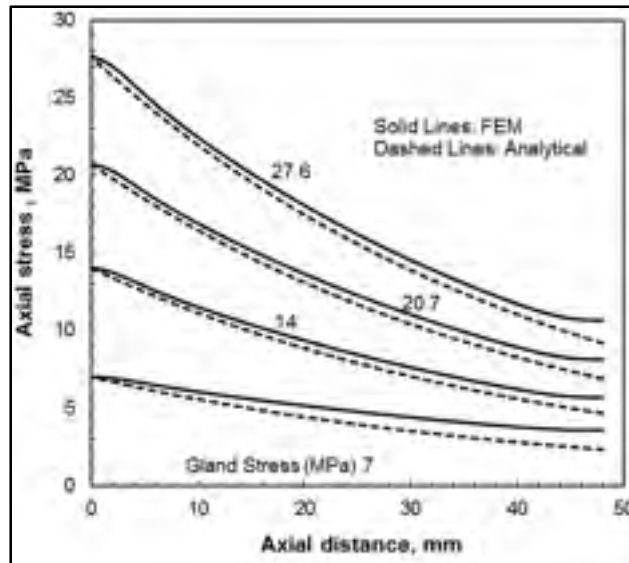
Figure 5.7 Axial stress distribution at different
gland stresses for 5 packing rings vs length

For the analytical capillary model with varying section and a first slip order boundary, the porosity parameters N and Rg used are those shown in Fig. 5.9 and are obtained experimentally using helium as a reference gas and a curve fitting of the leak rates on the basis of Eq.(10) as already pointed out. The methodology has been used for packings and gaskets successfully and is detailed in (Ochoński, 1988) (Grine et Bouzid, 2009). Figure 5.9 shows clearly the decrease of the capillary radius and its number in the packing set with the applied gland stress. Starting from 0.9 µm at the 7 MPa stress the radius of capillary reduce to 0.33 µm at 27.6 MPa whereas the number of capillaries reduces from 90000 to 10000 for the same stresses. Although the relationship with these two porosity parameters appears to be somewhat linearly deceasing one would expect to reach saturation. Has the gland stress been further increased a plateau known as tightness hardening where leak decreases in very small proportion with a drastic increase of load. This phenomenon has been observed generally with Teflon packing rings. Using these porosity parameters and the gas properties it is possible to predict the leak rate for all gases that do not interfere with the porous media structure.
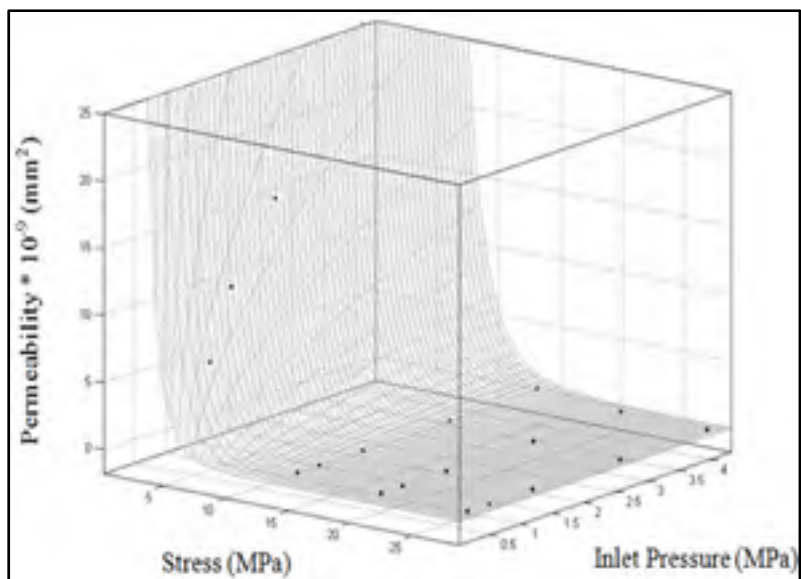
Figure 5.8 Permeability of Helium gas as function of
stress and pressure
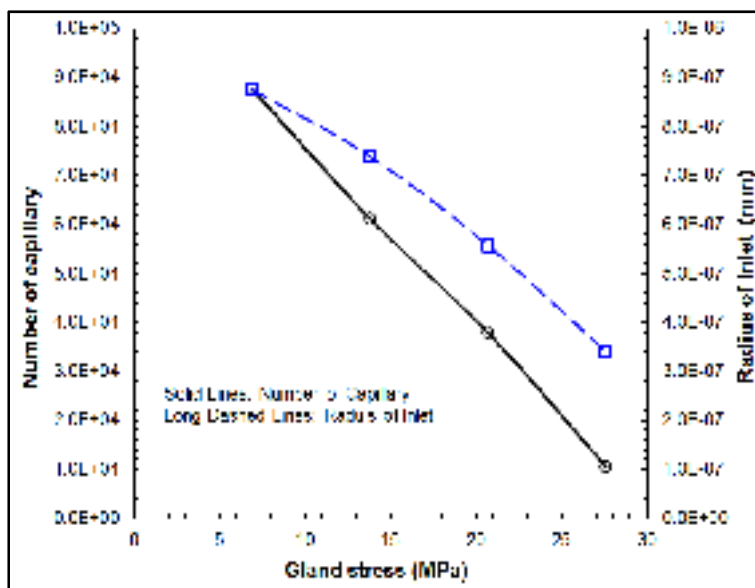
Figure 5.9 Number and inlet radius of capillary vs
gland stress
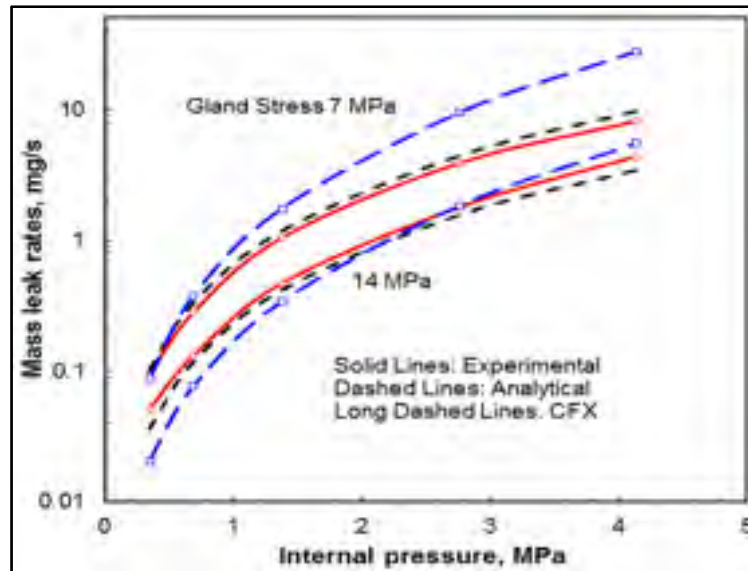
Figure 5.10 Prediction of leak rates of Nitrogen gas
at 7 & 14 MPa gland stress

In Figs. 5.10 and 5.11 the predictions using nitrogen gas are compared to those given numerically by CFX and the data obtained from tests under the same conditions of gland stress varying from 7 to 27.6 MPa and gas pressures varying from 0.34 to 4.14 MPa. These tests and comparisons are repeated in Figs. 5.12 and 5.13 for Argon and Fig. 5.14 and 5.15 for Air. In general the analytical and numerical models predict leak rate with reasonable accuracy. Both models give leak rate values close to those experimentally measured ones. The analytical model predicts slightly higher values while the numerical CFX model gives lower values. Nevertheless, in both cases the difference is not significant because the level of leak is small. At high stress levels the model seems to predict higher leak rate especially at those low leak rates obtained at the low pressure level. The dwell time to obtain leak rate stabilization may have been the cause. Had enough time been allocated for the leak to stabilize the values of leak rates would have increased, as higher dwell time is generally required for the gas to travel through the packing pores. Although the level leak rate and the applied gland stresses is representative of many existing applications, the analytical model is limited in terms of predicting leak rate to specific gases that do not change phase or react with the media. The model needs to be tested for low leak rate levels where other types of flow regimes predominates such as those with second order slip boundary condition and diffusion.

Finally, the flow is considered to pass only through the material pores. No surface flow or interfacial leak is considered in the analytical or the numerical models. The presence of the leak paths at the contact surface are the source of high leak especially at the low stress level as indicate in (Aweimer et Bouzid, 2018).

5.6 Conclusion

This study investigates the suitability of an exponential varying section capillary fluid flow model with first order condition to predict gaseous flow in soft flexible graphite packing. The capillary model section variation with length is based on the axial stress distribution. The model captures the true packing rings leakage behavior.
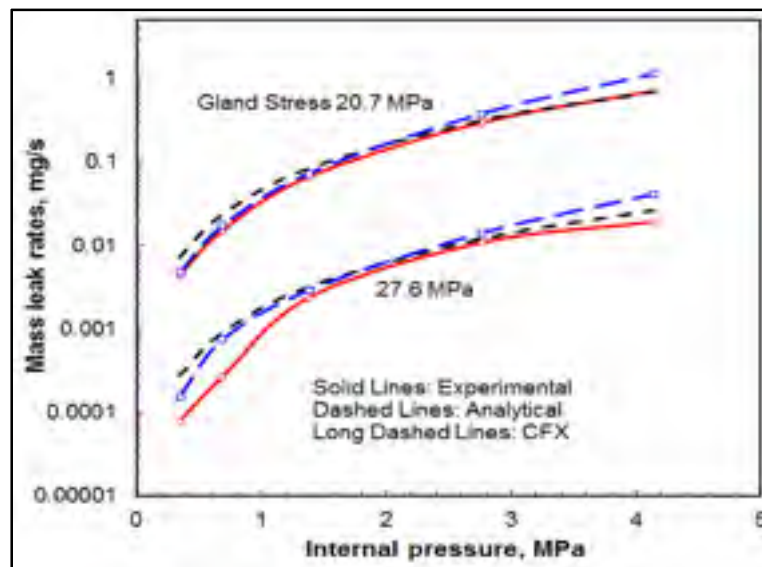
Figure 5.11 Prediction of leak rates of Nitrogen gas at
20.7 & 27.6 MPa gland stress
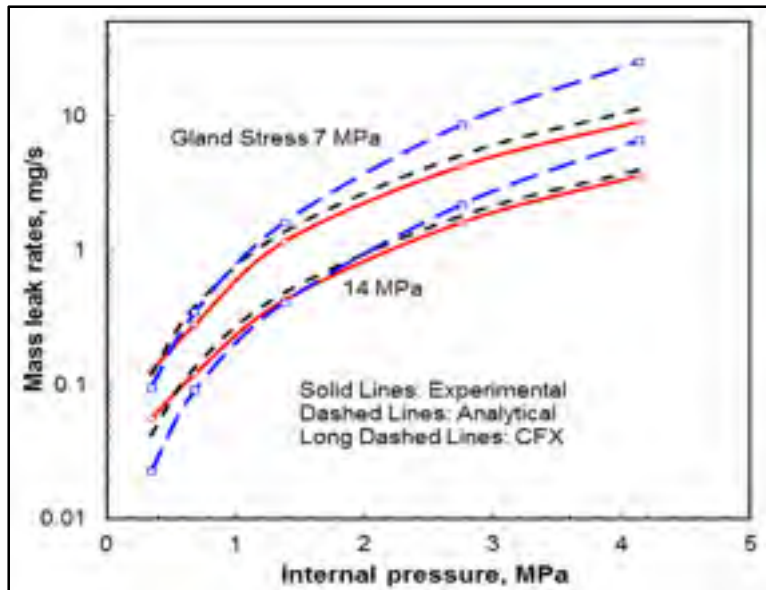
Figure 5.12 Prediction of leak rates of Argon gas at 7 &
14 MPa gland stress
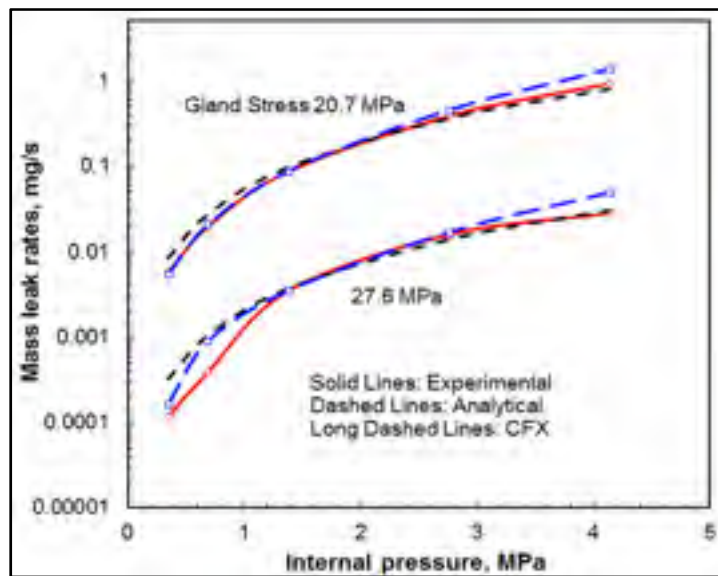
Figure 5.13 Prediction of leak rates of Argon gas at
20.7 & 27.6 MPa gland stress
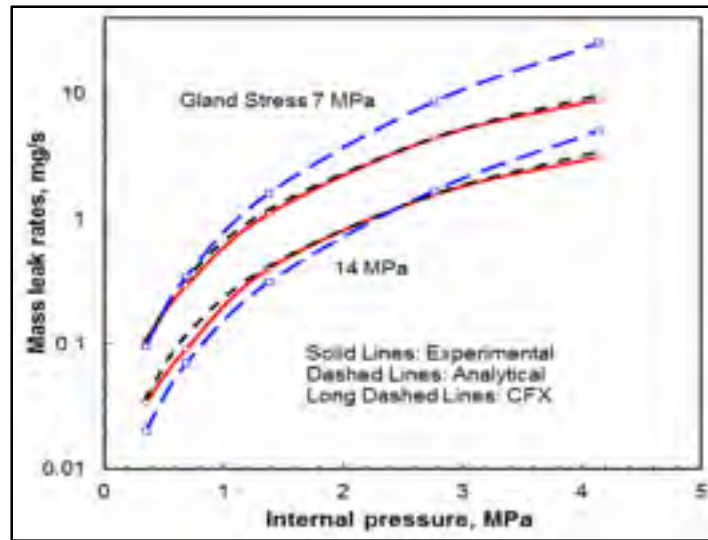
Figure 5.14 Prediction of leak rates of Air gas at 7 &
14 MPa gland stress
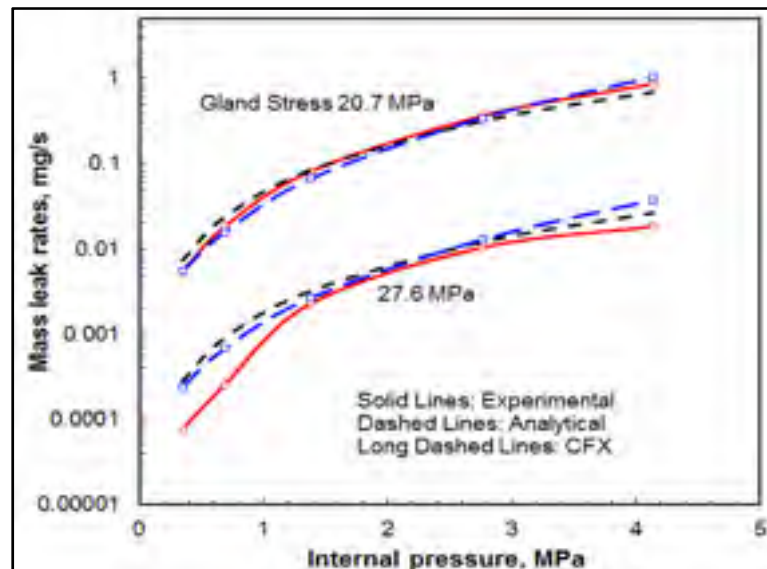
Figure 5.15 Prediction of leak rates of Air gas at 20.7 &
27.6 MPa gland stress

The validation of the analytical model was achieved experimentally at different operating conditions; tests are conducted with various types of gazes and under different internal pressures and applied gland stresses. A simulation using CFX module was run in parallel to support the analytical model. The CFX model is based on Darcy law and considers the porous

media to be a packed bed. The leak rates of the reference helium gas are used to obtain the porosity parameters required by the developed model. These parameters are then used to predict the gas flow for other types of gazes. The results demonstrate a good agreement between the predicted leak rates and those obtained from the experiments and the CFX model. The accuracy of the prediction may differ based on the type of gas, stress levels, and applied pressure levels.

CHAPITRE 6

PREDICTION OF LIQUID AND GAS LEAK RATES IN PACKED STUFFING BOX

[a] Ali Salah Omar Aweimer[1], [b] Abdel-Hakim Bouzid[2]

[a] Ph. D. student, Mechanical Engineering Department, École de technologie supérieure, 1100 Notre-Dame St. West, Montreal, Quebec, H3C 1K3
[b] ASME Fellow, Professor, Mechanical Engineering Department, École de technologie supérieure, 1100 Notre-Dame St. West, Montreal, Quebec, H3C 1K3

6.1   Abstract

The prediction of gas and liquid leak rate through packed stuffing boxes subjected to gas flow is a subject of very few studies in the literature. For better prediction of leakage, the change of porosity with length due to the non-uniform axial stress must be accounted for. There are few theoretical models on the prediction of leak rates in packing rings with capillary models. However, a model that incorporates the change of the capillary area with stress gives a better prediction.

In this paper, the first slip flow model is used to predict gas and liquid flow considering the straight capillaries and capillaries having an area dependent on the axial stress in the packing rings. An approach that uses an analytical-computational methodology based on the number and the size of pores obtained experimentally is adopted to predict gas and liquid leak rates in uniform and non-uniform compressed yarned packings. The Navier-Stokes equations associated with slip boundary condition at the wall are used to predict leakage. Experimental tests with helium, argon, nitrogen and air for gazes and water and kerosene for liquids will be used to validate the models. The porosity parameters characterization will be conducted experimentally with helium at a reference gas at different gland stresses and pressures.

130

Keywords: Predictions, compressible flow, incompressible flow, experimental approaches, analytical approaches, capillaries.

NOMENCLATURE

β	Packing ring coefficient
λ	Mean free path, m
μ	Dynamic viscosity, Pa s
ρ	Density, kg/m^3
σ	Tangential momentum accommodation coefficient = 1
σ_g	Gland Stress, MPa
$\mathfrak{R}$	Specific gas constant, J/kg K
∇P	Pressure difference between upstream and downstream, Pa
d	Inlet diameter of packing ring, m
k	Stem lateral pressure coefficient
Kn	Knudsen Number
D	Outlet diameter of packing ring, m
L	Leak rate, kg/s
ℓ	Length of packing, m
L_s	Slip flow in liquids, μm

N	Number of capillaries
NR^4	Porosity Parameters for tapered capillary, m^4
P	Pressure, Pa
R	Pore radius at outlet near the gland, m
R_g	Pore radius at the gland, m
r	Radial direction, m
T	Temperature, K
u	Axial velocity, m/s
z	Capillary axial direction, m

Subscripts and Superscripts

i	Inlet or upstream
o	Outlet or downstream
h	Refers to housing
s	Refers to stem
g	Refers to gland

6.2   Introduction

Valves with packed stuffing boxes have a wide range of applications in the chemical, petrochemical, and power plants industries. A valve is a mechanical device that controls the

flow of a fluid within a network of pipes. Valves are made with various components, the most important of which is the packed stuffing box mechanism. The stuffing box contains compression packing to prevent leaks of the confined fluid to the outer boundary. The packing rings with disordered porosity are subjected to a volumetric compression by the gland in the housing to produce a seal. They are made of square section yarned ropes or from a die, which are placed between the stem and the housing when compressed with the gland forms the packed stuffing box. They prevent fluid leaks in valve and protect the contact surfaces inside the valves from wear.

The leakage of valve stem packing is an important issue to scrutinize because of fugitive emission and their consequences on the environment, human health and safety. A few researchers concentrated their effort in studying the leakage performance of valve stem sealing and strived in documenting the leak test procedure and specifications in qualification and quality assurance standards. The leakage test set-up and leakage measurements in valve stuffing boxes are detailed and explained by (Hutchins, 1962) and (Baumann, 1966). Steinke et Abrahimzadeh (2000) also presented the results of different methods of leakage measurement in valves under different test conditions in order to show the correlations between them. They concluded that the different leakage measurement methods give different results, because the packing rings are affected by different parameters such as lubrication, load retention and stability of the parameter control loop. Reeves, Ross et Wasielewski (2004) developed a simple test bench for both packed valves and bellow seal valves that use different packing materials. The results show that careful valve stem packing material selection for a specific application minimizes fugitive emissions, decreases health hazard and reduces maintenance costs. Fugitive Emission performance, corrosion behaviour, and general physical and chemical attributes are the main parameters that are selected to identify the valve stem packing characterization. The API-622 standard test procedure evaluates mainly fugitive emission of a set of packing in a rotating stem valve fixture. The API-589 standard evaluates the performance of valve stem packing when it is exposed to a fire. It provides enough details about the stem packing materials strength and weakness under severe conditions. The API-622 500 ppm limit requirement has a significant impact on the manufacturing and material quality

of a valve stem packing (Harrison, 2004). Indeed, the leakage performance is the most important factor for fugitive emissions compliance. Most of the industrialized countries such as Canada, USA and others in Europe (Producers, February, 2014; Schaaf et Schoeckle, 2009a; Standards, April 2014) have implemented standards to regulate emissions of valves which are hazardous to the working personnel and the environment. Generally, the leak rate through compression packings is mostly affected by numerous parameters such as stress distribution in the stuffing box, the fluid pressure, and tolerances between the contact surfaces, the packing material, the number of packing rings and the type of fluid.

In order to control the leak rates an external axial force on the packing rings through the gland is applied. As a result, a radial force is generated in the packing rings, which reduces the pore size, the micro-channels and the leak paths at the interface between the packing and the stem and the housing. From this perspective, the stress distribution in the stuffing box is therefore the main parameter that controls leakage. Few models exit that treat the stress distribution (Jolly et Marchand, 2006; Masi, Bouzid et Derenne, 1998). The most recent work is by (Diany et Bouzid, 2006) who present a more accurate approach to evaluate the variation of the stress distribution in the axial direction and present an analytical solution of the lateral pressure coefficient of the interfaces between the packing and the stem and housing. Veiga et al. (2008a) investigates the seating stress necessary to assure a minimum leak rate in a valve packing stem in high pressure applications. They found that there is a minimum seating stress value for each compression packing material. Furthermore, when an applied seating stress increases, the level of fugitive emissions from the valve decreases. In addition, (Veiga, Girão et Cipolatti, 2009) designed a test rig to examine the different mechanical properties of the valve stem packing such as the relaxation and the effect of the number of packing rings on the leak rate. The results indicate that relaxation decreases when the applied gland stresses increases, and confirm that better tightness is achieved with higher number of packing rings. Nesbitt (2011) suggests that the number of packing rings used in valve stuffing boxes could be used to indicate the pressure rating of the valve.

For compressible fluids through packed stuffing boxes, (Diany et Bouzid, 2011) conducted experimental leak tests with different gases to investigate the effect of different materials and numbers of packing rings. The results confirm that the leak rate values with PTFE material are lower than flexible graphite material. And that the leak rate with four packing rings is much smaller than with two. Kazeminia et Bouzid (2016a) used three different analytical models to predict the leakage through packing rings. Capillary and concentric cylinder models with first order slip flow and modified Darcy model were used. Aweimer, Bouzid et Kazeminia (2019) used the first and second split models with the Ergun model to predict gas leak rates through graphite packing rings at different pressures and stresses. They conclude that the second slip flow model is more accurate than the other models for all range of Knudsen number. Unfortunately, in all these mentioned models, the porosity change of the packing with its length due to the axial stress distribution is not accounted for. The pores at the fluid inlet are greater than the once near the glad because the stress is much lower.

For incompressible fluids, the leakage rate through packing is very small compared to compressible fluids under the same conditions. Kockelmann et al. (2009) tested packed stuffing boxes with gas and water at high temperature. They found that flexible graphite packing relaxes more when exposed to air medium than water and steam. In addition, they conclude that PTFE packing produce less stem frictional forces when used with air media than water or steam.

This paper presents a method to characterize and predict the leak rates in porous braided packing rings used in valve stuffing boxes for gases and liquids through two types of packing rings namely PTFE and Flexible graphite. The porosity parameters N and R are estimated experimentally by tests conducted with helium used as a reference gas. The packing universal test bench is used to measure leak rates of packing rings with gases and liquids experimentally. Leakage under different conditions with gases namely helium, air, nitrogen and argon and liquids namely water and kerosene are measured with these two types of packing rings. The developed analytical models are then used to predicate leak rates with other gases and liquids. The analytical models are based on Navier-Stokes equations with the low-speed isothermal

gaseous fluid flow in micro- and nano-channels having straight cylindrical and tapered geometries with first order slip flow boundary conditions. Finally, the predicted leaks obtained from analytical approach are compared to the experimental data and a good correlation is observed.

6.3   Physical Models

The theoretical modelling of fluid flow and the leakage prediction through porous medium has become a spotlight during the past two decades. As a result, various flow models are applied for leak rate predications (Bauer, 1965; McGrew et McHugh, 1965; Vermes, 1960) in many applications such as valve stem sealing. The theoretical models related to leakage prediction are initiated from the Navier-Stokes equations. Many experimental results provided proofs to support these equations with different slip boundary conditions (Huang et Breuer, 2007; Lauga et Squires, 2005; Pit, Hervet et Leger, 2000). The leakage prediction requires the porosity parameters known as the number and diameter of the capillaries N and R) to be known. This is achieved by calibration of the model experimentally with a reference gas; helium in this case.
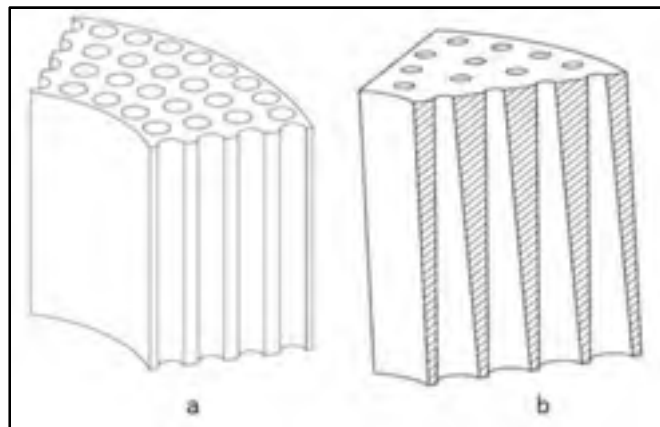
Figure 6.1 Capillary model a) Straight b) Tapered

The flow is assumed to be fully developed locally, permanent, and isothermal. Because the capillary section is small relative to its length, the velocity in the radial direction is neglected

and only the velocity in the axial direction is taken into account (Nield et Bejan, 2006). The analytical model derivation starts with fluid flow velocity obtained from the momentum conservation equation to which the boundary conditions applied to obtain the leak rate through the micro circular or tapered capillaries.

6.3.1 Tapered and straight capillary models for gas flow

The tapered and straight capillary models consider a one-dimensional flow due to the axisymmetric flow assumption where the r dependency is neglected because of the simplified consideration of the flow profile that is lumped by the introduction of the momentum correction factor. Therefore, the only explicit dependency of the flow is the z direction (Munson-McGee, 2002). The correlation between velocity and pressure for a capillary model based on the conservation of momentum is (Colin, 2006):

$$\frac{1}{r}\frac{d}{dr}\left(r\frac{du(r)}{dr}\right) = \frac{1}{\mu}\frac{dP}{dz} \tag{6.1}$$

Assuming a fully developed and isothermal flow is present in the channel, the boundary condition at the axis of tube would be:

$$\left.\frac{du(r)}{dr}\right|_{r=0} = 0 \tag{6.2}$$

The boundary condition at the wall, based on a first-order slip model is:

$$u(r,z) = -\frac{2-\sigma}{\sigma}\lambda\left.\frac{du}{dr}\right|_{r=R(z)} \tag{6.3}$$

Integrating equation (6.1) twice and applying the above boundary conditions gives the solution for the velocity in the z direction as a function of the radial position such that:

$$u(r,z) = \frac{1}{\mu}\frac{dp}{dz}\left[\frac{r^2}{4} - \frac{R^2(z)}{4} - \frac{2-\sigma}{\sigma}\lambda\frac{R}{2}\right] \tag{6.4}$$

The leak rate from N number of capillaries can be obtained by integrating the velocity through the capillary area such that:

$$L = N\int_0^R \rho\, 2\pi r * u\,(r,z)\,dr \tag{6.5}$$

6.3.2   Tapered capillary

The cross section of the capillary changes with the axial length or the z direction because in a yarned packing the radial compressive stress changes with the axial position on the stem. To obtain this variation, it is assumed that the cross section is inversely proportional to the radial stress, which is deduced from the axial stress and the lateral pressure coefficient. The axial stress distribution in the packing rings is given by an exponential form developed in (Diany et Bouzid, 2009) such that:

$$\sigma_x = \sigma_g\, e^{-\beta x} \tag{6.6}$$

The relationship between the capillary external radius and the axial position is therefore given by:

$$\frac{R^2(z)}{R_g^2} = \frac{\sigma_g}{\sigma_z} = \frac{\sigma_g}{\sigma_g e^{-\beta z}} = e^{\beta z}$$
$$R(z) = R_g e^{\frac{\beta z}{2}} \tag{6.7}$$

Where R_g is the capillary radius near the gland and σ_g is the gland stress. β is given by a rigorous analysis of the moment about the stem axis produced by the axial packing stress and friction forces at the walls neglecting the radial shear stress such that (Kazeminia et Bouzid, 2014b):

$$\beta = \frac{6\left(\mu_h K_h D^2 + \mu_s K_s d^2\right)}{\left(D^3 - d^3\right)} \tag{6.8}$$

Where D is the inside diameter of the stuffing box, d is the stem diameter, k is the lateral pressure coefficient ratio and μ is the friction coefficient at the interfaces between the packing and the stem and the housing. Substituting for the velocity u from equation (6.4) and R from Eq. (6.7) into Eq. (6.5) gives:

$$L = \frac{N\pi R_g^4 e^{2\beta z}}{4\mu R T}\left[\frac{1}{2}p\frac{dp}{dz} + 16\frac{2-\sigma}{\sigma}Kn\ p\frac{dp}{dz}\right] \tag{6.9}$$

It is to be noted that the quantity $K_n p$ is constant for an isothermal flow and can be written as a function of the outlet conditions by $Kn_o p_o$. Bearing in mind that the leak rate is constant and is independent of z, the integration with respect to z and p between the inlet and outlet gives the total leak rate passing through all capillaries such that:

$$L = \frac{N\pi\beta R_g^4 p_o^2\left(\Pi^2 - 1\right)}{8\mu R T\left(1 - e^{-2\beta l}\right)}\left[1 + 16\frac{2-\sigma}{\sigma}\frac{Kn_o}{(\Pi + 1)}\right] \tag{6.10}$$

For a flow through constant radius capillaries, it can be shown that incorporating Navier - Stocks flow equations gives, the total mass flow rates through all capillaries is (Aweimer, Bouzid et Kazeminia, 2019):

$$L = \frac{N \pi \beta R_g^4 p_o^2 \left(\Pi^2 - 1\right)}{8 \mu R T \left(1 - e^{-2\beta l}\right)} \left[1 + 16 \frac{2 - \sigma}{\sigma} \frac{Kn_o}{\left(\Pi + 1\right)}\right] \tag{6.11}$$

Where Kn is the Knudsen number defined as:

$$Kn = \frac{\lambda}{2R} \tag{6.12}$$

And Π is the pressure ratio and is given as follows:

$$\Pi = \frac{P_i}{P_o} \tag{6.13}$$

And λ is the mean free path given by:

$$\lambda = \frac{16 \mu}{5 P_o} \sqrt{\frac{RT}{2\pi}} \tag{6.14}$$

Equations (6.10) and (6.11) are dependent on the inlet to outlet pressure ratio Π and the two porosity parameters, namely the number and radius of capillaries N and R_g. The general technique used for the determination of these parameters is to perform a nonlinear regression approach on the leakage data obtained with a reference gas. In this paper the packing porosity parameters are function of the packing stress and are obtained using helium as the reference gas. They are then used to predict the mass leak rate for other gases.

6.3.3   Straight capillary model for liquid flow

For simplification, the straight capillary model is adopted for liquid leak predictions. The conservation of momentum equation (6.1) is the starting point as in the prediction of gas leak.

By assuming a fully developed and isothermal flow is present in the tube, the boundary condition at the middle of tube would be:

$$\frac{du(r)}{dr}\bigg|_{r=0} = 0 \tag{6.15}$$

The boundary condition at the wall, based on a first-order slip model of liquids, is:

$$u(r,z) = -L_s \frac{du}{dr}\bigg|_{r=R_g} = -L_s \left(\frac{du}{dr}\right)_w \tag{6.16}$$

Where L_s slip length in liquid condition in circular capillaries and is given by (Choi, Westin et Breuer, 2003):

$$L_s = 0.059|\gamma^{0.485} \quad \text{where} \quad \gamma = \frac{\Delta P R_g}{2\mu l} \tag{6.17}$$

Integrating Eq. (6.1) twice and applying the above boundary conditions gives the solution for the velocity in the z direction as a function of the radial position such that:

$$u(r,z) = \frac{1}{\mu}\frac{dp}{dz}\left[\frac{r^2}{4} - \frac{R_g^2}{4} - L_s \frac{R_g}{2}\right] \tag{6.18}$$

The leak rate from N number of capillaries can be obtained by integrating the velocity through the capillary area such that:

$$L = N\int_0^R \rho 2\pi r * u(r,z)dr \tag{6.19}$$

Finally, the total leak rate through all capillaries is given by:

$$L = \frac{N R_g \pi \rho \left(P_i - P_o \right)}{8 \mu l} \left[1 + \frac{4 L_s}{R_g} \right]$$

(6.20)

The packing porosity parameters are obtained from a curve fitting of the data obtained using helium as the reference gas. They are then used to predict the mass leak rate for liquids.

6.4 Experimental Setup

The experimental leak tests of compression packings were conducted on the universal packing test rig shown in Figure 6. 2. The universal packing rig has two staffing box modules one for gases and another one for liquids. It has three fluid systems: a hydraulic tensioner system, a gas pressurization system and a leak detection system for gases and a separate one for liquids. The load is applied to the gland through the stem using a hydraulic tensioner and a hand pump. The gland stress is deduced from the measurement of the load in the stem using a Wheatstone bridged strain gaged bounded to it.

Figure 6.2 Universal packing test rig for gases

The pressure is applied to the stuffing box and controlled by an electronic valve and regulator connected directly to the 2500 psi gas bottles. The rig has several instruments that are monitored through a data acquisition system and an interface program written under LabVIEW software. Among the monitored parameters are: pressure, gland stress, temperature, time and leak rates.

6.4.1   Gas leak test experiments

The gas test module and a housing of a total length of 104.8 mm (4.125 inches) in height and can accommodate up to 6 packing rings of 9.525mm (3/8 inch) square section. Only a set of five packing rings were inserted for the purpose of the gas test study.

The stuffing box housing has an outside diameter of 79.4mm (3.125 inches) and an inside diameter of 47.6 mm (1.875 inches). The stem is made of steel with a diameter of 28.6 mm (125 inches). The displacement of the packing rings due to compression is measured by mains of two LVDTs installed diametrically opposed. Depending on the level of the leak rate, four different leak measurement techniques are used: flow meter, pressure decay, pressurized rise and mass spectrometry, with the latter being able to detect down to 10^{-10} ml/s. For this study, only the flowmeter and the pressure rise methods were used to measure the leak rates. A gland stress ranging from 1000 to 4000 psi (6.9 to 27.6 MPa) in steps of 1000 psi is applied. For every gland stress level, pressures ranging from 50 to 600 psi (0.34 to 4.1 MPa) in steps are applied to the packed stuffing box. Four gazes, namely nitrogen, argon, air and helium were used in the experiment. The physical properties of these gases are presented in Table 6.1.

In order to avoid any effect of temperature variation on the leak measurements, the pressurization and leak detection tubing systems are thermally isolated. The experimental testing condition for gas tests are presented in Table 6.2.

Table 6.1 Physical properties of the gases

Gas	Helium	Argon	Nitrogen	Air
Viscosity (Pa, s) (m x10^{-5})	1.941	2.217	1.8	1.85
Density (mg/ml)	0.179	1.632	1.251	1.293
Specific Gas Constant (J/Kg,K)	2077	208.172	296.8	287
mean free path m x10^{-9}	17.65	6.441	6.044	1.205
Molecular Weight (g/mol)	4.003	39.94	28.01	28.95

Table 6.2 Experimental conditions and materials used in gas tests

Gas pressure (MPa)	0.345,0.69, 1.38, 2.76 & 4.14
Gland stress (MPa)	7, 14, 20.7 & 27.6
Packing materials	Flexible Graphite

6.4.2   Liquid leak test experiments

The liquid test module shown in Figure 6.3 has a housing of a total length of 105 mm (4.125 inches) in height and can accommodate up to 7 packing rings of 9.5 mm (3/8) inch square section. Only a set of four packing rings were inserted for the purpose of liquid tests with water and kerosene.

Figure 6.3 Capillary model a) Straight b) Tapered

The stuffing-box housing is specially designed to include a central hollow cylinder that is inserted inside the housing between the packing and the stem to make a tight chamber so that the packing rings can be installed in the stuffing box inside a bucket filled with the tested liquid to avoid air bubbles trapped into the system. The stuffing box has an outside diameter of 100.28 mm (3.94 in.) and can accommodate a packing of an outside diameter of 57 mm (2.25 in.) and inside diameter of 38 mm (1.5 in.). The stem is made of steel with a diameter of 28.6 mm (1.125 inches). In this study, a special liquid leak measuring device build previously which can measure leaks down to 10-5 mg/s of water is used (Grine et Bouzid, 2011b).

A gland stress ranging from 10.34 to 27.6 MPa (1500 to 4000 psi) is applied through a hydraulic tensioner fixed to the stem. For every gland stress level, helium gas pressures ranging from 0.34 to 2.76 MPa (50 to 400 psi) were applied in steps and leak rate was measured. The Physical properties the tested liquids are presented in table 6.3. Finally, the experimental conditions are presented in table 6.4.

Table 6.3 Physical properties of the liquids used in
experimental investigation

Liquids	Water	Kerosene
Dynamic viscosity (N.s/m^2 x 10^{-3})	0.798	2.17
Density (kg/m^3)	998.21	820

Table 6.4 Experimental conditions and materials
used in liquid tests

Gas pressure (MPa)	0.345,0.69, 1.03, 1.38, 1.72 and 2.06
Gland stress (MPa)	10.34, 13.79, 17.24, 20.68 and 24.14

6.5   Results and Discussion

6.5.1   Gas test results

Figure 6.4 shows the experimental leak rate results with helium gas under different gland stresses (7, 14, 20.7 and 27.6 MPa) and different internal pressures (0.34, 0.69, 1.38, 2.76 and 4.14 MPa). These leak test results are used as data source in order to identify the porosity parameters N and R for tapered and straight capillaries of flexible graphite packing rings using the curve fitting technique and Eqs. (10) and (11).
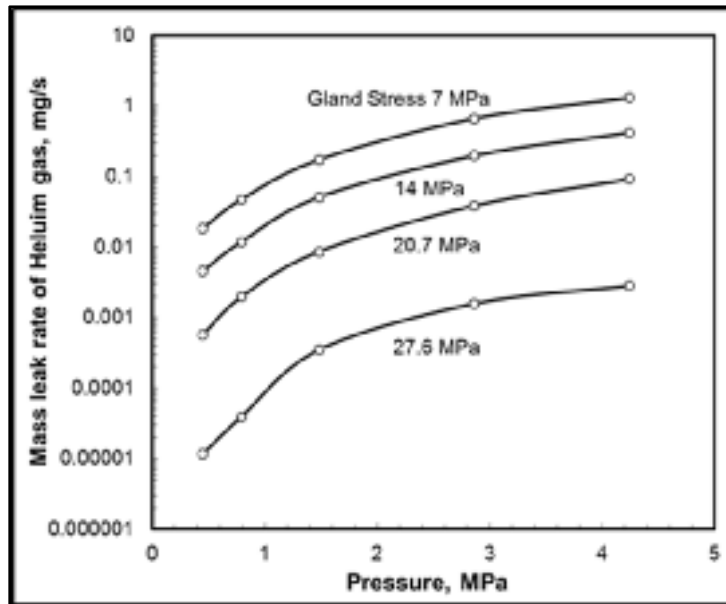
Figure 6.4 Leak rates of helium gas for different stresses

These parameters are then used to predict the leak rate for other gases, namely air, argon, and nitrogen in this case. The porosity parameters N and R for the tapered and straight capillaries with the first slip order boundary are shown in figures. 6.5 and 6.6, respectively. The porosity parameters are obtained experimentally using helium gas as already pointed out. It is to be noted that the porosity parameters of both tapered and straight capillary models tend to decrease as the gland stress increases. Figure 6.7 shows clearly the decrease of the capillary radius and its number with the applied gland stress. Although the relationship of both porosity parameters of the two cases appears to be decreasing somewhat linearly with the stress level one would expect to reach saturation.
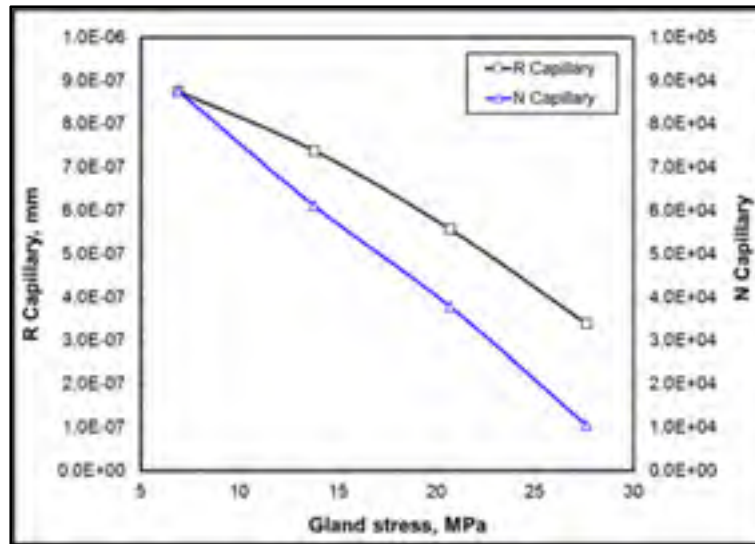
Figure 6.5 Tapered capillary flow model parameters
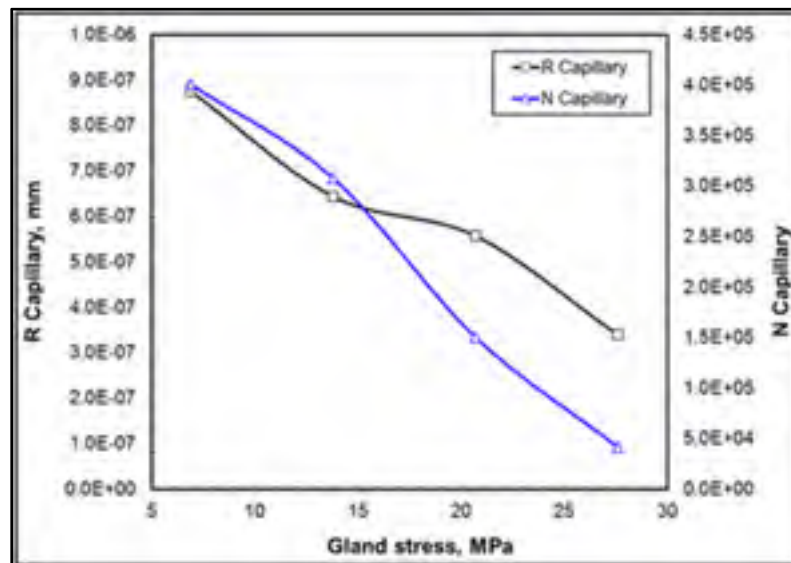
Figure 6.6 Straight capillary flow model parameters

This is characterized by a plateau known as tightness hardening where leak decreases very slowly with a considerable increase of load. Using the porosity parameters obtained with the reference gas, Eqs. (6.10) and (6.11) are used to predict the leak rate for air, nitrogen and argon.
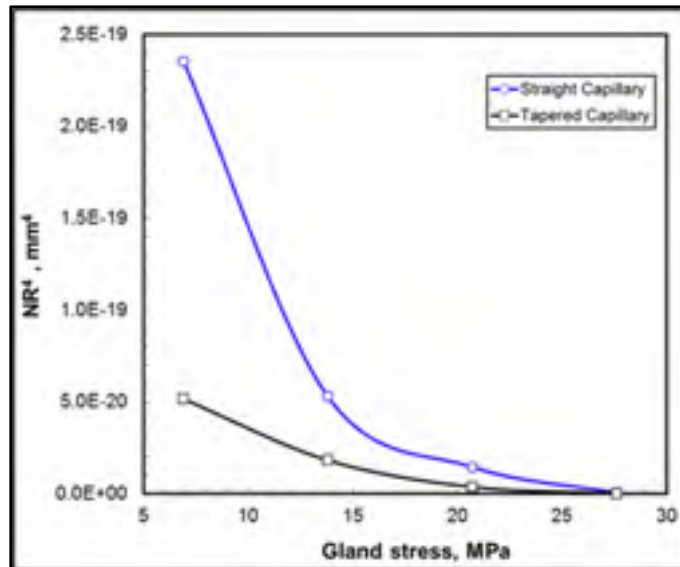
Figure 6.7 NR^4 Parameter for straight and tapered capillary
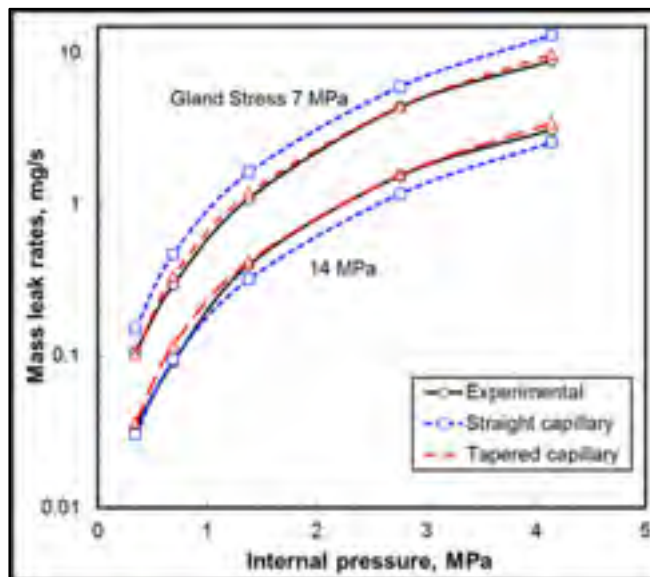
Figure 6.8 Prediction of Air gas for 7 and 14 MPa

In Figures 6.8 and 6.9 the predictions using air are compared to those measured experimentally under the same conditions. The straight capillary model gives slightly higher or lower values than those measured experimentally. However, the stress level plays an important role in the prediction. For the tapered capillary model, the prediction is more accurate than with the straight capillary model especially at the low stresses for all applied pressures.
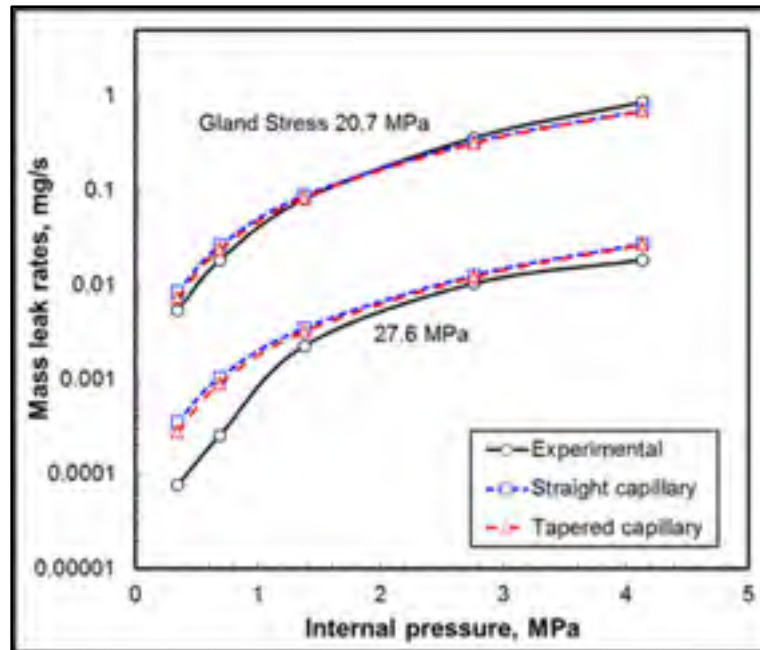
Figure 6.9 Prediction of Air gas for 20.7 and 27.6 MPa

In Figures 6.10 and 6.11, the predictions with nitrogen gas are compared to those measured experimentally under the same conditions of gland stress and same gas pressures as previously tests with air. The tapered capillary model predictions are closer to the experimental measure values than those of the straight capillary model especially at the low stress once again. In Figures 6.12 and 6.13 the predictions with argon also confirm the better predictions with the tapered capillary. At high stress levels the two models seems to predict higher leak rate especially at those low leak rates obtained at lower pressure levels. The dwell time to obtain leak rate stabilization may have been the cause. Had enough time been allocated for the leak to stabilise the values of leak rates would have increased slightly.
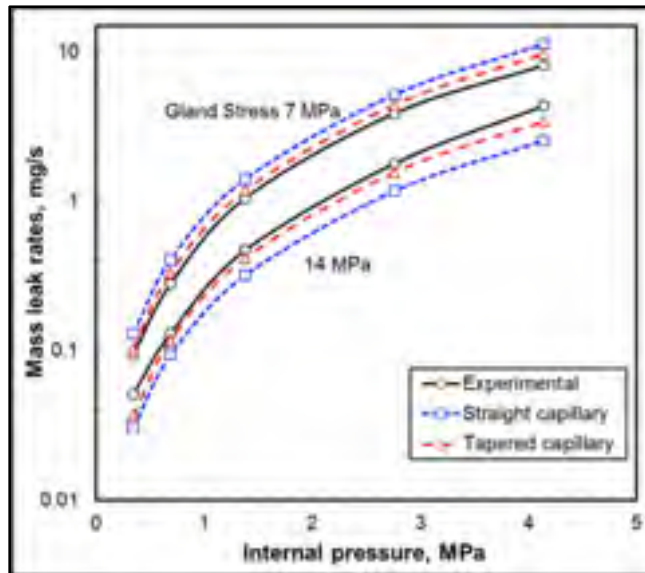
Figure 6.10 Prediction of Nitrogen gas for 7
and 14 MPa
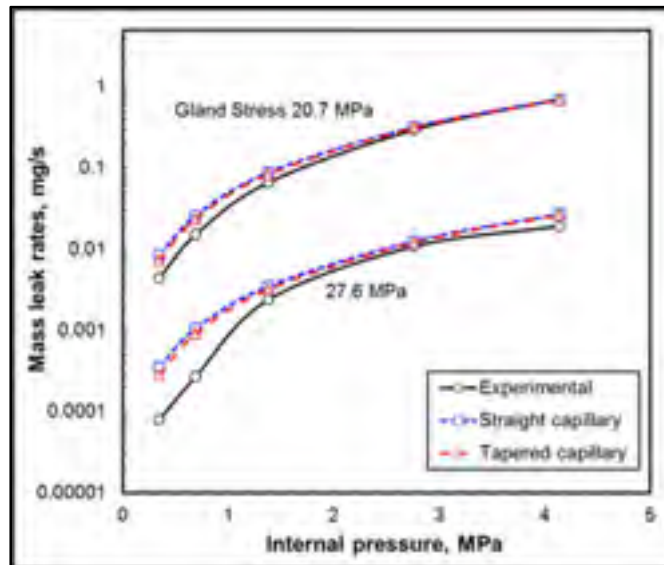
Figure 6.11 Prediction of Nitrogen gas for
20.7 and 27.6 MPa

A higher dwell time is generally required for a fluid to travel through the packing pores. Although the level of leak rate and the applied gland stresses are representative of many existing applications, the analytical model is limited in terms of predicting leak rate to specific gases that do not change phase or react with the media.
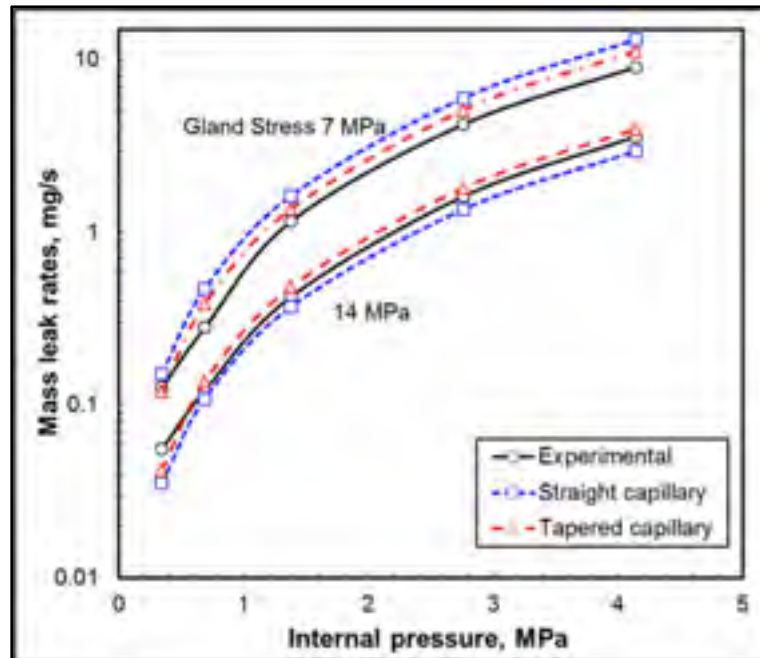
Figure 6.12 Prediction of Argon gas for 7 and 14 MPa

6.5.2   Liquid test results

Figures 6.14 and 6.15 show the experimental leak rate results with helium gas under different gland stresses (10.34, 13.79, 17.24, 20.68 and 24.14 MPa) and different internal pressures (0.345, 0.69, 1.03, 1.38, 1.72 and 2.06). The porosity parameters N and R for the straight liquid capillary with a first slip order boundary are shown in Figures 6.16 and 6.17, respectively for the flexible graphite and Teflon packing sets.

152
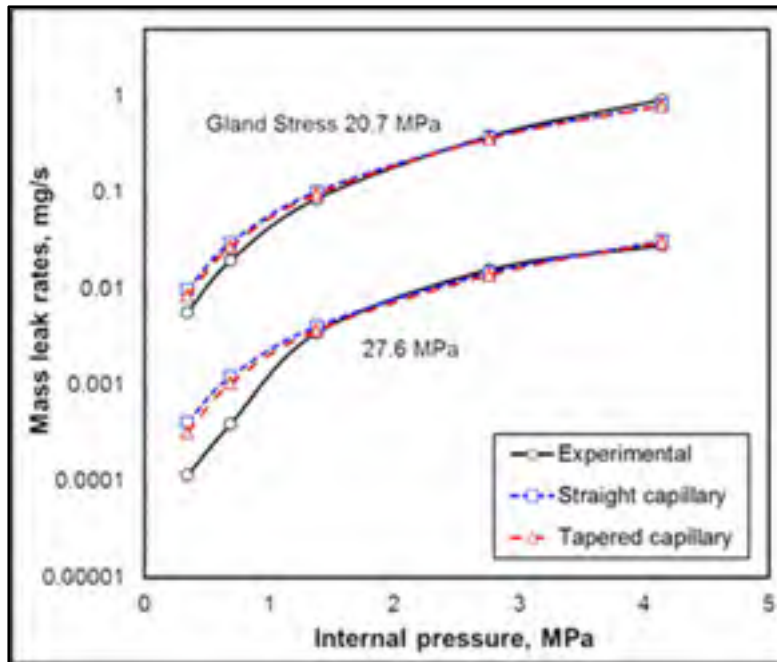
Figure 6.13 Prediction of Argon gas for 20.7 and 27.6 MPa
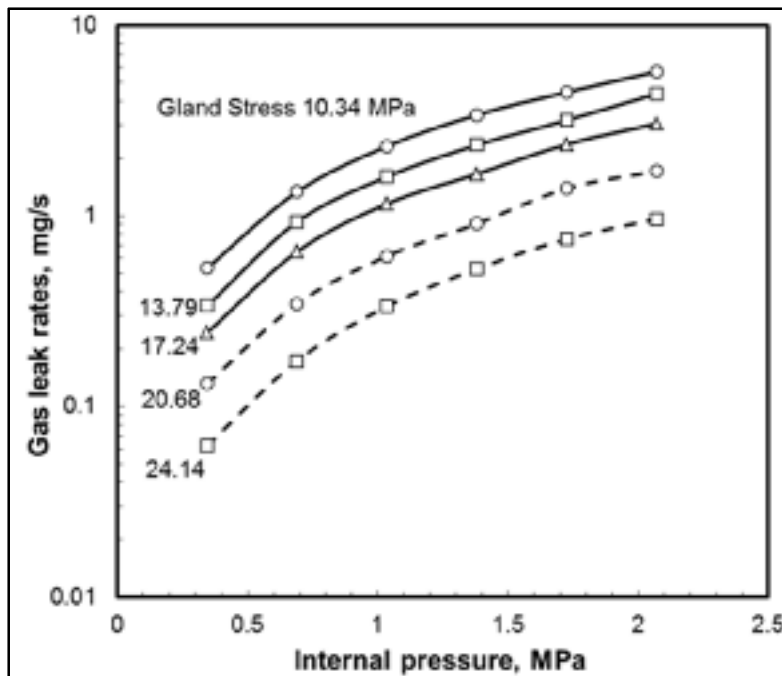
Figure 6.14 Leak rate measurements for helium gas at
different gland stresses of FG
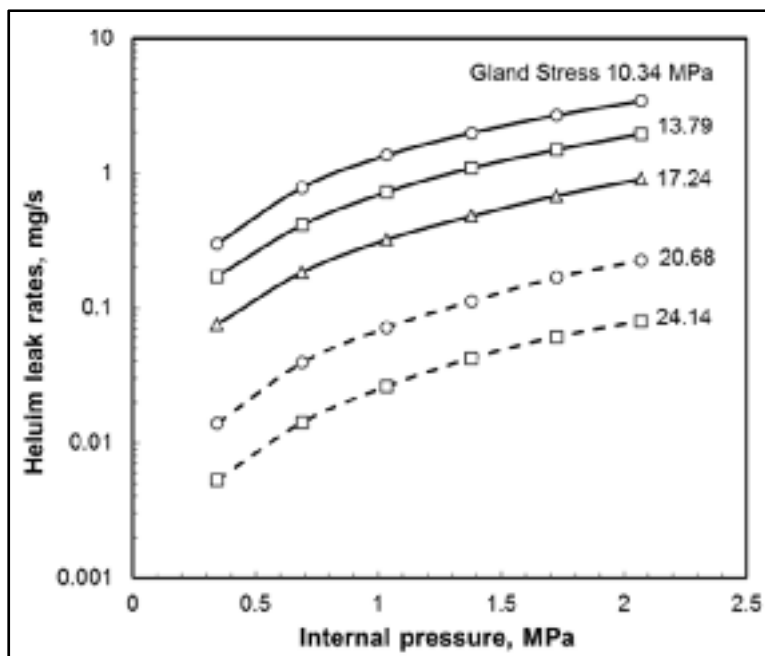
Figure 6.15 Leak rate measurements for helium gas at
different gland stresses of Teflon
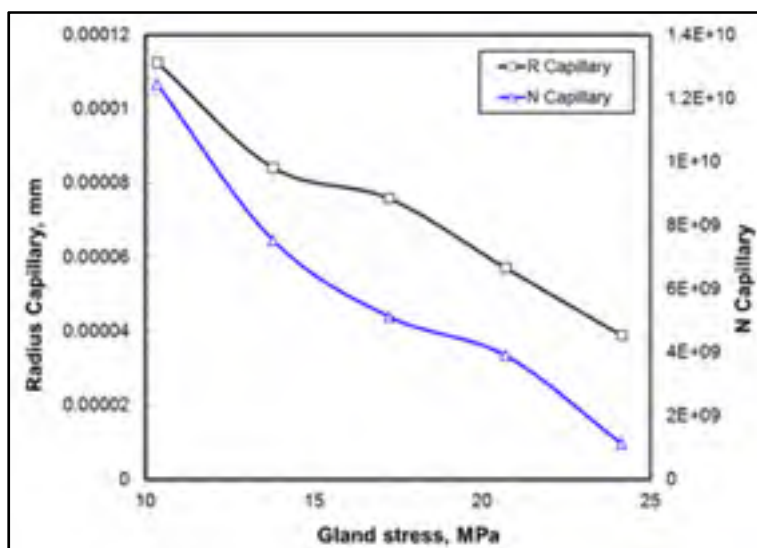
Figure 6.16 N& R capillaries for helium gas at different
gland stresses of FG
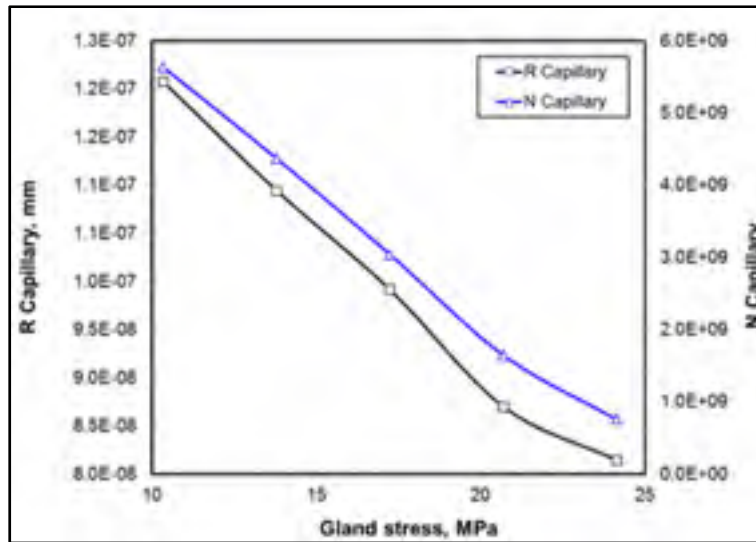
Figure 6.17 N& R capillaries for helium gas at different
gland stresses of Teflon

They are obtained experimentally using helium gas as already pointed out and will be used later to predict the leaks for liquids, namely for water and kerosene. In the same figures, both porosity parameters for both materials decrease as the gland stress increases. Starting from 0.15 μm at 10.34 MPa stress the radius of capillary reduce to 0.015 μm at 24.14 MPa stress, whereas the number of capillaries reduces from $1.3x10^{10}$ to 10^9 for the same stresses for FG material. The results with Teflon material are shown in Figure 6.18. The radius of capillary starts from 0.0125 μm at a 10.34 MPa stress and reduces to 0.08 μm at 24.14 MPa, whereas the number of capillaries reduces from $55x10^9$ to $1x10^9$ for the same stresses. Using the porosity parameters and the liquid properties, it is possible to predict the leak rate for other type of liquids such as kerosene and water in this case. In Figures 6.18 and 6.19 the predictions for kerosene are compared to those measured experimentally under the same conditions of gland stress varying from 10.34 to 24.14 MPa and gas pressures varying from 0.34 to 2.07 MPa for FG and Teflon materials, respectively.
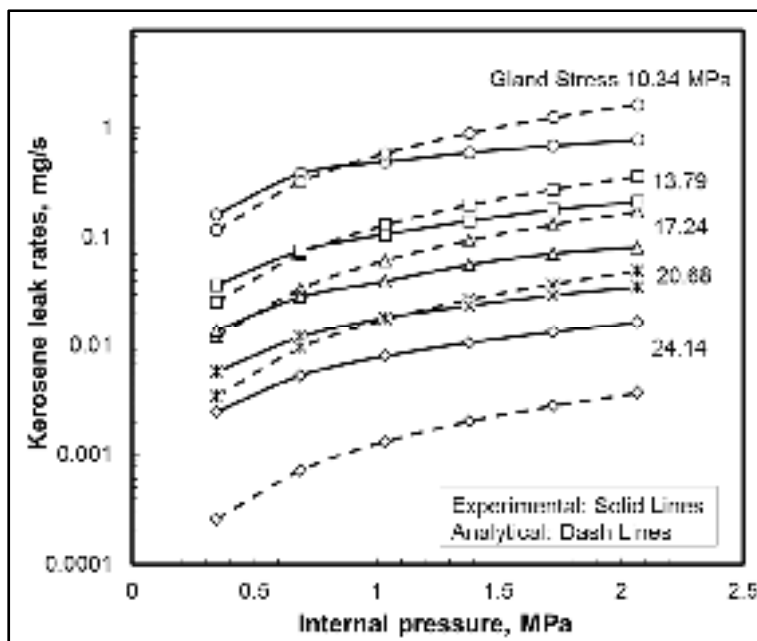
Figure 6.18 Prediction of kerosene for 10.34, 13.79,
17.24, 20.68 & 24.14 MPa for FG
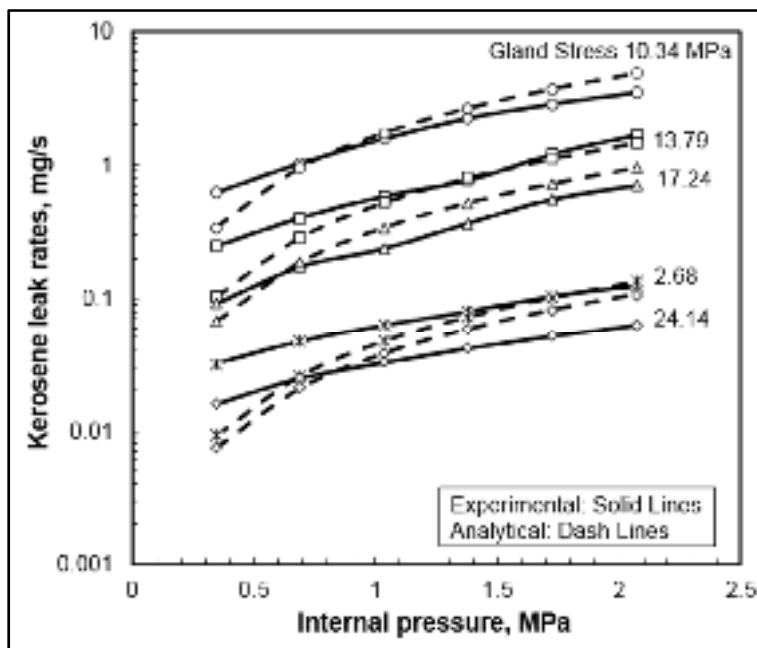
Figure 6.19 Prediction of Kerosene for 10.34, 13.79,
17.24, 20.68 & 24.14 MPa for Teflon

156
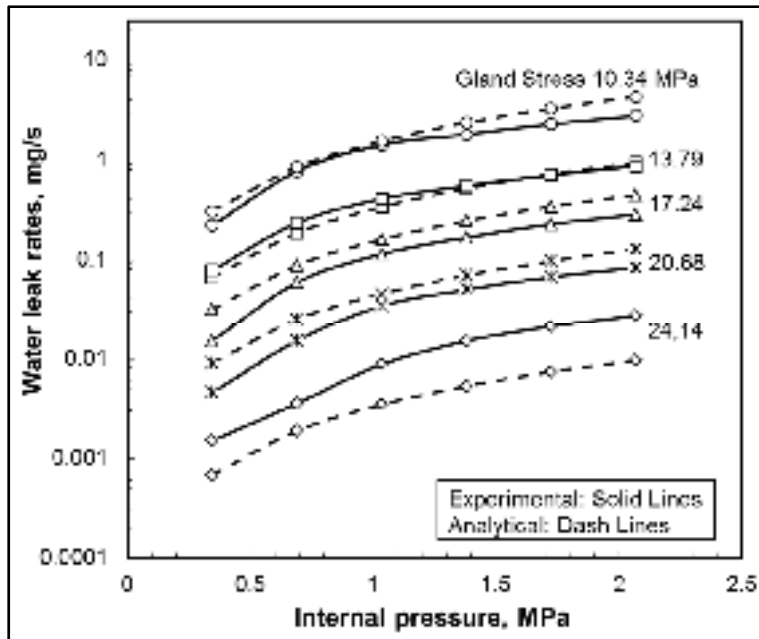
Figure 6.20 Prediction of Water for 10.34, 13.79, 17.24,
20.68 & 24.14 MPa for FGI
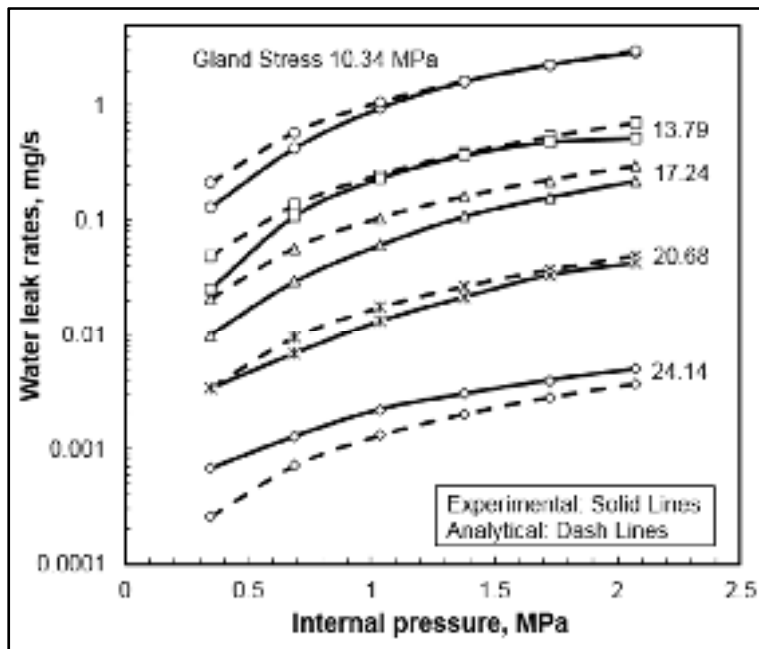
Figure 6.21 Prediction of water for 10.34, 13.79, 17.24,
20.68 & 24.14 MPa for Teflon

However, figures 6.20 and 6.21 present the predictions for water which are compared to those measured experimentally under the same conditions of gland stress varying from 10.34 to 24.14 MPa and gas pressures varying from 0.34 to 2.07 MPa for FG and Teflon materials, respectively. The prediction results for both materials and liquids are less accurate and show a considerable difference with the experimental measurements especially for high gland stresses as compared with the predictions of gases. The difference depends on the liquid pressure and the level of stress on the gland stress. Nevertheless, these predictions are considered acceptable because the level of leak is small. There are two reasons that explain this difference. The first one is related to surface tension that is present and not taken into account by the model and the second one is related to the presence of leak paths at the interface between the packing rings and the stem and housing. In addition the material variation between on packing to the other may play a role. It is to be noted that the gas leak test conducted for porosity characterization and the liquid leak tests are conducted with different packing sets.

6.6 Conclusion

In this study, firstly a comparison of leakage prediction using straight and tapered capillary flow models with first order condition to predict gaseous flow in soft flexible graphite packing was conducted. The tapered capillary model, the section of which varies with the length is based on the packing axial stress distribution. The model captures better the real packing rings leakage behavior than the straight tube model. A good agreement between the predicted leak rates and those obtained experimentally for all gases is found especially at the low stresses. The accuracy of the prediction may differ based on the type of gas, stress levels, and applied pressure levels in the case of compressible fluids. Secondly, for incompressible fluid, the slip flow model with straight capillary tested with water and kerosene on flexible graphite and Teflon packing materials showed less accuracy especially at the high stress level. Surface tension and interfacial leak paths are suspected to be the cause. Additional tests are underway to investigate the difference and extend the work to include other materials, fluids and the effect of temperature.

CONCLUSION

The impact of this research from an industrial point of view has been established; packing seals are mandatory components of valves to minimize the amount of leaks through these kinds of seals, in order to reduce fugitive emissions and to comply with related legislated restrictions. The use of a sealing system is essential for many applications, such as gaskets in bolted joints and packing rings in valves. Packing rings play a predominant role in conforming to environmental guidelines, especially in industrial plants. Many types of wide and high-pressure valves are employed in nuclear and petrochemical plants. Therefore, any leaks from valve sealing systems can cause failure of the piping system network, enhance pollution to the environment and health and human hazard. Furthermore, 60% of all equipment requiring sealing compliance are valves. From this standpoint, the necessity for innovative research leading to improvements of valve sealing performance is crucial. This thesis has met its objectives by fulfilling the following tasks:

- Characterize the sealing behavior of packing materials under different conditions;
- Implement analytical fluid flow models to predict leak rates through packing seals and validate them with various tests under multiple conditions of porous materials, gas types and liquids at room temperature;
- Modelling the leak rate of packing seals through ANSYS CFX using numerical approaches.

A methodology has been developed based on three major points. First, to develop analytical models to accurately predict the leak rates in packing rings. In more details, the analytical model of packing rings leak is based on the flow through porous medium at room temperature. Second, to modify the existing test rig to measure material properties of packing rings and conduct leakage tests with gases and liquids at room temperature. The test rig results were used to validate the analytical and numerical developed models and investigate the effect of interfacial leaks. Third, to model and simulate the packing valve leak rate with CFX in order to predict leak rates of packing rings under different conditions.

The leak controlling factors are discussed and investigated in the first paper via a comprehensive investigation using different approaches; namely experimental, analytical and numerical. The research study focuses on the prediction of leak through packed stuffing boxes under disparate conditions. The analytical studies show the capability of a few mathematical models to predict the leak rates through packed stuffing boxes over the wide range of gland stresses and fluid pressures. For the simulation part, only a few researchers have investigated the topic of leaks through sealing systems, such as packing rings. The suitability of capillary and porous medium models to predict gaseous leaks in flexible graphite packing rings of valve stuffing boxes is acknowledged. The porous agent for the slip and diffusive flow models was hypothetically constructed with micro-tubes in the direction of the fluid flow. For Ergun model, the porous medium was assumed to be a packed bed made of spheres. Helium was used as the reference gas to determine the porosity parameters of the numerous models. In general, the results showed a favorable agreement between the predicted leak rates and the rates measured experimentally. However, the second order slip model showed a better convergence over the four decades with a range of leak rates from 0.0001 to 1 mg/s (with helium). The relative error between prediction results and leak measurements are ranging between 40% to 60% for second order slip model, while it is 50% to 80% for other models.

The second paper presents an experimental work that investigates the contribution of the interfacial and permeation leaks on the total leak present in packed stem and in bolted gasketed joints. The gaskets were made of CF, FG and PTFE sheet materials, while the packing rings were made of FG and PTFE yarn materials. Interfacial leak is predominant in valve stem packing rings, accounting for approximately 95% of the total leaks, at low stress as shown in this study. The results for gaskets indicate that, at low stress, interfacial leak is predominant with low and high surface finish. The amount of interfacial leak rate is affected by diverse factors such as the material type and the surface finish of the matting surfaces. In more details, CF and FG gaskets showed a significant contribution of the interfacial leak, with an average of 80% of the total leak, while PTFE showed on average a little less than 50%. Pre-compression technique of sealing performance is shown to be useful, because it reduces the leak rate to a minimum, for packing rings and gaskets, as observed in paper 2.

Paper 3 investigates the suitability of an exponential varying section capillary fluid flow model, with pristine conditions, to predict gaseous flow in soft flexible graphite packing. The capillary model section variation with length is based on the packing axial stress distribution. The validation of the analytical model was achieved experimentally at different operating conditions. Tests were conducted with various types of gases and were under different internal pressures and gland stresses. A simulation using a CFX module was ran in parallel to support the analytical model. The CFX model is based on the Darcy's law and considers the porous medium to be a packed bed. The leak rates of the reference helium gas are used to obtain the porosity parameters required in the developed model. The results show a good agreement between the predicted leak rates and those obtained from the experiments and the CFX model.

Paper 4 implements a comparative investigation for both straight and tapered capillary flow models with first order condition to predict gaseous and liquid flow in soft flexible graphite packing and PTFE packing materials. The results obtained from tapered capillary demonstrate a superior accuracy in predicting leak rates and confirmed by experiments with several gasses. For incompressible results, the slip flow model with liquids for water and kerosene was examined with flexible graphite and Teflon packing materials. In general, the analytical results for packing rings were found slightly higher at the higher stresses for both liquid water and kerosene.

Finally, the prediction of the sealing performance of packing rings through different approaches, under different conditions, is mandatory to reduce the fugitive emissions and reduce safety hazard from valves.

RECOMMENDATIONS

This study focuses primarily on the leak predictions of packing rings under distinctive conditions. The developed models were tested with few materials and under specific working conditions. Therefore, in order to generalise the study, the work could be extended to include other material products, operating conditions and applications.

The suggested recommendations are specified below:

1. Conduct leak tests with other types of packing ring materials that have distinct porosity characteristics.
2. Use bigger size gas molecules such as SF6 and methane and other type of liquids such as diesel to cover a wider range of properties (viscosity, surface tension, volatility etc…).
3. Consider high temperature effect including fluid and porous media property changes, thermal expansion, creep, aging and corrosion.
4. Consider the tribological effects such as lubrication, friction and wear.
5. Two-phase flow conditions when using certain liquids that experience phase change such as steam-water.
6. Study the interfacial leak and its influence by the surface finish. The development of an analytical approach which can be used to anticipate the interfacial leak contribution is desirable.

SECOND ORDER SLIP FLOW MODEL FOR STRAIGHT CAPILLARY FOR GASES

The theoretical model commences by assuming the packing rings as a set of uniform straight capillaries to which Navier and Stockes flow equations apply. The capillaries are specifically considered as Nano or micro-tubes with circular cross-section. Furthermore, the model will be driven with the effect of slip condition on the wall. The general form of Navier and Stoke equations are mentioned on equations (A I-1) and (A I-2) below:

$$\frac{\partial p}{\partial t} + \frac{\partial (\rho u_k)}{\partial x_k} = 0 \tag{A I-1}$$

$$\frac{\partial (\rho u_i)}{\partial t} + \frac{\partial (\rho u_k u_i)}{\partial x_k} = -\frac{\partial p}{\partial x_i} + \frac{\partial (\tau_{ik})}{\partial x_k} \tag{A I-2}$$

Generally, for Newtonian fluid with isotropic effect, the stress tensor is found as follows:

$$\tau_{ik} = \mu \left(\frac{\partial u_i}{\partial x_k} + \frac{u_k}{x_i} \right) + \lambda \left(\frac{\partial u_j}{\partial x_j} \right) \delta_{ik} \tag{A I-3}$$

Where μ, λ are the first and second viscosities. δ is the delta from Kronecker. The equations of conversation of mass for compressible fluid (such as gas) in cylindrical coordinates considered as:

$$\frac{\partial P}{\partial t} + \frac{\partial (\rho u_z)}{\partial z} + \frac{1}{r} \frac{\partial (r \rho u_r)}{\partial r} = 0 \tag{A I-4}$$

The velocity in z direction is u_z, and the velocity in r direction is u_r. The equations of momentum conversation in the z direction for compressible fluid in cylindrical coordinates is given by equation (A I-5):

$$\frac{\partial\left(\rho u_z\right)}{\partial t} + \frac{\partial\left(\rho u_z u_z\right)}{\partial z} + \frac{1}{r}\frac{\partial\left(\rho r u_z u_r\right)}{\partial r} - \frac{\partial}{\partial z}\left(\mu\frac{\partial u_z}{\partial z}\right) - \frac{1}{r}\frac{\partial}{\partial r}\left(r\mu\frac{\partial u_z}{\partial r}\right)$$
$$= -\frac{\partial}{z}\left(p + 2/3\mu\nabla.V\right) + \frac{\partial}{z}\left(\mu\frac{\partial u_z}{\partial z}\right) + \frac{1}{r}\frac{\partial}{\partial r}\left(r\mu\frac{\partial u_r}{\partial z}\right)$$

(A I-5)

But, knowing that:

$$\nabla.V = \frac{\partial u_z}{\partial z} + \frac{1}{r}\frac{\partial\left(r u_r\right)}{\partial r}$$

(A I-6)

The relation between the inertia terms and diffusion terms is significant parameter and is shown by equation (A I-7) below:

$$\frac{\rho u\dfrac{\partial u}{\partial z}}{\mu\dfrac{\partial^2 u}{\partial z^2}} \approx \frac{\rho u^2/l}{\mu.u/h^2} = \frac{\rho u L}{\mu}\left(\frac{h}{l}\right) = \mathrm{Re}\left(\frac{h}{l}\right)$$

(A I-7)

Generally, for the fluid flow with low Reynolds number Re <<< 1 in Nano and Micro channels with a combination of a high ratio of $\left(\dfrac{h}{l}\right)$ >>>1, gives an indication whether to neglect the inertia term. Therefore, in this case all the terms, which are multiplies by the speed, are zero $\left(u*(.......)\right) = 0$.

$$-\frac{1}{r}\frac{d}{dr}\left(\mu r\frac{du_z}{dr}\right) = -\frac{dP}{dz}$$

(A I-8)

Now, the equations of conservation of momentum in cylindrical coordinates for an ideal gas simplified to:

$$\frac{1}{r}\frac{d}{dr}\left(r\frac{du_z}{dr}\right) = \frac{1}{\mu}\frac{dP}{dz} \tag{A I-9}$$

In the case of isothermal flow with second order slip on the wall of micro tapered and exponential tubes, the first and second boundary conditions are:

$$\left.\frac{du}{dr}\right|_{r=0} = 0$$

$$\left.u\right|_{r=R} = -\frac{2-\sigma}{\sigma}\lambda\left.\frac{du}{dr}\right|_{r=R} + A_2\lambda^2\left.\frac{d^2u}{dr^2}\right|_{r=R} \tag{A I-10}$$

Where, σ is the tangential momentum accommodation coefficient taken as 1 for considering the particles case in diffuse reflections and λ is the mean free path.

$$r\frac{du_z}{dr} = \frac{r}{\mu}\frac{dP}{dz}dr$$

$$r\frac{du_z}{dr} = \int_0^r \frac{r}{\mu}\frac{dP}{dz}dr$$

$$r\frac{du_z}{dr} = \frac{1}{\mu}\frac{dP}{dz}\left[\frac{1}{2}r^2 + c_1\right] \tag{A I-11}$$

$$\frac{du_z}{dr} = \frac{1}{\mu}\frac{dP}{dz}\left[\frac{1}{2}r + \frac{c_1}{r}\right]$$

$$\int_0^{u_z} du_z = \frac{1}{\mu}\frac{dP}{dz}\int_0^r \left[\frac{1}{2}r + \frac{c_1}{r}\right]dr$$

So, after integration the velocity in z direction is given by:

$$u_z = \frac{1}{\mu}\frac{dP}{dz}\left[\frac{1}{4}r^2 + c_1 \ln r + c_2\right]$$

(A I-12)

Now the constants in the velocity equation can be found by implementing both boundaries conditions, which were mentioned in equation (A I-10). So, equation (A I-13) shows that:

$$\frac{du_z}{dr} = \frac{1}{\mu}\frac{dP}{dz}\left[\frac{1}{2}r + \frac{c_1}{r}\right]$$
$$r \neq 0$$

(A I-13)

Therefore, $c_1 = 0$, and the velocity in z direction becomes as:

$$u_z = \frac{1}{\mu}\frac{dP}{dz}\left[\frac{1}{4}r^2 + c_2\right]$$

(A I-14)

The same technique is followed to get c_2 after applying the second boundary condition:

$$c_2 = -\frac{2-\sigma}{\sigma}\lambda\frac{R}{2} + \frac{A_2\lambda^2}{2} - \frac{R^2}{4}$$

(A I-15)

Finally, the velocity shown in equation (A I-16):

$$u(r,z) = \frac{1}{\mu}\frac{dP}{dz}\left[\frac{r^2}{4} - \frac{R^2}{4} - \frac{2-\sigma}{\sigma}\lambda\frac{R}{2} + A_2\lambda^2\frac{1}{2}\right]$$

(A I-16)

When the effect of rarefaction is not considered (Kn≈0), the speed at the center of the Nano and micro tube explained as u_{zo}:

$$u_{zo} = -\frac{R^2}{4}\frac{1}{\mu}\frac{dP}{dz} \tag{A I-17}$$

The non-dimensional velocity descried as $\frac{u_z}{u_{zo}} = u_z{}^*$ is given by:

$$\frac{u_z}{u_{zo}} = u_z{}^* = \left[\frac{r^2}{R^2} - \frac{2-\sigma}{\sigma}\lambda 4\frac{1}{2R} + A_2\,\lambda^2 8\frac{1}{4R^2} - 1\right] \tag{A I-18}$$

By considering, $r^* = \frac{r}{R}$, $Kn_0 = \frac{\lambda}{2R}$ we get:

$$u_z{}^* = \left[r^{*2} - 1 - \frac{2-\sigma}{\sigma}4\,kn_o + 8\,A_2\,kn_o^2\right] \tag{A I-19}$$

Now the non-dimensional average velocity $\overline{u_z{}^*}$ can be found after implementing the integration on $u_z{}^*$:

$$\overline{u_z{}^*} = \frac{1}{\pi}\int_0^1 u_z{}^*\,2\pi r^*\,dr^* \tag{A I-20}$$

$$\overline{u_z}{}^* = \frac{\overline{u_z}}{u_{zo}} = \left[\frac{1}{2} + \frac{2-\sigma}{\sigma}4\,Kn_o - 8\,A_2\,Kn_o^2\right] \tag{A I-21}$$

The average velocity in the second order slip model can be expressed as below:

$$\overline{u_z} = -\frac{R^2}{4\mu}\frac{dP}{dz}\left[\frac{1}{2} + \frac{2-\sigma}{\sigma}4\,Kn_o - 8\,A_2\,Kn_o^2\right] \tag{A I-22}$$

Considering the first-order slip flow model, the mass flow rate of a gas pass through the straight capillary with circular cross section in a micro-tube is expressed as the equation follow:

$$L = \overset{\bullet}{m}_{ts} = \rho \overline{u_z} A = P . \overline{u_z} . \pi R^2 / \Re T \tag{A I-23}$$

$$\overset{\bullet}{m}_{ts} = \frac{-PR^4 \pi}{4\mu \Re T} \frac{dP}{dz} \left[\frac{1}{2} + \frac{2-\sigma}{\sigma} 4 Kn_o - 8 A_2 Kn_o^2 \right] \tag{A I-24}$$

$$\overset{\bullet}{m}_{ts} = \frac{-\pi P R^4}{dz 4\mu \Re T} \left[\frac{1}{2} dP + \frac{2-\sigma}{\sigma} 4 Kn_o \, dP - 8 A_2 Kn_o^2 \, dP \right] \tag{A I-25}$$

$$\overset{\bullet}{m}_{ts} = \frac{-\pi R^4}{dz 4\mu \Re T} \left[\frac{1}{2} P dP + \frac{2-\sigma}{\sigma} 4 Kn_o \, P_o dP - 8 P_o^2 A_2 Kn_o^2 \frac{dP}{P} \right] \tag{A I-26}$$

$$\int_0^l \frac{-4\mu R T \overset{\bullet}{m}_{ts}}{\pi R^4} dz = \int_{P_i}^{P_o} P dP \frac{1}{2} + \int_{P_i}^{P_o} P_o dP \frac{2-\sigma}{\sigma} 4 Kn_o \, - \int_{P_i}^{P_o} \frac{P_o^2}{P} dP 8 A_2 Kn_o^2 \tag{A I-27}$$

Now, after integration of the left side of equation (A I-27) we get:

$$\int_0^l \frac{-4\mu R T \overset{\bullet}{m}_{ts}}{\pi R^4} dz = \frac{-4l\mu R T \overset{\bullet}{m}_{ts}}{\pi R^4} \tag{A I-28}$$

Integrating the right side of equation (A I-27) we get:

$$\int_{P_i}^{P_o} P\,dP \frac{1}{2} = \frac{1}{4}\left[P_o^2 - P_i^2 \right]$$

$$\int_{P_i}^{P_o} P_o\,dP \frac{2-\sigma}{\sigma} 4\,Kn_o = \frac{2-\sigma}{\sigma} 4\,Kn\left[P_o^2 - P_i P_o \right] \tag{A I-29}$$

$$\int_{P_i}^{P_o} -\frac{P_o^2}{P}\,dP\, 8\,A_2\,Kn_o^2 = -8\,P_o^2\,A_2\,Kn_o^2 \ln\left(\frac{P_o}{P_i} \right)$$

Equation (A I-27) becomes:

$$\overset{\bullet}{m}_{ts} = \frac{R^4\pi}{4\mu R\,Tl}\left[\frac{1}{4}\left[P_o^2 - P_i^2 \right] + 4\frac{2-\sigma}{\sigma}Kn_o\left[P_o^2 - P_i P_o \right] + 8P_o^2 A_2\,Kn_o^2 \ln\left(\frac{P_i}{P_o} \right) \right] \tag{A I-30}$$

$$\overset{\bullet}{m}_{ts} = \frac{\pi R^4 P_o^2 \left(\Pi^2 - 1 \right)}{16\mu R\,Tl}\left[1 + 16\frac{2-\sigma}{\sigma}Kn_o\frac{1}{(\Pi+1)} - 32\,A_2\,Kn_o^2\frac{\ln(\Pi)}{(\Pi^2-1)} \right] \tag{A I-31}$$

Finally, leak rate through N capillaries can be estimated as follow:

$$\overset{\bullet}{m}_{ts} = \frac{NR^4 P_o^2 \pi \left(\Pi^2 - 1 \right)}{16\mu R\,Tl}\left[1 + 16\frac{2-\sigma}{\sigma}Kn_o\frac{1}{(\Pi+1)} - 32\,A_2\,Kn_o^2\frac{\ln(\Pi)}{(\Pi^2-1)} \right] \tag{A I-32}$$

FIRST ORDRE SLIP FLOW MODEL FOR STRAIGHT CAPILLARY FOR GASES

The theoretical modeling commencement by assuming the packing rings as a set of uniform straight radius capillaries incorporating Naiver Stocks flow equations. The capillaries are specifically existed as Nano or micro-tubes with circular cross-section. Furthermore, the model will be drive with the effect of slip condition on the wall. Now, the equations of conservation of momentum in cylindrical coordinates for an ideal gas simplified as below as mentioned in second order flow model in equation (A I-9):

$$\frac{1}{r}\frac{d}{dr}\left(r\frac{du_z}{dr}\right) = \frac{1}{\mu}\frac{dP}{dz}$$

(A II-1)

In the case of isothermal flow with first order slip on the wall of micro straight tubes, the first and second boundary conditions are:

$$\left.\frac{du}{dr}\right|_{r=0} = 0$$

$$u\Big|_{r=R} = -\frac{2-\sigma}{\sigma}\lambda\left.\frac{du}{dr}\right|_{r=R}$$

(A II-2)

Simply, the same techniques as APPENDIX I are flow to estimate the lake rate with first slip, where the average velocity with first order slip can be exist as below:

$$\overline{u_z} = -\frac{R^2}{4\mu}\frac{dP}{dz}\left[\frac{1}{2} + \frac{2-\sigma}{\sigma}4Kn_o\right]$$

(A II-3)

Considering the first-order slip flow model, the mass flow rate of a gas pass through circular cross section in micros tubes is expressed as the equation follow:

$$\dot{m}_{ts} = \frac{-\pi P R^4}{dz\,4\,\mu R T} \left[\frac{1}{2} dP + \frac{2-\sigma}{\sigma} 4\,Kn_o\,dP \right]$$ (A II-4)

The amount of $(Kn\,P)$ is constant for an isothermal flow, where it can be written as a function of the outlet conditions only $Kn_o P_o = Kn\,P$

$$\dot{m}_{ts} = \frac{-\pi R^4}{dz\,4\,\mu R T} \left[\frac{1}{2} P dP + \frac{2-\sigma}{\sigma} 4\,Kn_o\,P_o dP \right]$$ (A II-5)

Now, after perform the integral of equation (A II-5) as followings:

$$\int_0^l \frac{-4\,\mu R T\,\dot{m}_{ts}}{\pi R^4} dz = \int_{P_i}^{P_o} P dP \frac{1}{2} + \int_{P_i}^{P_o} P_o dP \frac{2-\sigma}{\sigma} 4\,Kn_o$$ (A II-6)

Finally, the total mass flow rate which passes through all capillaries considered as:

$$\dot{m}_{ts} = \frac{N\,\pi R^4 P_o^2 \left(\Pi^2 - 1 \right)}{16\,\mu R T l} \left[1 + 16 \frac{2-\sigma}{\sigma} Kn_o \frac{1}{(\Pi+1)} \right]$$ (A II-7)

APPENDIX III

DIFFUSIVITY MODEL FOR GASES

The theoretical modeling commencement by assuming the packing rings as a set of uniform straight radius capillaries incorporating Naiver Stocks flow equations. The capillaries are specifically existed as Nano or micro-tubes with circular cross-section. Furthermore, the model will be drive with the effect of slip condition on the wall.

Simply, the same techniques as APPENDIX I are flow to estimate the lake rate with diffusivity condition, where the boundary conditions are:

$$\frac{du}{dr}\bigg|_{r=0} = 0$$
$$u\bigg|_{r=R} = -\frac{\mu}{\rho P}\frac{dP}{dz}$$

(A III-1)

Finally, the total mass flow rate which passes through all capillaries considered as:

$$L = \frac{N\pi R^4 P_o^2 \left(\Pi^2 - 1\right)}{16\mu R T l}\left(1 + \frac{16\mu^2 R T}{R^2 P_o^2}\frac{In\left(\Pi\right)}{\left(\Pi^2 - 1\right)}\right)$$

(A III-2)

Note: the total mass flow rate which passes through all capillaries with diffusivity can be estimated easily from equation (A I-32), by ignoring the slip condition and consider the flow in diffusion condition only.

APPENDIX IV

FIRST ORDRE SLIP FLOW MODEL FOR TAPERED CAPILLARY FOR GASES

The theoretical modeling commencement by assuming the packing rings as a set of uniform tapered capillaries incorporating Naiver Stocks flow equations. The capillaries are specifically existed as Nano or micro-tubes with circular cross-section. Furthermore, the model will be drive with the effect of slip condition on the wall.

Simply, the same techniques as APPENDIX II are flow to estimate the lake rate with slip condition, where the boundary conditions are:

$$\left. \frac{du}{dr} \right|_{r=0} = 0$$

$$u\Big|_{r=R(z)} = -\frac{2-\sigma}{\sigma} \lambda \left. \frac{du}{dr} \right|_{r=R(z)}$$

(A IV-1)

The average velocity derived as (A II-3), but in equation below the R is varying with z:

$$\overline{u_z} = -\frac{R^2(z)}{4\mu} \frac{dP}{dz} \left[\frac{1}{2} + \frac{2-\sigma}{\sigma} 4 Kn \right]$$

(A IV-2)

Considering the first-order slip flow model, the mass flow rate of a gas pass through the tapered capillary with circular cross section is expressed as the below:

$$\int_0^l \frac{-4\mu RT \dot{m}_{ts}}{\pi R^4(z)} dz = \int_{P_i}^{P_o} PdP \frac{1}{2} + \int_{P_i}^{P_o} P_o dP \frac{2-\sigma}{\sigma} 4 Kn_o$$

(A IV-3)

Because $R(z)$ is varying with z direction, so as the cross section of the capillary changes with the axial length in the z direction because in a yarned packing the compressive stress changes with axial position on the stem. As mentioned in equation (5.7) in chapter 5 the relation between the $R(z)$ and the R near the gland is:

$$R(z) = R_g e^{\frac{\beta z}{2}} \qquad \text{(A IV-4)}$$

Where R_g is the capillary radius near the gland and σ_g is the gland stress. β is given by a rigorous calculation of the moment about the stem axis produced by the axial packing stress and friction forces at the walls neglecting the radial shear stress such that:

$$\beta = \frac{6\left(\mu_h K_h D^2 + \mu_s K_s d^2\right)}{\left(D^3 - d^3\right)} \qquad \text{(A IV-5)}$$

Finally, the total mass flow rate, which passes through all tapered capillaries, considered as:

$$\overset{\bullet}{m}_{ts} = \frac{N \pi \beta R_o^4 P_o^2 \left(\Pi^2 - 1\right)}{8 \mu R T \left(1 - e^{-2\beta l}\right)} \left[1 + 16 \frac{2 - \sigma}{\sigma} Kn_o \frac{1}{(\Pi + 1)}\right] \qquad \text{(A IV-6)}$$

FIRST ORDRE SLIP FLOW MODEL FOR STRAIGHT CAPILLARY OF LIQUIDS

The theoretical modeling commencement by assuming the packing rings as a set of uniform tapered capillaries incorporating Naiver Stocks flow equations. The capillaries are specifically existed as Nano or micro-tubes with circular cross-section. Furthermore, the model will be drive with the effect of slip condition on the wall. The momentum equation as mention in APPENDIX I can be obtained as follow:

$$\frac{1}{r}\frac{d}{dr}\left(r\frac{du_z}{dr}\right) = \frac{1}{\mu}\frac{dP}{dz}$$

(A V-1)

Simply, the same techniques as APPENDIX II are flow to estimate the lake rate with slip condition, where the boundary conditions for liquid condition are:

$$\frac{du}{dr}\bigg|_{r=0} = 0$$

$$u\big|_{r=R} = -L_s \frac{du}{dr}\bigg|_{r=R}$$

(A V-2)

Where L_s slip condition in liquid condition in circular capillary:

$$L_s = 0.059\big|\gamma^{0.485} \text{ where } \gamma = \frac{\Delta PR}{2\mu l}$$

(A V-3)

Integrating equation (A V-1) twice and applying the above boundary conditions gives the solution for the velocity in the z direction as a function of the radial position such that:

$$u(r,z) = \frac{1}{\mu}\frac{dp}{dz}\left[\frac{r^2}{4} - \frac{R^2}{4} - L_s\frac{R}{2}\right] \tag{A V-4}$$

The volume flow rate of capillaries can be obtained by integrating the velocity through the capillary area such that:

$$Q = \int_0^{2\pi}\int_0^R \frac{1}{\mu}\frac{dp}{dz}\left[\frac{r^2}{4} - \frac{R^2}{4} - L_s\frac{R}{2}\right]rd\theta\,dr \tag{A V-5}$$

After implement the integration the leak rate for each capillary found as:

$$Q = \frac{p(P_i - P_o)R^4}{8\mu l}\left[1 + L_s\frac{4}{R}\right] \tag{A V-6}$$

Finally the total leak rate passing through all capillaries are:

$$L = \frac{NR^4\pi\rho(P_i - P_o)}{8\mu l}\left[1 + \frac{4L_s}{R}\right] \tag{A V-7}$$

BIBLIOGRAPHY

Adanhounmè, Villevo, François de Paule Codo et Alain Adomou. 2012. « Solving the Navier Stokes Flow Equations of Micro-Polar Fluids by Adomian Decomposition Method ». *Bulletin of Mathematical Sciences and Applications,* vol. 2, p. 30-37.

Adler, PM, CG Jacquin et JA Quiblier. 1990a. « Flow in simulated porous media ». *International Journal of Multiphase Flow,* vol. 16, nº 4, p. 691-712.

Agrawal, Amit, et Nishanth Dongari. 2012. « Application of Navier-Stokes equations to high Knudsen number flow in a fine capillary ». *International Journal of Microscale and Nanoscale Thermal and Fluid Transport Phenomena,* vol. 3, nº 2, p. 125.

Aikin, John. 1994. « Packing developments improve valve availability ». *Power Engineering,* vol. 98, nº 1, p. 29-33.

Amyx, J , D Bass et R Whiting. 1960a. « PERMEABILITY MEASUREMENT ». In *Petroleum Reservoir Engineering: Physical Properties*. p. 1-9. New York: McGraw-Hill Book Co.

Amyx, James W, Daniel M Bass et Robert L Whiting. 1960b. *Petroleum reservoir engineering: physical properties*, 1. McGraw-Hill College.

API-622. 2011. « Type testing of process valve packing for fugitive emissions. ». *American Petroleum Industries*.

Araki, Takuto, Min Soo Kim, Hiroshi Iwai et Kenjiro Suzuki. 2002. « An experimental investigation of gaseous flow characteristics in microchannels ». *Microscale Thermophysical Engineering,* vol. 6, nº 2, p. 117-130.

Arghavani, J, M Derenne et L Marchand. 2003. « Effect of surface characteristics on compressive stress and leakage rate in gasketed flanged joints ». *The International Journal of Advanced Manufacturing Technology,* vol. 21, nº 10, p. 713-732.

Arkili, Errol Bernard. 1994. « Gaseous flow in micron-sized channels ». Massachusetts Institute of Technology.

Arkilic, Errol B, Martin A Schmidt et Kenneth S Breuer. 1994. « Slip flow in microchannel ». In *Proceeding of Rarefield Gas Dynamic Symposium*. (Oxford, UK).

Arkilic, Errol B, Martin A Schmidt et Kenneth S Breuer. 1997. « Gaseous slip flow in long microchannels ». *Journal of Microelectromechanical systems,* vol. 6, nº 2, p. 167-178.

Aweimer, Ali Salah Omar, et Abdel-Hakim Bouzid. 2018. « Experimental investigation of interfacial and permeation leak rates in sheet gaskets and valve stem packing ». In *ASME 2018 Pressure Vessels and Piping Conference*. p. V002T02A036-V002T02A036. American Society of Mechanical Engineers.

Aweimer, Ali Salah Omar, Abdel-Hakim Bouzid et Mehdi Kazeminia. 2017. « Leak rates of gasses through packing seals with different analytical approaches ». In *ASME 2017 Pressure Vessels and Piping Conference*. p. V002T02A023-V002T02A023. American Society of Mechanical Engineers.

Aweimer, Ali Salah Omar, Abdel-Hakim Bouzid et Mehdi Kazeminia. 2019. « Predicting Leak Rate Through Valve Stem Packing in Nuclear Applications ». *Journal of Nuclear Engineering and Radiation Science,* vol. 5, nᵒ 1, p. 011009.

Bahrami, M, A Tamayol et P Taheri. 2009. « Slip-flow pressure drop in microchannels of general cross section ». *Journal of Fluids Engineering,* vol. 131, nᵒ 3, p. 031201.

Bartonicek, Jaroslav, Hahn Rolf, Hans Kockelmann, Eberhard Roos et Friedrich Schöckle. 2001. « Characteristics of Packings for Stuffing Boxes for the Proof of Strength, Function and Tightness of Valves ».

Bauer, Paul. 1965. *Investigation of Leakage and Sealing Parameters*. IIT RESEARCH INST CHICAGO IL.

Baumann, HD. 1966. « Should a control valve leak/ques/(Control valve seat leakage as function of fluid viscosity, density, pressure drop and cube function of gap between two surfaces) ». *Instruments and Control Systems,* vol. 39, p. 111-115.

Bayreuther, D. 2012. « Fugitive emission testing and certification for valves ». In *Valve Manufacturers Association of America, 2012 Technical Seminar Presentations, Houston, TX, Mar*. p. 8-9.

Bazergui, André, et GQOPQQS Louis. 1987. « Predicting Leakage for various gases in Gasketed Joints ». In *Spring Conference, Society of Experimental Mechanics, Jun*. p. 15-19.

Beskok, Ali, George Em Karniadakis et William Trimmer. 1996. « Rarefaction and compressibility effects in gas microflows ». *Journal of Fluids Engineering,* vol. 118, nᵒ 3, p. 448-456.

Boqin, Gu, Chen Ye et Zhu Dasheng. 2007. « Prediction of Leakage Rates Through Sealing Connections with Nonmetallic Gaskets** Supported by the Funds for Outstanding Scientists of Jiangsu Province of China (No. 2005-6) ». *Chinese Journal of Chemical Engineering,* vol. 15, nᵒ 6, p. 837-841.

Bouzid, Abdel-Hakim, et Hichem Beghoul. 2003. « The design of flanges based on flexibility and tightness ». In *ASME 2003 Pressure Vessels and Piping Conference*. p. 31-38. American Society of Mechanical Engineers.

Bouzid, Hakim, Michel Derenne et Marwan El-Rich. 2004. « Effect of flange rotation and gasket width on leakage behavior of bolted flanged joints ». *Welding Research Council Bulletin*, nᵒ 496, p. 1-23.

Carman, Philip Crosbie. 1956. *Flow of gases through porous media*. Academic press.

Choi, Chang-Hwan, K Johan A Westin et Kenneth S Breuer. 2003. « Apparent slip flows in hydrophilic and hydrophobic microchannels ». *Physics of fluids,* vol. 15, nᵒ 10, p. 2897-2902.

Colin, Stéphane. 2006. « Single-phase gas flow in microchannels ». *Heat transfer and fluid flow in minichannels and microchannels*, p. 9-86.

Davis, Rich. 2012. « What are the current emission standards for valve packing? ».

Denny, DF. 1957. *A force analysis of the stuffing-box seal*.

Diany, Mohammed, et Abdel-Hakim Bouzid. 2009. « Short term relaxation modeling of valve stem packings ». *Journal of Tribology,* vol. 131, nᵒ 3, p. 032201.

Diany, Mohammed, et Abdel-Hakim Bouzid. 2011. « An experimental-numerical procedure for stuffing box packing characterization and leak tests ». *Journal of Tribology,* vol. 133, nᵒ 1, p. 012201.

Diany, Mohammed, et Abdel-Hakim Bouzid. 2012. « Creep constitutive law of packing materials based on relaxation tests ». *Journal of Tribology,* vol. 134, nᵒ 1, p. 012202.

Diany, Mohammed, et Abel-Hakim Bouzid. 2006. « Evaluation of contact stress in stuffing box packings ». In *ASME 2006 Pressure Vessels and Piping/ICPVT-11 Conference*. p. 87-92. American Society of Mechanical Engineers.

Dongari, Nishanth, Abhishek Agrawal et Amit Agrawal. 2007. « Analytical solution of gaseous slip flow in long microchannels ». *International journal of heat and mass transfer,* vol. 50, nᵒ 17, p. 3411-3421.

Dongari, Nishanth, et Amit Agrawal. 2012. « Modeling of Navier–Stokes equations for high Knudsen number gas flows ». *International Journal of Heat and Mass Transfer,* vol. 55, nᵒ 15, p. 4352-4358.

Dongari, Nishanth, Ashutosh Sharma et Franz Durst. 2009. « Pressure-driven diffusive gas flows in micro-channels: from the Knudsen to the continuum regimes ». *Microfluidics and nanofluidics,* vol. 6, n° 5, p. 679-692.

Ergun, Sabri. 1952. « Fluid flow through packed columns ». *Chem. Eng. Prog.,* vol. 48, p. 89-94.

Ewart, Timothée, Pierre Perrier, Irina Graur et J Gilbert Méolans. 2006. « Mass flow rate measurements in gas micro flows ». *Experiments in fluids,* vol. 41, n° 3, p. 487-498.

Flitney, Robert K. 2011. *Seals and sealing handbook*. Elsevier.

Gaft, Ya Z, VG Krivonogov et VA Petushkov. 1989. « Investigation into the mechanism of sealing in shaft stuffing boxes ». *Wear,* vol. 132, n° 1, p. 39-48.

Gauvin, Rea, F Trochu, Y Lemenn et L Diallo. 1996. « Permeability measurement and flow simulation through fiber reinforcement ». *Polymer composites,* vol. 17, n° 1, p. 34-42.

Geoffroy, S, et Marc Prat. 2004. « On the leak through a spiral-groove metallic static ring gasket ». *TRANSACTIONS-AMERICAN SOCIETY OF MECHANICAL ENGINEERS JOURNAL OF FLUIDS ENGINEERING,* vol. 126, n° 1, p. 48-54.

Grine, Lotfi, et Abdel-Hakim Bouzid. 2009. « Correlation of gaseous mass leak rates through micro and nano-porous gaskets ». In *ASME 2009 Pressure Vessels and Piping Conference*. p. 41-47. American Society of Mechanical Engineers.

Grine, Lotfi, et Abdel-Hakim Bouzid. 2011a. « Correlation of gaseous mass leak rates through micro-and nanoporous gaskets ». *Journal of Pressure Vessel Technology,* vol. 133, n° 2, p. 021402.

Grine, Lotfi, et Abdel-Hakim Bouzid. 2011b. « Liquid leak predictions in micro-and nanoporous gaskets ». *Journal of Pressure Vessel Technology,* vol. 133, n° 5, p. 051402.

Gu, B.Q. 1999. « Application of model of gases flowing through porous media to gasket sealing ». *Journal of Nunjing University of Chemical Technology,* vol. 21, n° 1, p. 19-22.

Guo, Z. Y., and Wu, X. B. 1998. « Further Study on Compressibility Effects on the Gas Flow and Heat Transfer in a Microtube ». *Nanoscale Microscale Thermophys. Eng,* vol. 2, p. 111–120.

Handley, D, et PJ Heggs. 1968. « Momentum and heat transfer mechanisms in regular shaped packings ». *Transactions of the Institution of Chemical Engineers and the Chemical Engineer,* vol. 46, n° 9, p. 251-264.

Harrison, David. 2004. « Valve fugitive emission measurement standards ». *Sealing Technology,* vol. 2004, nº 2, p. 9-12.

Harrison, David. 2006. « ISO valve emission standards are published ». *Sealing Technology,* vol. 2006, nº 12, p. 10.

Haruyama, Shigeyuki, Didik Nurhadiyanto, Moch Agus Choiron et Ken Kaminishi. 2013. « Influence of surface roughness on leakage of new metal gasket ». *International Journal of Pressure Vessels and Piping,* vol. 111, p. 146-154.

Hayashi, K, et K Hirasata. 1989. « Experimental derivation of the basic characteristics of asbestoid and graphitic packings in mounted condition, 12 Int ». In *Conf. Fluid sealing, Paper A*. Vol. 4, p. 1989.

Hellström, Gunnar, et Staffan Lundström. 2006. « Flow through porous media at moderate Reynolds number ». In *International Scientific Colloquium Modelling for Material Processing: 08/06/2006-09/06/2006*. p. 129-134.

Hong, Chungpyo, Yutaka Asako et Jae-Heon Lee. 2009. « Estimation of leak flow rates through narrow cracks ». *Journal of Pressure Vessel Technology,* vol. 131, nº 5, p. 05140501-05140508.

Huang, Peter, et Kenneth S Breuer. 2007. « Direct measurement of slip length in electrolyte solutions ». *Physics of fluids,* vol. 19, nº 2, p. 028104.

Hutchins, WC. 1962. « Leak Test Specifications ». *Instruments and Control Systems,* vol. 35, p. 107-109.

Jim Drago. June 2010. « Containing Fugitive Emissions ». *Chemical Engineering*.

Jolly, Pascal, et Luc Marchand. 2006. « Leakage predictions for static gasket based on the porous media theory ». In *ASME 2006 Pressure Vessels and Piping/ICPVT-11 Conference*. p. 151-158. American Society of Mechanical Engineers.

Jones, D. P, et H Krier. 1983. « Gas Flow Resistance Measurements Through Packed Beds at High Reynolds Numbers1 ». *Urbana,* vol. 3, p. 186-172.

Karniadakis, GEM, Ali Beskok et M Gad-el-Hak. 2002. « Micro flows: fundamentals and simulation ». *Applied Mechanics Reviews,* vol. 55, p. B76.

Kazeminia, M, et A Bouzid. 2016a. « Predicting leakage in packed stuffing boxes ». In *23rd International Conference on Fluid Sealing Manchester, UK*. p. 45-59.

Kazeminia, M, et AH Bouzid. 2016b. « Predicting leakage in packed stuffing boxes ». In. BHR Group.

Kazeminia, M, et AH Bouzid. 2016c. « Predicting leakage in packed stuffing boxes ». In *23rd International Conference on Fluid Sealing*. (Manchester, UK), p. 45-59.

Kazeminia, Mehdi, et Abdel-Hakim Bouzid. 2014a. « Analysis of stresses and strains in packed stuffing-boxes ». In *ASME 2014 Pressure Vessels and Piping Conference*. p. V005T11A019-V005T11A019. American Society of Mechanical Engineers.

Kazeminia, Mehdi, et Abdel-Hakim Bouzid. 2014b. « Effect of tapered housing on the axial stress distribution in a stuffing box packing ». *International Journal of Advancements in Mechanical and Aeronautical Engineering–IJAMAE,* vol. 1, nᵒ 3, p. 115-120.

Kazeminia, Mehdi, et Abdel-Hakim Bouzid. 2015. « Prediction of leak rates in porous braided packing rings ». In *ASME 2015 Pressure Vessels and Piping Conference*. p. V002T02A015-V002T02A015. American Society of Mechanical Engineers.

Kazeminia, Mehdi, et Abdel-Hakim Bouzid. 2018. « Leak prediction through porous compressed packing rings: A comparison study ». *International Journal of Pressure Vessels and Piping,* vol. 166, p. 1-8.

Knudsen, M. 1909a. « The law of the molecular flow and viscosity of gases moving through tubes. ». *Ann. Phys.,* vol. 28 p. 75-130.

Knudsen, Martin. 1909b. « The law of the molecular flow and viscosity of gases moving through tubes ». *Ann. Phys,* vol. 28, nᵒ 1, p. 75-130.

Kockelmann, H, et R Hahn. 2006. « High Grade Performance Proof on Gaskets for Bolted Flange Connections With Organic Fluids ». In *ASME 2006 Pressure Vessels and Piping/ICPVT-11 Conference*. p. 273-279. American Society of Mechanical Engineers.

Kockelmann, Hans, Jaroslav Bartonicek, Eberhard Roos, Rolf Hahn et Werner Ottens. 2009. « Long Term Behaviour of Stuffing Box Packings Under the Influence of Fluids at High Temperature ». In *ASME 2009 Pressure Vessels and Piping Conference*. p. 35-39. American Society of Mechanical Engineers.

Kumar, Sanjeev, et Sanjeet Kumar. 2009. « A Mathematical model for Newtonian and non-Newtonian flow through tapered tubes ». *Indian Journal of Biomechanics*, p. 191.

Lasseux, Didier, Pascal Jolly, Yves Jannot et Emmanuel Sauger Benoit Omnes. 2011. « Permeability measurement of graphite compression packings ». *Journal of Pressure Vessel Technology,* vol. 133, nᵒ 4, p. 041401.

Lauga, Eric, et Todd M Squires. 2005. « Brownian motion near a partial-slip boundary: A local probe of the no-slip condition ». *Physics of Fluids,* vol. 17, nº 10, p. 103102.

Liu, Shijie, Artin Afacan et Jacob Masliyah. 1994. « Steady incompressible laminar flow in porous media ». *Chemical engineering science,* vol. 49, nº 21, p. 3565-3586.

Ljung, Anna-Lena, T Staffan LUNDSTRÖM et Kent Tano. 2006. « Simulation of heat transfer and fluid flow in a porous bed of iron ore pellets during up-draught drying ». *SIMULATION,* vol. 13, p. 15.

Luft, TA. 2007. « Emission measurements of industrial valves according to TA Luft and EN ISO 15848-1 ». *perspective,* vol. 506, p. 2440.

Lv, Zhi Kai, Shun Li He, Shao Yuan Mo et Hai Yong Zhang. 2013. « The Effect of Gas Slippage on Laboratory Results and Gas Well Production ». In *Applied Mechanics and Materials*. Vol. 318, p. 437-441. Trans Tech Publ.

Macdonald, IF, MS El-Sayed, K Mow et FAL Dullien. 1979. « Flow through porous media-the Ergun equation revisited ». *Industrial & Engineering Chemistry Fundamentals,* vol. 18, nº 3, p. 199-208.

Masi, Vincent, Abdel-Hakim Bouzid et Michel Derenne. 1998. « Correlation between gases and mass leak rate of gasketing materials ». *ASME-PUBLICATIONS-PVP,* vol. 367, p. 17-24.

Maurer, Jean, Patrick Tabeling, Pierre Joseph et Herve Willaime. 2003. « Second-order slip laws in microchannels for helium and nitrogen ». *Physics of Fluids,* vol. 15, nº 9, p. 2613-2621.

McGrew, JM, et JD McHugh. 1965. « Analysis and test of the screw seal in laminar and turbulent operation ». *Journal of Basic Engineering,* vol. 87, nº 1, p. 153-162.

Munson-McGee, Stuart H. 2002. « An approximate analytical solution for the fluid dynamics of laminar flow in a porous tube ». *Journal of membrane science,* vol. 197, nº 1-2, p. 223-230.

Nesbitt, Brian. 2011. *Handbook of valves and actuators: valves manual international.* Elsevier.

Nield, DA, et A Bejan. 1999a. « Convection in Porous Media2 Springer-Verlag New York Google Scholar ».

Nield, Donald A, et Adrian Bejan. 1999b. *Convection in porous media*, 1. Coll. « Mechanics of Fluid Flow Through a Porous Medium ». Springer.

Nield, Donald A, et Adrian Bejan. 2006. *Convection in porous media*, 3. Springer.

Ochoński, W. 1988. « Radial stress distribution and friction forces in a soft-packed stuffing-box seal ». *Tribology International,* vol. 21, nº 1, p. 31-38.

Ottens, Werner, Eberhard Roos, Hans Kockelmann et Rolf Hahn. 2010. « Optimization of stuffing box stem sealings in valves by means of surface treatment and coating ». In *ASME 2010 Pressure Vessels and Piping Division/K-PVP Conference*. p. 191-201. American Society of Mechanical Engineers.

Parkhouse, JG, et A Kelly. 1995. « The random packing of fibres in three dimensions ». In *Proceedings of the Royal Society of London A: Mathematical, Physical and Engineering Sciences*. Vol. 451, p. 737-746. The Royal Society.

Pengyun, Song, Chen Kuangmin et Dong Zongyun. 1997. « A theoretical analysis of the lateral pressure coefficients in a soft-packed stuffing-box seal ». *Tribology International,* vol. 30, nº 10, p. 759-765.

Pérez-Ràfols, Francesc, Roland Larsson et Andreas Almqvist. 2016. « Modelling of leakage on metal-to-metal seals ». *Tribology International,* vol. 94, p. 421-427.

Pit, R, H Hervet et L Leger. 2000. « Direct experimental evidence of slip in hexadecane: solid interfaces ». *Physical review letters,* vol. 85, nº 5, p. 980.

Pogodin, VK, DM Dubrovin, VA Venediktov et PM Kon'kov. 1995. « Determination of required conditions for nonleakage of valve stuffing-box seals ». *Chemical and Petroleum Engineering,* vol. 31, nº 7, p. 391-394.

Producers, Canada`s Oil and Nutral Gas. February, 2014. « Update of Fugitive Equipment Leak Emission Factors ».

Reeves, David W, JW Bill Ross et M Wasielewski. 2004. « Assessing fugitive emissions performance in valves and packing ». *Valve World*, p. 208228.

Roe, M, et AA Torrance. 2008. « The surface failure and wear of graphite seals ». *Tribology International,* vol. 41, nº 11, p. 1002-1008.

Saeed, Hasan Aftab, Satoshi Izumi, Shinsuke Sakai, Shigeyuki Haruyama, Masato Nagawa et Hideki Noda. 2008. « Development of new metallic gasket and its optimum design for leakage performance ». *Journal of Solid Mechanics and Materials Engineering,* vol. 2, nº 1, p. 105-114.

Schaaf, Manfred, Thomas Klenk, Ralf Vogel et Jaroslav Bartonicek. 2005a. « Tightness characteristics of packings ». In *ASME 2005 Pressure Vessels and Piping Conference*. p. 147-154. American Society of Mechanical Engineers.

Schaaf, Manfred, Thomas Klenk, Ralf Vogel et Jaroslav Bartonicek. 2005b. « Tightness characteristics of packings ». In *2005 ASME PVP Conference, Montreal*.

Schaaf, Manfred, et Friedrich Schoeckle. 2009a. « Technical Approach for the Reduction of Fugitive Emissions ». In *ASME 2009 Pressure Vessels and Piping Conference*. p. 251-257. American Society of Mechanical Engineers.

Schaaf, Manfred, et Friedrich Schoeckle. 2009b. « Technical Approach for the Reduction of Fugitive Emissions ». In *Proceedings of the ASME 2009 Pressure Vessels and Piping Division Conference*. Vol. 2, p. 251-257.

Schaaf, Manfred, Friedrich Schoeckle et Jaroslav Bartonicek. 2008. « Concept for the Guarantee of the Integrity of Bolted Flanged Connections in a German Nuclear Power Plant ». In *ASME 2008 Pressure Vessels and Piping Conference*. p. 81-88. American Society of Mechanical Engineers.

Singh, Narendara, Nishanth Dongari et Amit Agrawal. 2014. « Analytical solution of plane Poiseuille flow within Burnett hydrodynamics ». *Microfluidics and nanofluidics,* vol. 16, nº 1-2, p. 403-412.

Sreekanth, AK. 1969. « Slip flow through long circular tubes ». *ACADEMIC PRESS, INC.,* vol. 1, nº 1969, p. 667-680.

Standards, U.S. EPA Office of Air Quality Planning and. April 2014. « Oil and Natural Gas Sector Leaks ».

Steinke, Joe, et Jay Abrahimzadeh. 2000. « FUGITIVE EMISSIONS EXPERIMENTAL MEASUREMENTS AND EQUIVALENCY ». p. 1-9.

Tahir, Mohammad Waseem, Stefan Hallström et Malin Åkermo. 2014. « Effect of dual scale porosity on the overall permeability of fibrous structures ». *Composites Science and Technology,* vol. 103, p. 56-62.

Tashiro, Hisao, et Fusahito Yoshida. Jun 1991. *Sealing characteristics of gland packing. (5th Report, leakage rate measurement and its evaluation)*. Japanese: Transactions of the Japan Society of Mechanical Engineers, 2047-2051 p.

Thomson, JL. 1961. « A Theory of Sealing With Particular Reference to the Packed Stuffing Box ». In *British Hydromechanics Research Association, International Conference on Fluid Sealing, Paper Bl*.

Tison, SA. 1993. « Experimental data and theoretical modeling of gas flows through metal capillary leaks ». *Vacuum,* vol. 44, nº 11-12, p. 1171-1175.

Ueda, T, et M Fujiwara. 1997. « Improved gland packings for volatile fluids ». In *BHR GROUP CONFERENCE SERIES PUBLICATION*. Vol. 26, p. 145-158. MECHANICAL ENGINEERING PUBLICATIONS LIMITED.

Vallabh, Rahul, Pamela Banks-Lee et Abdel-Fattah Seyam. 2010. « New Approach for Determining Tortuosity in Fibrous Porous Media ». *Journal of Engineered Fabrics & Fibers (JEFF),* vol. 5, nº 3.

Vasse, Christophe. 2009. « Developing a Numerical Model to Describe the Mechanical Behavior of Compressed Expanded Graphite for Valve Stem Sealing ». In *ASME 2009 Pressure Vessels and Piping Conference*. p. 81-87. American Society of Mechanical Engineers.

Veiga, José C, Carlos Cipolatti, Carlos Girão, Leandro Ascenco et Fabio Castro. 2008a. « Valve Packings Seating Stress ». In *ASME 2008 Pressure Vessels and Piping Conference*. p. 101-106. American Society of Mechanical Engineers.

Veiga, José C, Carlos Cipollati, Carlos Girão, Leandro Ascenco et Fabio Castro. 2008b. « Valve Packings Seating Stress ». *ASME Paper No. PVP2008-61214*.

Veiga, José, Carlos D Girão et Carlos F Cipolatti. 2009. « The influence of different braided packing materials and number of rings on stem torque and sealability ». In *ASME 2009 Pressure Vessels and Piping Conference*. p. 115-123. American Society of Mechanical Engineers.

Vermes, Géza. 1960. « A fluid mechanics approach to the labyrinth seal leakage problem ». In *ASME 1960 Gas Turbine Power and Hydraulic Divisions Conference and Exhibit*. p. V001T02A012-V001T02A012. American Society of Mechanical Engineers.

Wang, S. 2000. *Sealing model of nonmetallic gaskets and calculation of leakage rate of bolted flanged connections* chinese: Master D. Thesis, Nanjing University of Technology, 4-5 p.

Yanagisawa, T, M Sanada, H Tanoue, T Koga et H Hirabayashi. 1990. « Fundamental study of the sealing performance of a C-shaped metal seal ». In *Proceedings of the 2nd International Symposium on Fluid Sealing*. p. 389-398.

Zahorulko, Andriy. 2015. « Experimental investigation of mechanical properties of stuffing box packings ». *Sealing Technology,* vol. 2015, nº 8, p. 7-13.

Zhang, Qiang, Xiaoqian Chen, Yiyong Huang et Xiang Zhang. 2018. « An Experimental Study of the Leakage Mechanism in Static Seals ». *Applied Sciences,* vol. 8, nº 8, p. 1404.

Zou, RP, et AB Yu. 1996. « Evaluation of the packing characteristics of mono-sized non-spherical particles ». *Powder technology,* vol. 88, nº 1, p. 71-79.